ERDC/CHL TR-06-8

Coastal and Hydraulics Laboratory

US Army Corps of Engineers®
Engineer Research and Development Center

Houston-Galveston Navigation Channels, Texas Project

Navigation Channel Sedimentation Study, Phase 1

J. N. Tate and R. C. Berger

August 2006

ERDC/CHL TR-06-8
August 2006

Houston-Galveston Navigation Channels, Texas Project

Navigation Channel Sedimentation Study, Phase 1

J.N. Tate and R.C. Berger

Coastal and Hydraulics Laboratory
U.S. Army Engineer Research and Development Center
3909 Halls Ferry Road
Vicksburg, MS 39180

Final report

Prepared for U.S. Army Corps of Engineers
Washington, DC 20314-1000

Under Work Unit 33143

Abstract: The U.S. Army Engineer District, Galveston, has recently enlarged the Houston Ship Channel from a 40-ft (12.2-m) depth by 400-ft (122-m) width to a 45-ft (13.7-m) depth by 530-ft (162-m) width. Previously, a three-dimensional (3-D) numerical model study was implemented at the U.S. Army Engineer Research and Development Center's Coastal and Hydraulics Laboratory to evaluate the salinity and circulation impact of this enlargement. The enlarged channel is nearly complete. Preliminary evaluations indicate a higher than anticipated rate of deposition in the channel reach near Atkinson Island. The purpose of this investigation was to determine if this new shoaling rate was a permanent feature of this new channel or a single anomalous event. If this considerably larger deposition is a permanent condition then the planned disposal locations must be expanded. The project will determine the possible effects on sedimentation in the channel based on dredging records, field data, vessel effects, and hydrodynamic changes due to the channel's enlargement.

Contents

Figures and Tables

Figures

Tables

Preface

This report represents the findings of an investigation of the possible causes of increased shoaling in the Houston Ship Channel after its dimensions were increased from 40 ft x 400 ft (12.2 m x 122 m) to 45 ft x 530 ft (13.7 m x 162 m). This unexpected increase in shoaling may subside in time if due to the dredging itself or the channel side slopes reestablishing equilibrium. It, however, may be due to the larger channel dimensions. In which case the increased shoaling would be a permanent condition. Additional disposal capability would then be required.

This investigation was conducted from August 2004 through August 2005 at the U.S. Army Engineer Research and Development Center (ERDC) by Dr. R. C. Berger, A. R. Carrillo, L. M. Lee, and J. N. Tate of the Coastal and Hydraulics Laboratory (CHL). The data collection was conducted 20-22 August 2004. In addition to Dr. Berger, the data collection group included J. R. Bull, H. A. Benson, and Dr. K. R. Barry. Funding was provided by the U.S. Army Engineer District, Galveston.

The work was performed under the general direction of Thomas W. Richardson, Director, CHL, Dr. William D. Martin, Deputy Director, CHL, B. A. Ebersole, Chief, Flood and Storm Protection Division, CHL, and Dr. R. T. McAdory, Chief, Estuarine Engineering Branch, CHL.

COL Richard B. Jenkins was Commander and Executive Director.
Dr. James R. Houston was Director of ERDC.

Unit Conversion Factors

Multiply	By	To Obtain
cubic feet	0.02831685	cubic meters
cubic yards	0.7645549	cubic meters
degrees (angle)	0.01745329	radians
Feet	0.3048	meters
Knots	0.5144444	meters per second
Microns	1.0 E-06	meters
miles (nautical)	1,852	meters
miles (U.S. statute)	1,609.347	meters
miles per hour	0.44704	meters per second
pounds (force)	4.448222	newtons
Slugs	14.59390	kilograms
square feet	0.09290304	square meters
square miles	2.589998 E+06	square meters
square yards	0.8361274	square meters
Yards	0.9144	meters

1 Introduction

Background

The U.S. Army Engineer District, Galveston, recently enlarged the Houston Ship Channel from a 40-ft (12.2-m) depth by 400-ft (122-m) width to a 45-ft (13.7-m) depth by 530-ft (162-m) width. Previously, a three-dimensional (3-D) numerical model study was implemented at the U.S. Army Engineer Research and Development Center's (ERDC's) Coastal and Hydraulics Laboratory (CHL) to evaluate the salinity and circulation impact of this enlargement. In Berger et al. (1995a) the model was shown to represent the salinity and circulation in the earlier channel configuration. Then in Berger et al. (1995b), it was used to predict the impact of the enlarged channel. This model was again used in Carrillo et al. (2002) to evaluate the addition of barge lanes along the ship channel flanks. The enlarged channel is nearing completion, and preliminary evaluations indicate a higher than anticipated rate of deposition in the channel reach near Atkinson Island. The purpose of this investigation was to determine if this new shoaling rate was a permanent feature of this enlarged channel or a single anomalous event. If this considerably larger deposition is a permanent condition, then the planned disposal locations must be expanded.

The historical record shows that once the bay channel became deeper than the natural depth over its entire length (mid-1920's), the dredging rate has been fairly constant. This may mean that the material moves into the channel from the sides and is simply moved about along the channel by the currents and vessel entrainment, or this could be the result of other conditions. The historical rate of dredging within the bay segment of the channel has been about 2 million cu yd (765,000 cu m) per year. The model and field data show that the residual near-bed currents are relatively large over most of the southern part of the bay channel, approximately from the Texas City dike up to about where the Bayport Channel intersects the main channel. The residual near-bed currents in the channel near Atkinson Island are small. Over the entire length of the bay channel, the near-bed currents are flood-directed. That is, they are directed landward rather than toward the ocean. Any material that falls into the southern part of the channel will tend to move upstream to the region near Atkinson Island. If the currents are not strong enough, the material may deposit before it reaches this area. The vessel traffic along the Hous-

ton Ship Channel can cause resuspension even if the tidal currents are weak.

The preliminary evaluation of the required dredging quantity for the new channel configuration appears to be perhaps 4 million cu yd (3 million cu m) per year in just the channel section near Atkinson Island. It is possible that this additional dredging quantity is material that has escaped from the disposal sites or low density fluff. It may also be due to the adjustment of the channel side slopes to the new configuration. However, it could also be that the hydrodynamics of the channel and bay have changed enough to result in this change.

Another possible reason that the dredging quantity could have increased is from the effect of vessel traffic. This may include vessel-induced erosion of the surrounding shallows. With a larger channel, the vessels can move faster. The vessel speed is limited by the ability of the water to move out of the way and return behind the vessel. The wave speed in the shallows around the vessel may be slower than the vessel. In this circumstance, the condition is like that of supercritical flow in open channel flow. The drawdown wave results in high currents and substantial shock waves moving along and behind the vessel. It is possible that this is causing more sediment to move into the channel. Also, a vessel moving in the channel can reduce the deposition rate or cause erosion. The enlarged channel may have reduced the erosion potential of the passing vessels.

Approach

The study focuses on determining what the ultimate deposition rate should be in the navigation channel, especially in the Atkinson Island reach, for the 45- x 530-ft (13.7- x 162-m) channel (hereafter referred to as the "plan" condition). The original channel configuration of 40 x 400 ft (12.2 x 122 m) is termed the "base" condition. Several different components of the study are undertaken.

The initial step is to analyze the dredging records obtained from the Corps of Engineers District, Galveston. These will be used to determine the pattern of deposition before the enlargement and any correlation with flow rate.

Next, field data collection will be conducted:

a. To provide sediment parameters for the model.

b. To try to determine the source of the extensive sedimentation in the Atkinson Island reach of the Houston Ship Channel.

Sediment data include bed and water column samples. These data are used to estimate critical shear stress, settling velocity, grain-size distribution, etc. In addition to characterizing sediment along the channel, nearby shallows are also sampled. A preliminary assessment of resuspension due to ship induced currents is made as well. This is used to determine the potential reduction in net shoaling in the base and enlarged channel conditions due to the presence of ships.

The next step is to analyze the currents from the model for both channel configurations - before and after the channel enlargement. The average residual currents can provide an indicator of the shear stress vector for the before and after enlargement conditions. The questions to be answered are as follows:

a. Is there substantially larger erosion of the surrounding shallows with the increased channel size?

b. Is there a substantial decrease in shear stress in the channel?

c. Do the residual currents suggest a large shift in the distribution of sediment similar to that noticed for this first maintenance cycle?

The final step is to improve the previous 3-D model to include more detailed representation of areas that are of interest for this particular study. The model is then used to analyze the impact of the channel enlargement by introducing a sediment tracer in the model channel for the 40- x 400-ft (12.2- x 122-m) channel and the “as built” 45- x 530-ft (13.7- x 162-m) conditions. This gives an idea of the change one should see in the dredging distribution and an indication of any change in trapping efficiency. This reflects only the impact of the change in hydrodynamics and therefore is only a rough estimate of the expected permanent change in shoaling.

The analysis of the dredging data is in the second chapter. The third chapter discusses the data collection, the fourth chapter discusses the vessel-induced effects on sedimentation, and the fifth chapter details model results. First the impact of the hydrodynamic change due to the channel enlargement and its likely effect on sedimentation is investigated. Second,

the model is run with a sediment tracer. The final chapter is a summary with conclusions from the entire report.

2 Dredge Data Analysis

The dredging records of the Houston Ship Channel for the period in which the channel was in the 40-ft (12.2-m) deep by 400-ft (122-m) wide condition are analyzed. There are two goals of this analysis: a) Determine the distribution of sedimentation during the period in which the channel was in the 40- x 400-ft (12.2- x 122-m) configuration. This is to be used as validation data for the sediment model; which will be reported on later. b) Determine the change in shoaling over time during this same period, and attempt to find a causal relationship with freshwater inflow to the system or other factors.

Figure 1 shows the Houston Ship Channel area and locations of interest for this analysis.

Figure 1. Houston Ship Channel area map.

Historical dredging records were received from the U.S. Army Corps of Engineer District, Galveston, in EXCEL spreadsheet form for all reaches along the Houston Ship Channel over a time period from 1949 to 2003. These data were sorted, and the reaches of Bolivar Roads to Red Fish Reef and Red Fish Reef to Morgan's Point were separated from the other

reaches. The data were provided as total yardage dredged on a given date for a given station range. The stations were given as an upstream station number and a downstream station number for each yardage total, with station numbers being 1000 ft (302.8 m) increments. The station numbers were used as the guide to join the two reaches together into one data set. Bolivar Roads was taken as sta 130, with the station numbers decreasing as one travels upstream to Morgan's Point and sta 0 (see Figure 2). The analysis presented here is to determine if a correlation can be made between the dredging records and the freshwater flows into the system during this time.

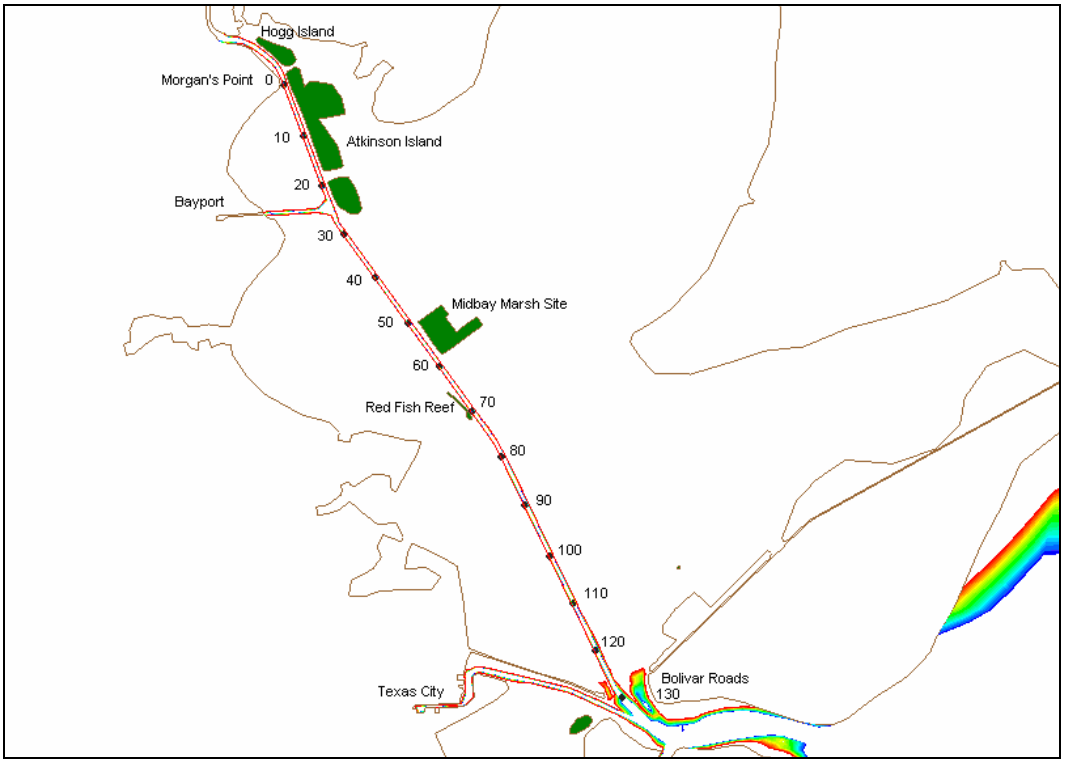

Figure 2. Houston Ship Channel station map (emergent features are shaded green).

In order to determine a yardage for each station, the number of stations included in each dredging segment was divided into the total yardage for that segment. The yardage was summed over time for each of the stations and averaged by the total amount of time, ~34 years. Note that the time of interest for this project is after the navigation channel was dredged to 40 ft (12.2 m). It was determined that this deepening was performed by Fiscal Year 1964. The dredge data prior to this deepening were not included in the analysis presented here. These sections were last dredged, for maintenance only, in 1998, to maintain the enlarged – widened and deepened - channel. This manipulation allowed for the determination of an average

shoaling rate per station over the entire dredging period for each of the stations. The average shoaling rate per station is given in Figure 3.

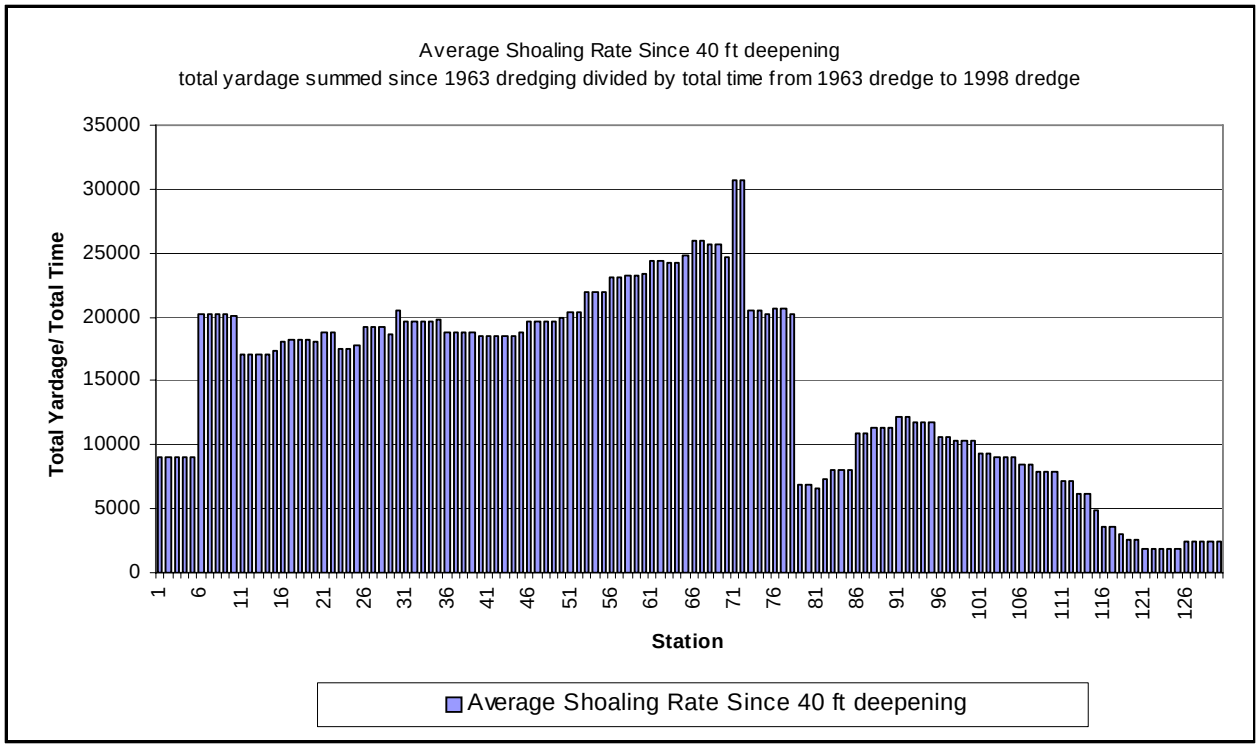

Figure 3. Average shoaling rate per station (total cubic yards per total number of years for each station).

The dredge data were separated by reach with station 72 as the dividing line for Red Fish Reef. The total yardage for each dredge occurrence was summed over the reach (Morgan's Point to Red Fish Reef: stations 0-72 and Red Fish Reef to Bolivar Roads: stations 72-130). Each yardage sum was averaged by the number of stations in the reach and divided by the time since the previous dredge event for that reach in order to obtain an average shoaling per year over the reach. The average shoaling rate per reach over time is shown in Figure 4 for Morgan's Point to Red Fish Reef and in Figure 5 for Red Fish Reef to Bolivar Roads.

Results of this analysis showed that the shoaling rate was higher in the upper half of the bay channel for the 40- x 400-ft (12.2- x 122-m) condition (this is in the region north of Redfish Reef and along Atkinson Island). In this upper reach the sedimentation dredging volume dropped dramatically and fairly consistently over the 34 years of this channel configuration. The dredging rate in the recent years was only about one-fourth of that required immediately after the enlargement to 40 x 400 ft (12.2 x 122 m).

The decline is steady throughout the 34 years. In the lower bay there was no strong trend over this period.

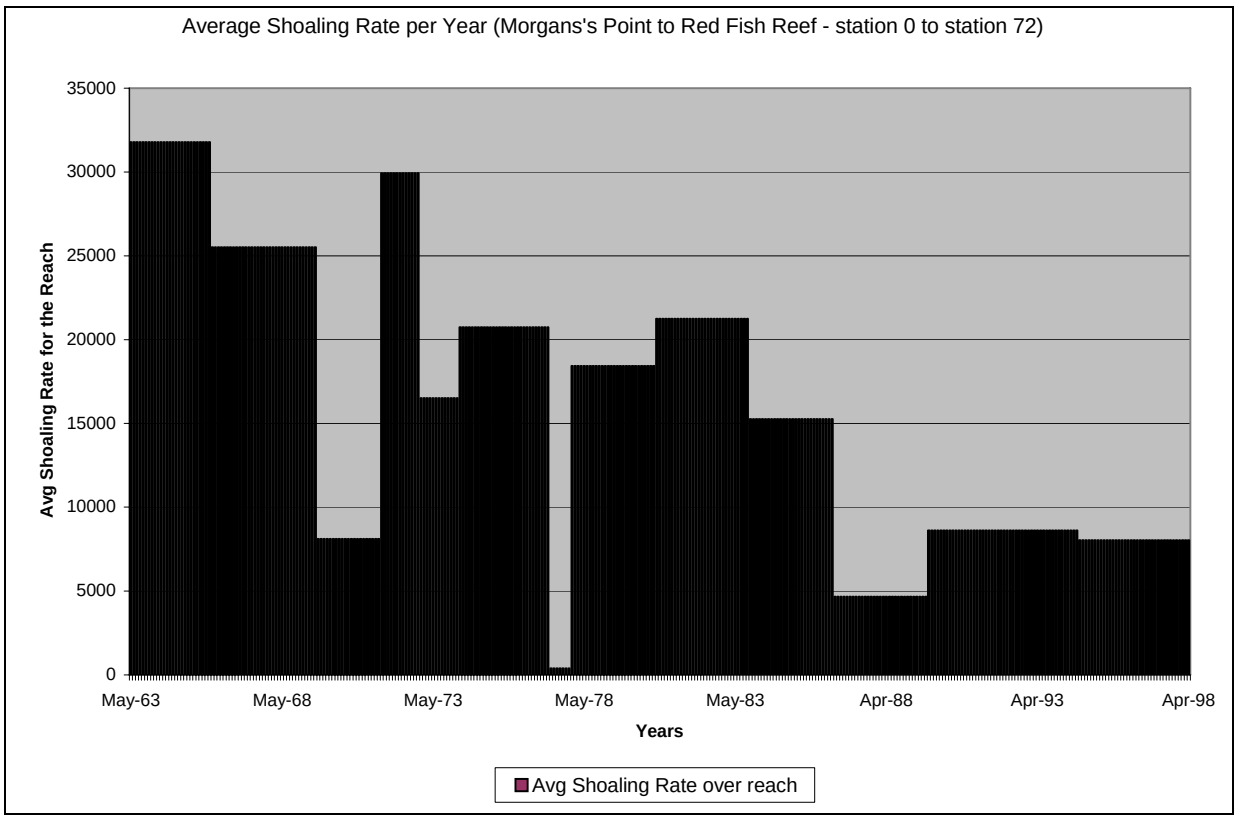

Figure 4. Average shoaling rate for Morgan's Point to Red Fish Reef (total cubic yards per station in the reach per year between dredging).

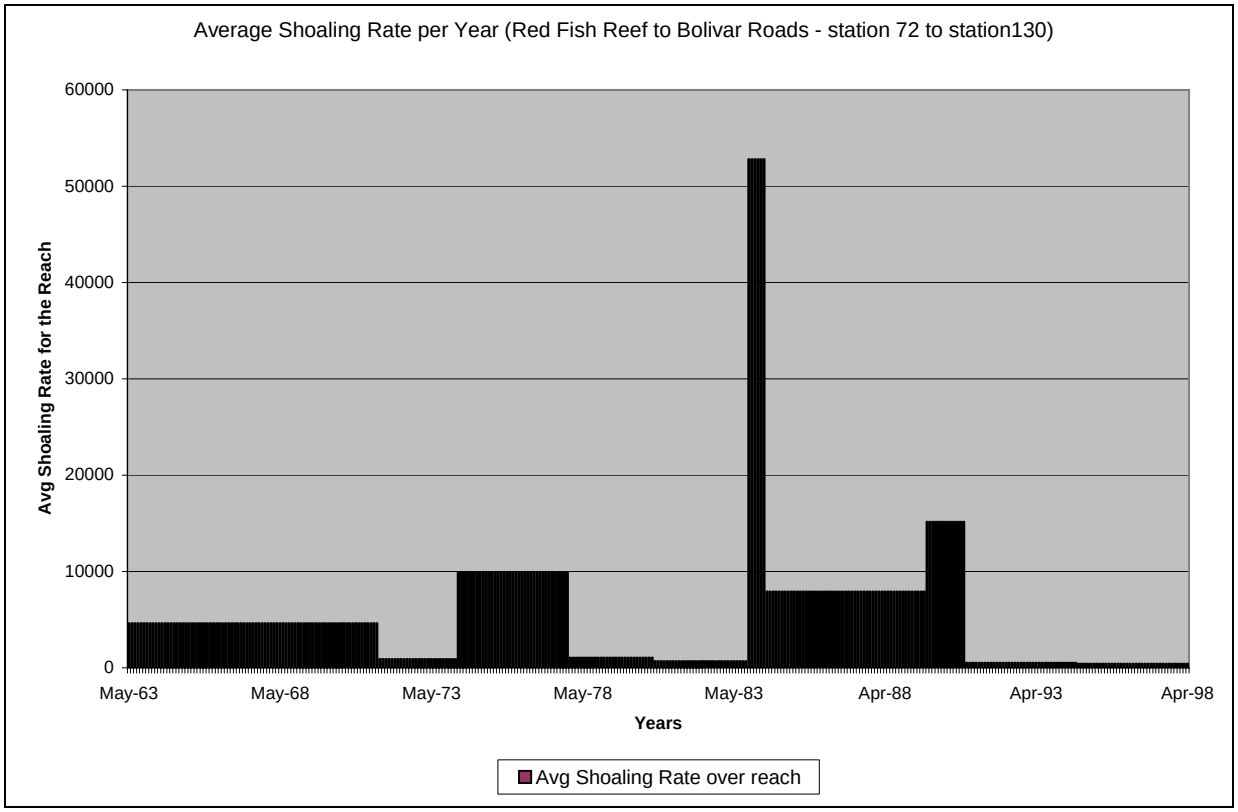

Figure 5. Average shoaling rate for Red Fish Reef to Bolivar Roads (total cubic yards per station in the reach per year between dredging).

Stream flow data for the Trinity River and the San Jacinto River over the same time period as the dredging records were obtained from the U.S. Geological Survey (USGS) Web site. In order to get data over the entire period needed, data sets were taken from gauges upstream of the rivers' entrances to the Houston Ship Channel model domain. Trinity River data were taken from the gauge at Liberty, TX, while San Jacinto data were taken from the western fork at Conroe, TX, and the eastern fork at Cleveland, TX. The purpose of the stream flow data was to determine if a correlation exists between it and the dredging records; therefore a general trend was only necessary at this point and data from gauges slightly upstream were reasonable. The flow data are presented in Figures 6-8.

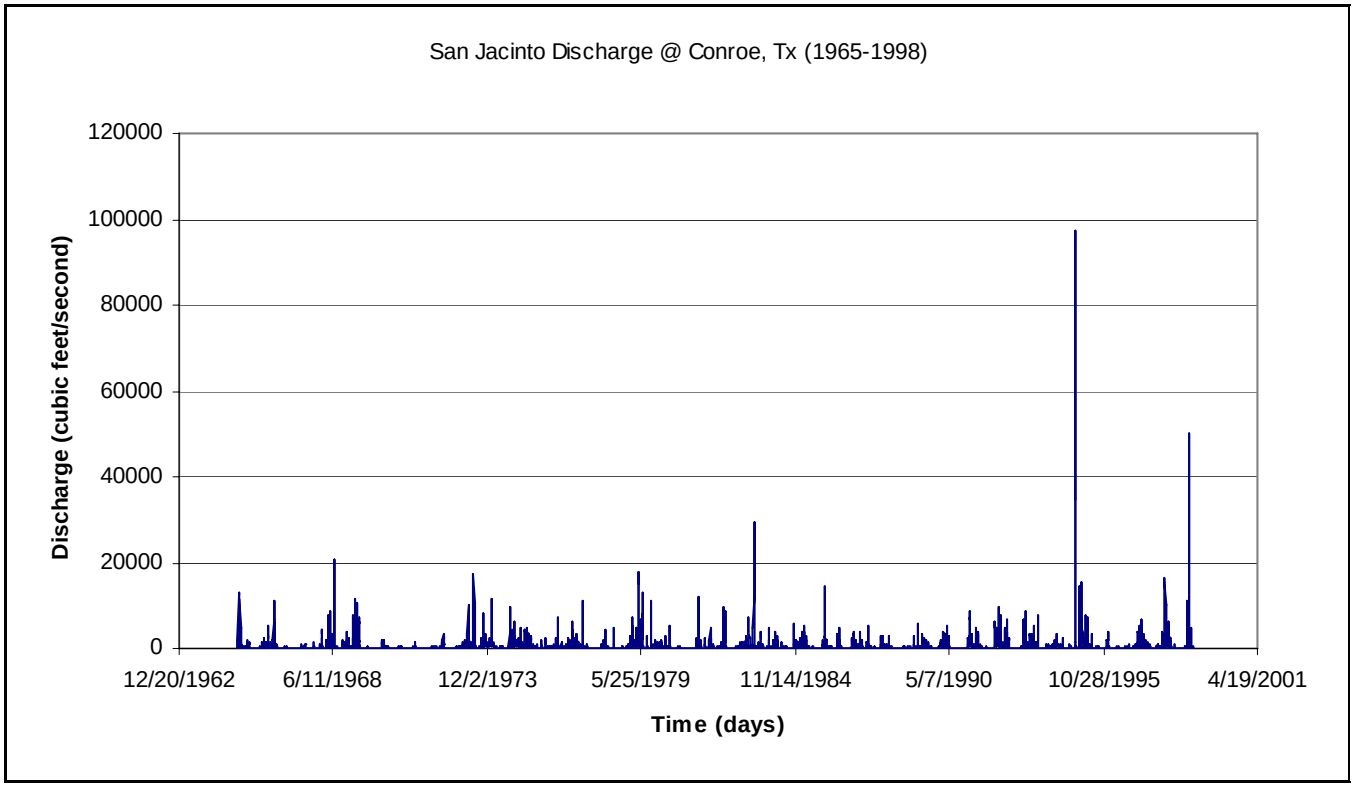

Figure 6. Flow data for San Jacinto River western fork.

It was thought that perhaps the freshwater inflow decreased dramatically leading to this drop in sedimentation. However, the flow data do not support this hypothesis since the data showed somewhat more average flow during the years of less dredging.

It is possible that the channel stabilized over time causing less sediment to erode from its banks. Perhaps dredging practices improved so that less dredged material was allowed to reenter the channel. Another possibility for the drop in dredging over this period is the change in the sediment load

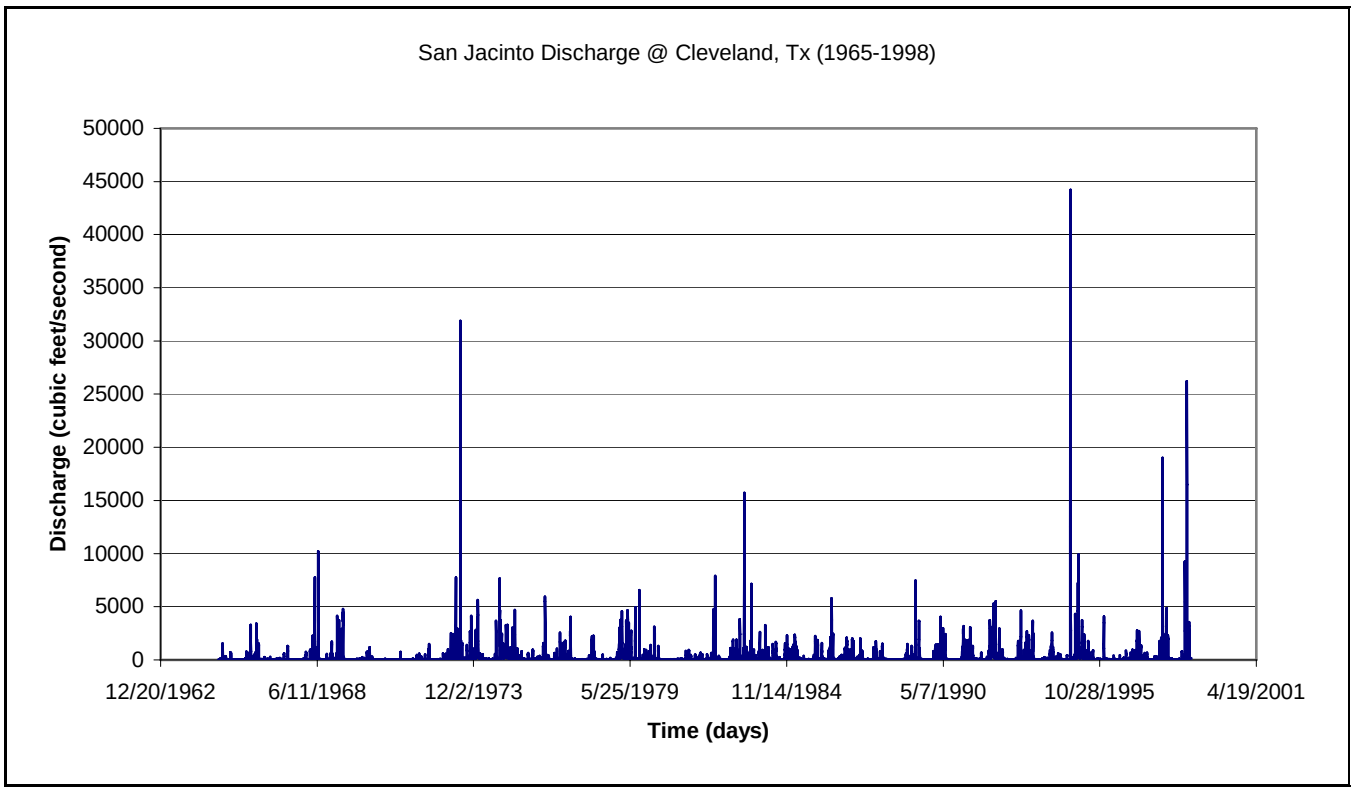

Figure 7. Flow data for San Jacinto River eastern fork.

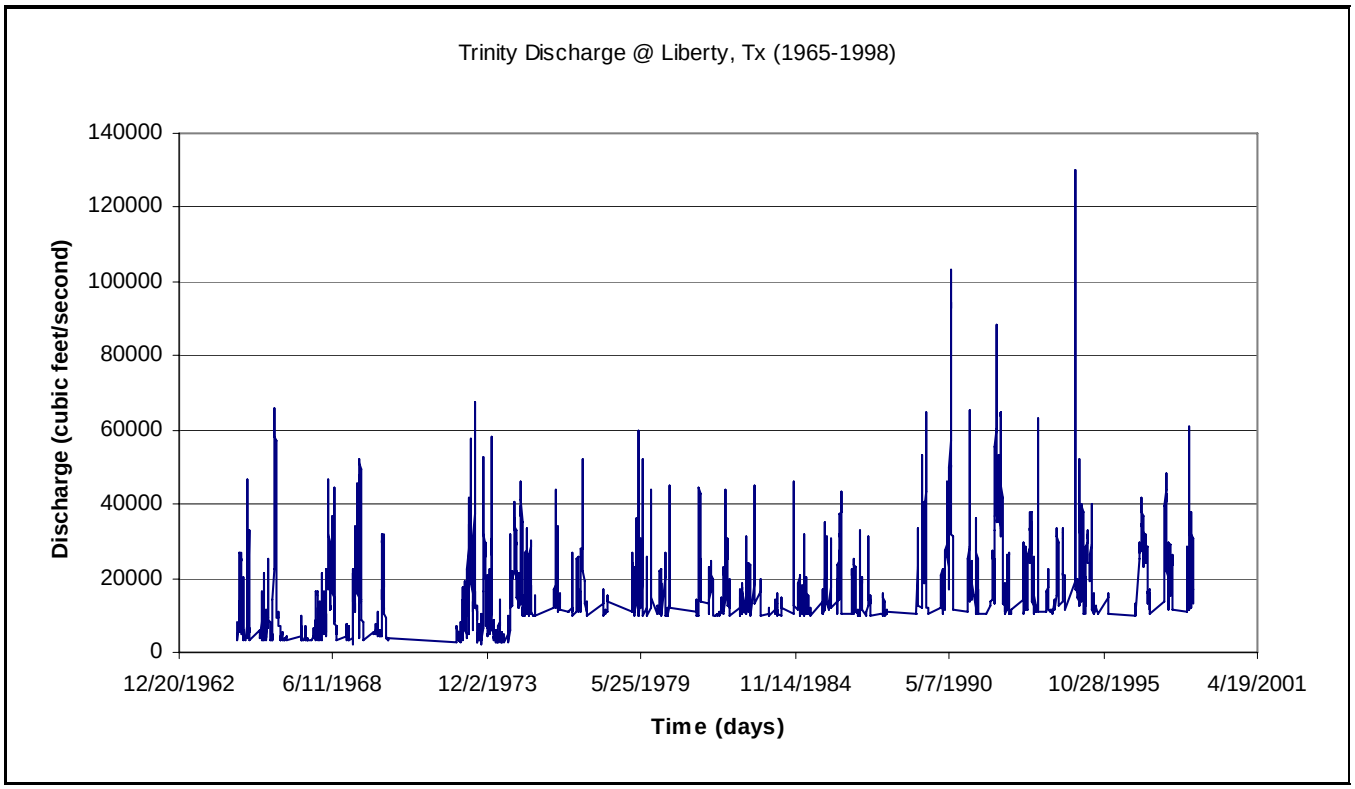

Figure 8. Flow data for Trinity River.

from upstream sources to the bay. Ward and Armstrong (1993) found that the suspended solids in the upper Houston Ship Channel had dropped to one-third of that from 25 years earlier. They attribute this reduction to improved waste treatment, altered land use, and impoundments on the principal rivers. Solis et. al. (1994) found that the Trinity River gauge at Romayor, TX (USGS gauge 08066500 located approximately 74 km (46 miles) upstream from the river's entrance to the bay) shows a significant reduction in downstream sediment inputs after the completion of Lake Livingston in 1968. White et. al. (2002) indirectly confirmed this finding by noting that the Trinity River delta was prograding through most of the 20th century, with a transition to degradation beginning sometime between 1956 and 1974.

There actually is a decline in total suspended sediment throughout most of the bay. The goal of this analysis was to study the link between dredging quantities and the freshwater inflow to the system. There does not appear to be a clear link. It appears that the perception that the historical shoaling rate in the channel had not increased with channel enlargement may in fact be due to reduced sediment load caused by other factors, such as the impoundment of the rivers, waste treatment, altered land use, or improved dredge disposal practices.

3 Field Data Collection and Analysis

The ERDC-CHL Measurement and Analysis Group sent a team to the Houston Ship Channel – Galveston Bay area to gather field data from 20 to 22 August 2004. A summary of observations is given in this chapter along with the actual data and analysis performed.

Generally the channel was found to contain significant deposits along the edges with the center maintaining the 49 ft. (14.9-m) or so depth dredged during channel construction. When not meeting or passing other vessels the ship's path was along the centerline. It appears that the forces (return currents and propeller) are enough to keep deposits away from the channel centerline.

Bed samples were collected using a 3-in.- (7.62-cm-) diam drag bucket bed sampler and 1-1/2-in.- (3.81-cm-) diam push core samples. Many more samples were collected than were analyzed. In the case of the push core samples many were collected to note the type of material present. Analysis of a few representative samples was then made, rather than the entire group. Suspended sediment concentrations were collected using a 3-1/2-in.- (8.89-cm-) diam Niskin tube. The complete analysis data for calculating suspended sediment concentrations, fall velocity, erodibility parameters, bulk density, and sediment gradations are supplied in the appendix. This chapter summarizes the findings.

The shallows on the east side of the channel in the Atkinson Island reach were of coarser material than on the west side at about the same distance from the channel and depth. This can be seen from the data in Table 1 and Figure 9 that give the fraction of the sample that is silt/clay and that which is coarser (here it is referred to as sand). The samples at 090009, 112445, and 123924 on the east side of the channel show silt/clay fractions of less than 10 percent. While on the west side of the channel, stations 114554, 121418, and 123028 have silt/clay fractions of around 20 to 35 percent. The east side of the channel is exposed to somewhat greater wave forces due to the reflection caused by the presence of Atkinson Island. This would be true for vessel-produced waves in particular.

On the west side of the channel the bed material becomes progressively finer as one moves away from the channel. The progression from stations

121418, 082124, and 074151 results in silt/clay fractions of about 15, 55, and 90 percent, respectively. This could be the usual delta formation of a river moving into a bay, the larger sizes settling out sooner than the finer size particles. Of course, near the channel the vessel return currents and waves also play a part.

Table 1. Sand-silt/clay separation analysis results giving percentage of each at several points.

Sand-Silt/Clay Separation Analysis										
PROJECT: Houston Ship Channel						Analysis complete		9/22/04		
P.I.: C. Berger						Analyst: D. B.				
Sampling date: 8/20/04										
Date	Range	Time	Depth	Sed.	Tare	Gross	Pan	Net	Total sed.	Sed.
	Sta. #	CST	(ft.)	type	wt. g	wt. g	wt. g	wt. g	wt. g	%
8/20/04		090009	10.0	sand	72.75	83.10	0.1991	10.15	11.21	90.55
				silt/clay	152.25	153.11		1.06		9.45
8/20/04		093838	48.0	sand	72.42	72.50	0.0163	0.06	3.20	1.99
				silt/clay	152.67	155.79		3.14		98.01
8/20/04		112445	6.0	sand	72.07	80.79	0.1743	8.55	9.44	90.53
				silt/clay	161.82	162.54		0.89		9.47
8/20/04		114554	11.0	sand	73.06	78.99	0.3016	5.63	7.29	77.21
				silt/clay	160.96	162.32		1.66		22.79
8/20/04		121418	13.0	sand	71.96	81.39	0.4552	8.97	10.75	83.49
				silt/clay	154.82	156.14		1.78		16.51
8/20/04		123028	11.0	sand	72.60	79.85	0.8610	6.39	9.95	64.21
				silt/clay	164.28	166.98		3.56		35.79
8/20/04		123924	9.0	sand	72.18	80.33	0.1235	8.03	8.62	93.11
				silt/clay	163.78	164.25		0.59		6.89
8/22/04	Push core #1	074151	10.5	sand	88.31	89.04	0.1458	0.58	5.33	10.96
	10/26/04			silt/clay	164.40	169.00		4.75		89.04
8/22/04	Push core #3	082124	9.0	sand	88.31	94.18	1.0701	4.80	11.03	43.52
	11/2/04			silt/clay	164.40	169.56		6.23		56.48

Now consider the channel bed material. Figures 10-14 show stations 093838, 110820, 114205, 120447, and 123417, respectively. These show the sediment gradations by volume using a Coulter counter. The order of the figures begins upland in the bayou section of the Houston Ship Channel and then moves south along the channel to near the midreach of Atkinson Island. These plots show modes at about 100 microns (0.0039 in.) (very fine sand), 20 microns (0.00079 in.) (silt), and approximately 4 microns (0.00016 in.) (clays). The trend moving down the channel through these stations is a shift toward coarser material. That is, the upland stations are predominantly clays and silts. The lower stations are more sand. This trend would be consistent with material moving upland in the channel and it is known that the channel's net drift is upland. This has been noted in Bobb et al. (1973); Ward (1980); and Berger et al. (1995a). These references confirmed that over most of the lower bay channel, the drift is in the flood direction (upland) over the water column. From Bobb et. al.

(1973), at about the southern tip of Atkinson Island, the channel becomes more stratified. In this region of the channel and upland, the bottom currents are usually flood-directed while the surface currents tend to be ebb-directed. The radioactive sediment tracer study by Hart (1969) demonstrated that the sediments were moving strongly upland (flood) in the channel.

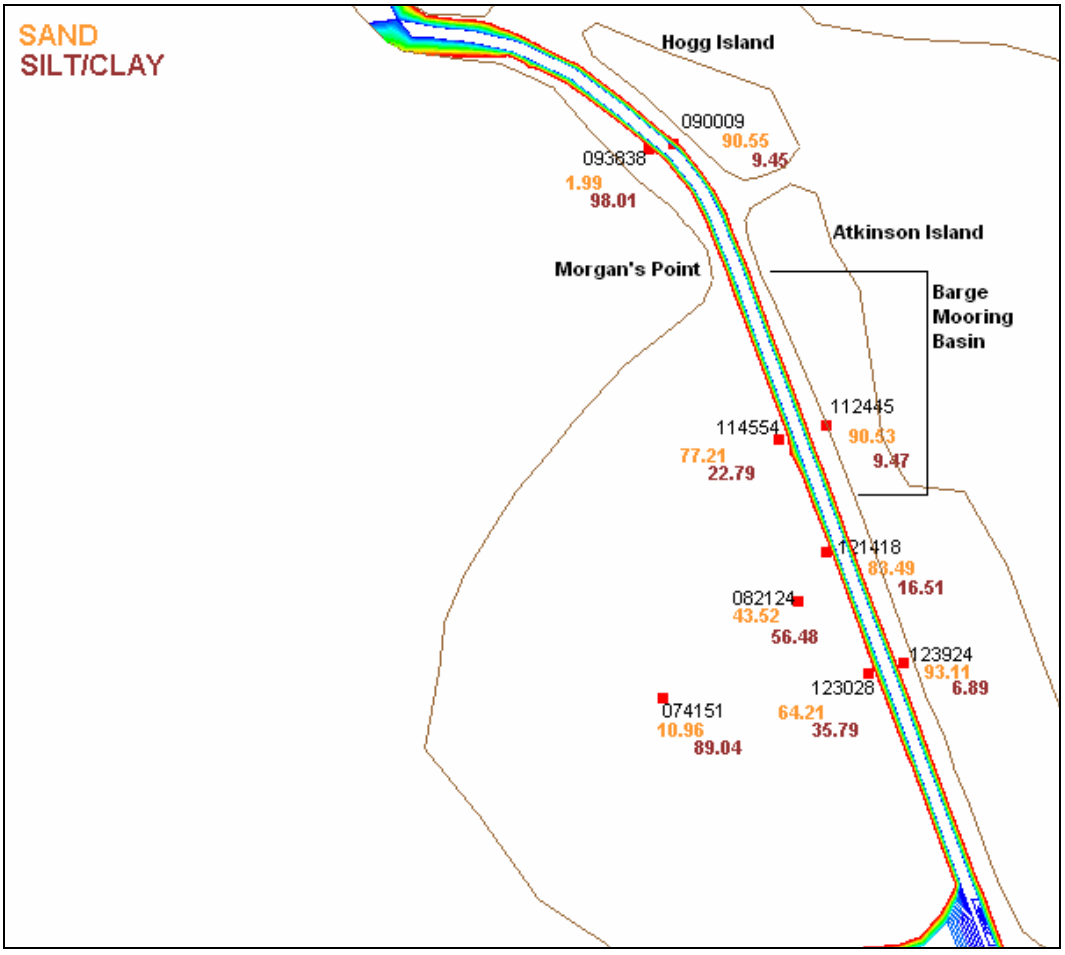

Figure 9. Grain class separation percentages for several field data points

The open bay regions in the vicinity of Atkinson Island (west of the navigation channel and also the region east of the island) contain a great deal of silts and clays. The areas exposed to ship traffic are sandier, as a likely result of natural armoring. This is noticeable at the northern tip of Atkinson Island. Along the shore to the west are shells and sands. To the east is finer material. The disposal site just south of Atkinson Island is more firm material.

Some vessels passing along the waterway created bores of about a foot in height in shallow areas. These include the area along Hogg Island and pe-

riodically along Atkinson Island. These locations were shallow and the bed material was found to be firm. Easily erodable material would have been swept away by the wave.

Stations 164015 and 163007 are shown in Figures 15 and 16, respectively. These stations are in the channel and the nearby shallows. Both show significant fine material. There is a midbay marsh site being created nearby.

Coulter® LS Particle Size Analyzer

File name:	093838	Group ID:	Houston Ship Channel
Sample ID:	093838 48 ft. 8-20-04	Location:	Range 1, channel
Operator:	DB		
Comments:	oxi. 3 times		
Optical model:	Fraunhofer.rfz		
LS 100Q	Fluid Module		

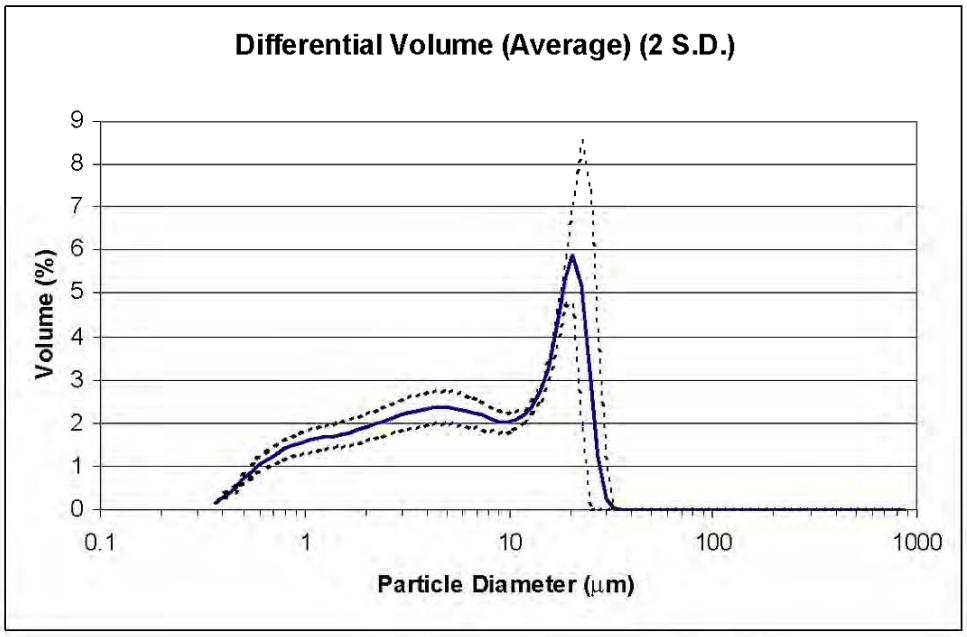

Volume Statistics (Arithmetic) 093838

Calculations from 0.375 µm to 948.3 µm

Volume:	100%		
Mean:	9.679 µm	S.D.:	8.424 µm
Median:	6.384 µm	C.V.:	87.0%
D(3,2):	2.852 µm	Skewness:	0.658 Right Skewed
Mode:	21.69 µm	Kurtosis:	-0.947 Pltykurtic

%<	10	25	50	75	90
µm	1.012	2.257	6.384	17.28	22.67

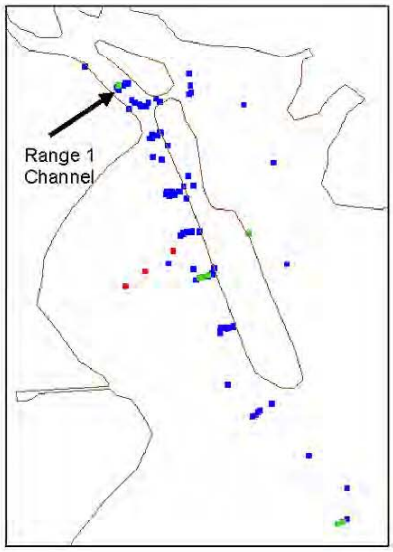

Figure 10. Coulter counter analysis for Point 093838.

Coulter® LS Particle Size Analyzer

File name:	110820	Group ID:	Houston Ship Channel
Sample ID:	110820 39 ft. 8-20-04	Location:	Range 3, channel, Morgan's Point
Operator:	DB		
Comments:	oxi. 3 times		
Optical model:	Fraunhofer.rfz		
LS 100Q	Fluid Module		

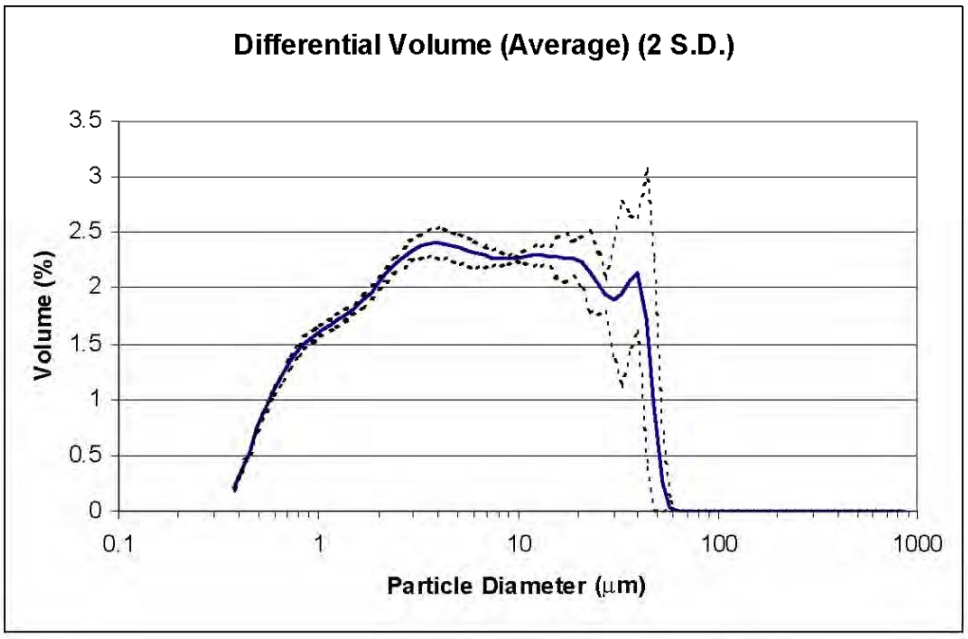

Volume Statistics (Arithmetic) 110820

Calculations from 0.375 µm to 948.3 µm

Volume:	100%		
Mean:	11.30 µm	S.D.:	12.44 µm
Median:	5.914 µm	C.V.:	110%
D(3,2):	2.776 µm	Skewness:	1.445 Right Skewed
Mode:	4.047 µm	Kurtosis:	1.251 Leptokurtic

%<	10	25	50	75	90
µm	0.990	2.164	5.914	16.43	31.62

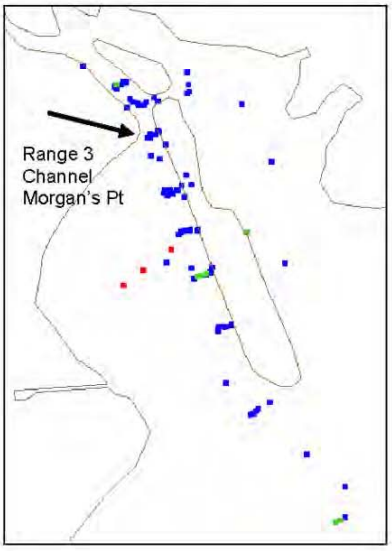

Figure 11. Coulter counter analysis for Point 110820.

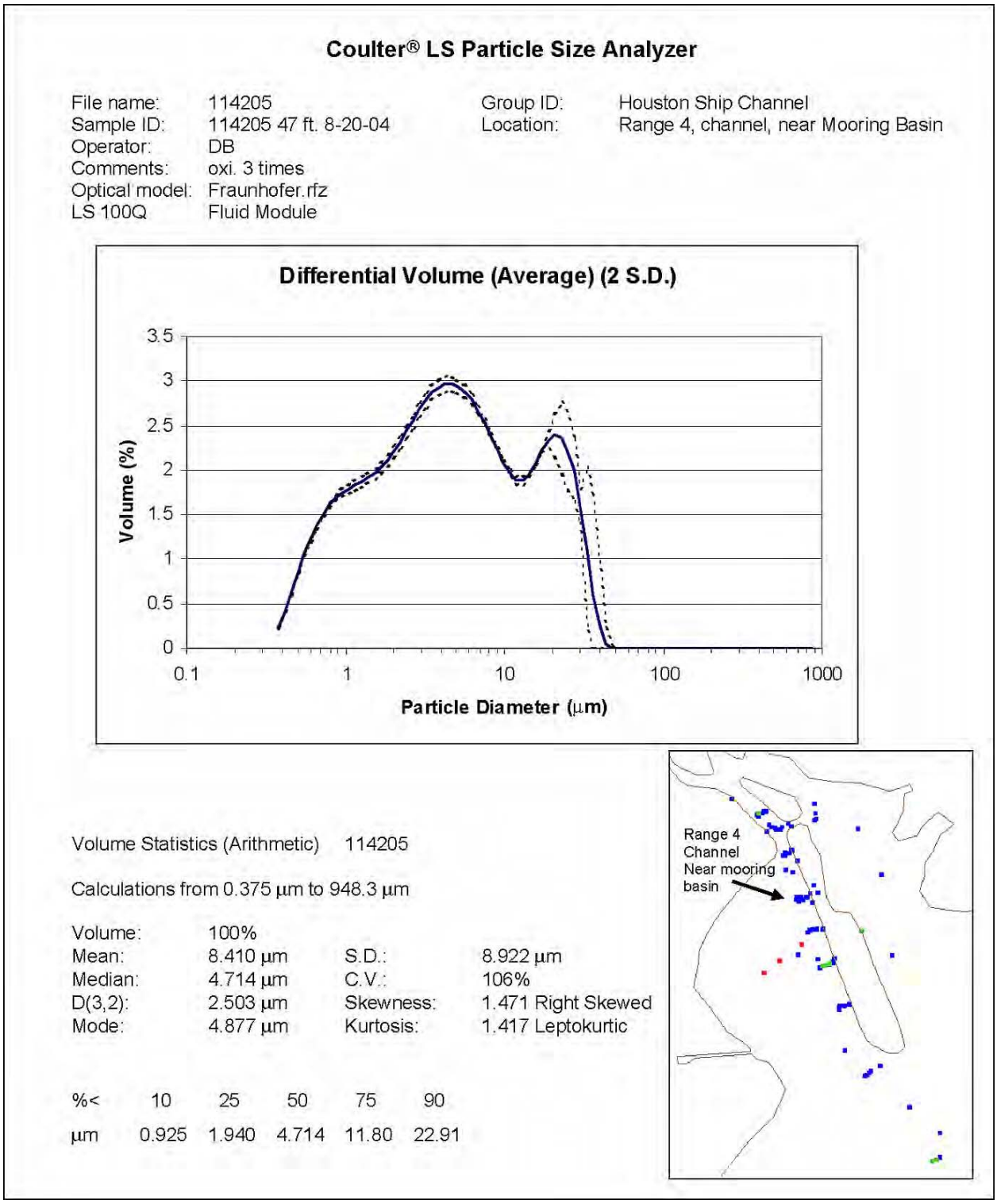

Figure 12. Coulter counter analysis for Point 114205.

Coulter® LS Particle Size Analyzer

File name:	120447	Group ID:	Houston Ship Channel
Sample ID:	120447 37 ft. 8-20-04	Location:	Range 5, channel
Operator:	DB		
Comments:	oxi. 3 times		
Optical model:	Fraunhofer.rfz		
LS 100Q	Fluid Module		

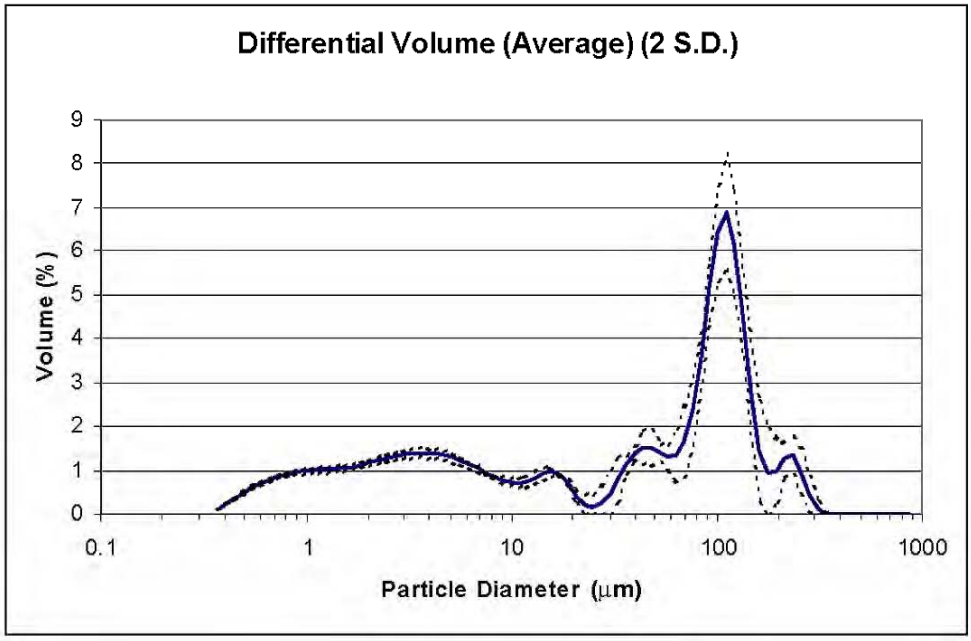

Volume Statistics (Arithmetic) 120447

Calculations from 0.375 µm to 948.3 µm

Volume:	100%		
Mean:	68.61 µm	S.D.:	67.74 µm
Median:	55.97 µm	C.V.:	98.7%
D(3,2):	4.623 µm	Skewness:	0.899 Right Skewed
Mode:	116.3 µm	Kurtosis:	0.429 Leptokurtic

%<	10	25	50	75	90
µm	1.386	4.311	55.97	115.3	147.8

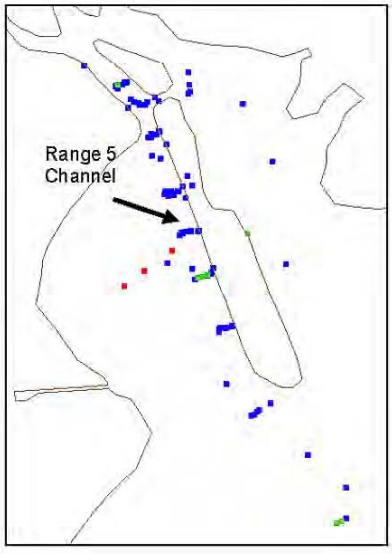

Figure 13. Coulter counter analysis for Point 120447.

Coulter® LS Particle Size Analyzer

File name:	123417	Group ID:	Houston Ship Channel
Sample ID:	123417 39 ft. 8-20-04	Location:	Range 6, channel
Operator:	DB		
Comments:	oxi. 3 times		
Optical model:	Fraunhofer.rfz		
LS 100Q	Fluid Module		

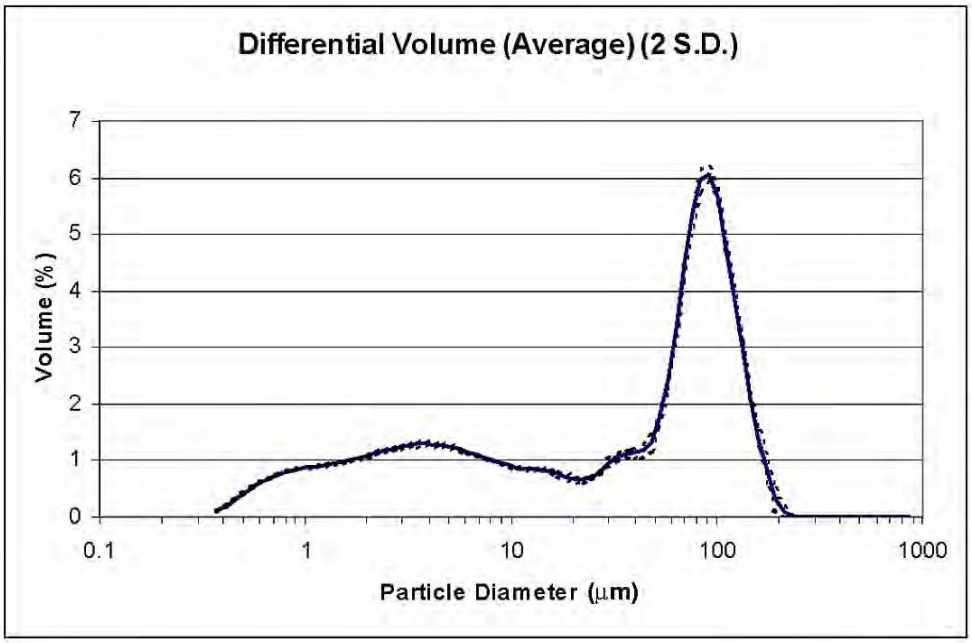

Volume Statistics (Arithmetic) 123417

Calculations from 0.375 µm to 948.3 µm

Volume:	100%		
Mean:	57.19 µm	S.D.:	50.91 µm
Median:	55.14 µm	C.V.:	89%
D(3,2):	5.072 µm	Skewness:	0.483 Right Skewed
Mode:	96.49 µm	Kurtosis:	-0.801 Platykurtic

%<	10	25	50	75	90
µm	1.567	5.135	56.14	96.51	126.2

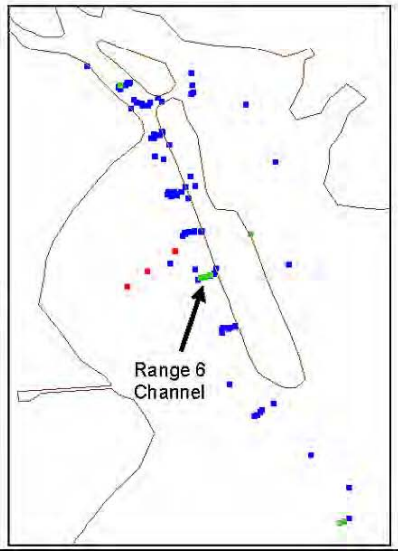

Figure 14. Coulter counter analysis for Point 123417.

Coulter® LS Particle Size Analyzer

File name:	164015	Group ID:	Houston Ship Channel
Sample ID:	164015 51 ft. 8-21-04	Location:	Channel, near marsh site
Operator:	DB		
Comments:	oxi. 3 times		
Optical model:	Fraunhofer.rfz		
LS 100Q	Fluid Module		

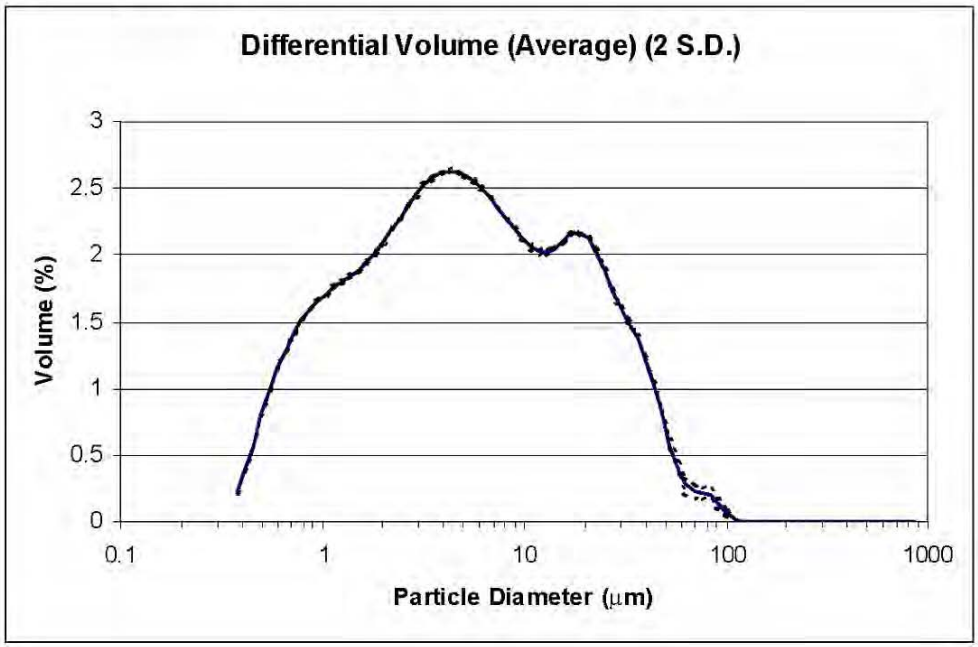

Volume Statistics (Arithmetic) 164015

Calculations from 0.375 µm to 948.3 µm

Volume:	100%		
Mean:	11.11 µm	S.D.:	14.18 µm
Median:	5.314 µm	C.V.:	128%
D(3,2):	2.657 µm	Skewness:	2.460 Right Skewed
Mode:	4.443 µm	Kurtosis:	7.947 Leptokurtic

%<	10	25	50	75	90
µm	0.959	2.054	5.314	14.88	29.56

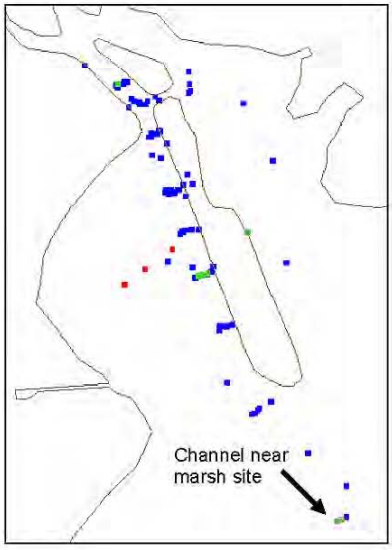

Figure 15. Coulter counter for Point 164015.

Coulter® LS Particle Size Analyzer

File name:	163007	Group ID:	Houston Ship Channel
Sample ID:	163007 13 ft. 8-21-04	Location:	East shallows, near marsh site
Operator:	DB		
Comments:	oxi. 3 times		
Optical model:	Fraunhofer.rfz		
LS 100Q	Fluid Module		

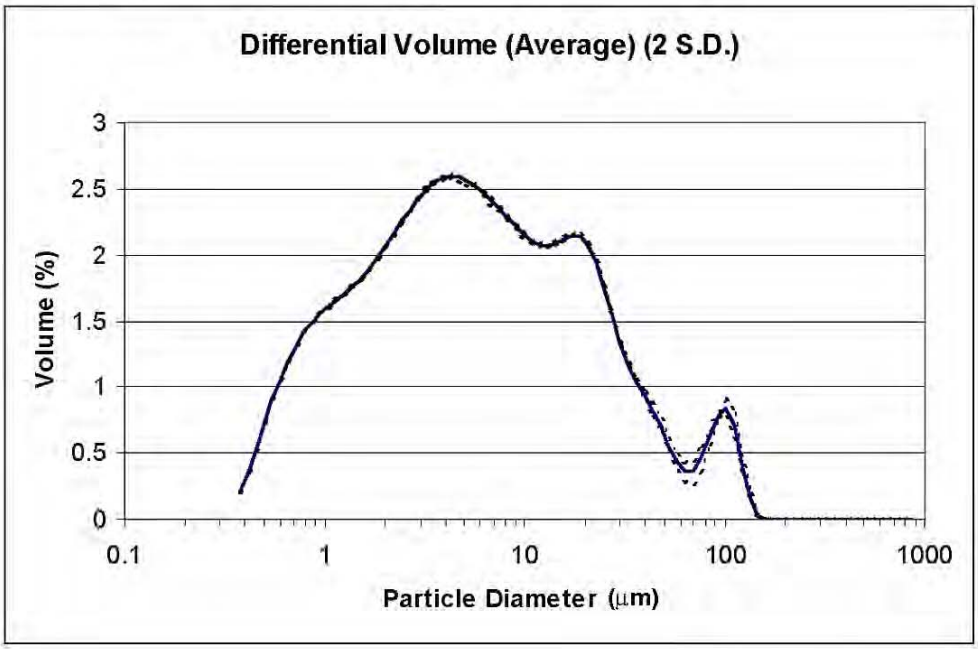

Volume Statistics (Arithmetic) 163007

Calculations from 0.375 µm to 948.3 µm

Volume:	100%		
Mean:	14.15 µm	S.D.:	22.42 µm
Median:	5.654 µm	C.V.:	158%
D(3,2):	2.784 µm	Skewness:	3.072 Right Skewed
Mode:	4.443 µm	Kurtosis:	10.23 Leptokurtic

%<	10	25	50	75	90
µm	1.001	2.182	5.654	15.97	34.14

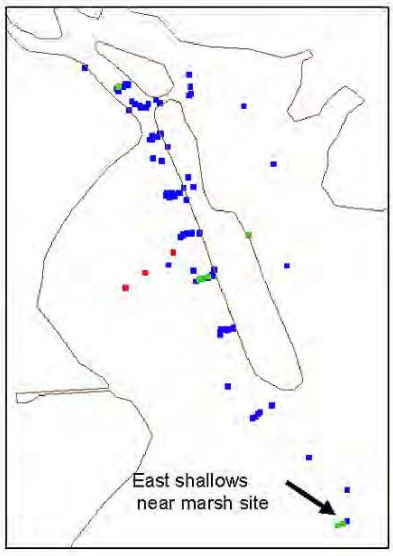

Figure 16. Coulter counter for Point 163007.

Surveys of the region have shown that material spreads a considerable distance from the midbay marsh site and appears to be entering the channel, so these fines may be from that location. However, they could be from the large sources to the east and west of the channel, and unrelated to this marsh site.

4 Vessel Effects on Sediment Suspension

In this chapter, the influence of the enlarged channel on the speeds attainable by vessels in the Houston-Galveston Navigation Channel is examined. This investigation compares the same vessels in the previous and current configurations using a typical cross section for each. The year 1990 configuration of the bay part of the Houston Ship Channel consists of a 40-ft (12.2-m) mlw depth and a 400-ft (122-m) base width. It is assumed that the side slopes are 1Vertical:7Horizontal up to a depth at mlw of 10 ft (3 m). For the enlarged channel (which is the present configuration) the depth is 45-ft (13.7-m) mlw and 530-ft (162-m) base width. The same side slope and ultimate depth at the shoulder of 10-ft (3-m) mlw is used. The first section estimates the drawdown and return currents due to moving vessels, then describes this impact to the waterway. The second section estimates the erosion due to vessel passage.

Vessel Hydrodynamics in Houston Ship Channel

The equations developed by Jansen and Shijf (1953) are used to calculate the cross-section average return current and drawdown. The section containing just the channel center section and the side slopes is treated as the cross section and does not consider the surrounding shallows of the bay. This equation is actually just Bernoulli's energy equation about the vessel along with conservation of mass. The two equations are as follows:

$$z = \frac{(V_s + V_r)^2 - V_s^2}{2g}$$

$$V_s A_c = (V_r + V_s) A_w \tag{1}$$

where:

z = the drawdown

V_s = the speed of the vessel relative to a fixed reference frame

V_r = the return current

g = the acceleration due to gravity

A_c = the cross-sectional area in front of the vessel

A_w = the cross-sectional area at midlength of the vessel.

This method assumes uniformity over a cross-section, no friction losses, and zero ambient currents.

Maynord (2005b) recorded vessel speeds along with water data in the channel near Atkinson Island. This vessel data will be used as an indicator of vessels that demonstrated strong hydraulic impacts. Table 2 contains information on these vessels.

Table 2. Description of vessel dimensions found to be hydraulically significant in Houston Ship Channel near Atkinson Island.

Boat Number	Length, ft (m)	Beam, ft (m)	Draft, ft (m)
1	760 (232)	106 (32.3)	30.5 (9.30)
2	760 (232)	140 (42.7)	30.5 (9.30)
3	899 (274)	180 (54.9)	34.6 (10.5)

This section calculates the maximum ship velocity, V_{max}, for the two channels. This is the maximum speed attainable, however, this is fuel inefficient. The speed that is typically used is about 85 percent of the maximum. Table 3 records the drawdown, return current, and the depth h_{cr} at which the Froude number is 1 for this ship speed. h_{cr} then is just equal to $\frac{V_s^2}{g}$.

Table 3. Effect of channel size on vessel speed, drawdown, return current, and critical depth.

Boat	Channel, ft (m)	V_{max}, f/s (m/s)	85 percent V_{max}			
			V_s, f/s (knots)	z, ft (m)	V_r, f/s (m/s)	h_{cr}, ft (m)
1	40X400 (12.2X122)	17.3 (5.27)	14.7 (8.7)	1.5 (0.46)	3.0 (0.91)	6.7 (2.04)
	45X530 (13.7X162)	20.4 (6.22)	17.3 (10.2)	1.4 (0.43)	2.5 (0.76)	9.3 (2.84)
2	40X400 (12.2X122)	15.4 (4.70)	13.1 (7.8)	1.6 (0.49)	3.5 (1.07)	5.3 (1.62)
	45X530 (13.7X162)	18.5 (5.64)	15.7 (9.3)	1.6 (0.49)	2.9 (0.88)	7.7 (2.35)
3	40X400 (12.2X122)	12.4 (3.78)	10.5 (6.2)	1.6 (0.49)	4.2 (1.28)	4.8 (1.46)
	45X530 (13.7X162)	15.5 (4.73)	13.2 (7.8)	1.7 (0.52)	3.6 (1.10)	5.4 (1.65)

The important point of this table is that the larger channel allows the vessels to travel faster. The vessel can travel faster in the channel than a free surface wave can travel in the surrounding shallows. If the shallows have a depth less than h_{cr} then a bore will be formed. The enlarged channel lowers the return current magnitude and had little impact on the drawdown. However, since the vessels can move faster in the larger channel, the critical depth is much deeper. Therefore ships will produce bores from the drawdown over a number of the surrounding shallows.

The importance of this effect is that the measured shoaling has shown a significant increase since the channel was deepened. Since the deepened channel has only been in place a short time, there is little certainty whether this is going to be the typical shoaling rate or if this is within the variability found in dredging requirements. There is ample evidence that there is erosion of shoreline and shallow regions, which seems to have been going on even before the channel was enlarged. Examples are the erosion of Goat Island (Maynord 2000) and also the islands separating the barge mooring basin (Maynord 2005a) from the main channel. If the increased deposition results from vessel-induced shoreline erosion, then one would expect this to decline over time as the nearby areas are eroded and naturally armored.

Effects of Vessels on Shoaling

As a vessel moves along the waterway, it creates a drawdown and a return current around the vessel. The return currents will create a stress on the bed that can cause erosion. These periods of erosion will reduce the longer term channel deposition. The increased channel size could decrease the stress caused by the vessel passage and result in an apparent increase in channel shoaling. The propeller may also create erosion. However, in this analysis only cross-sectional effects of the vessel body are determined (not including the propeller effects). To perform this analysis, the estimated return currents for the largest of the three previously mentioned vessels, information from the analysis of the field collected sediment, and a crude estimate of ship traffic are utilized. This analysis will show how significant the vessel traffic may be on the actual deposition in the channel for the two channel configurations.

The bed shear stress is estimated using the quadratic relationship

$$\tau_b = \tfrac{1}{2} C_f \rho V^2 \quad (2)$$

where:

C_f = a coefficient of friction
ρ = density
V = velocity

The value of C_f depends upon the nature of the velocity being used. If the velocity is the near-bed velocity the coefficient can be large. In this case, the velocity is a cross-section average value and the coefficient is relatively small. For established open channel flow, the coefficient is about 0.005 (Maynord 2005b). However, in this case, the boundary layer is quite thin since the flow profile does not have time to reach a quasi-steady condition. In this case Maynord (2005b) recommends using C_f =0.01. Using this coefficient one now estimates the shear stress for the largest vessel in the two channel configurations (see Table 4).

Table 4. Erosion rate for a vessel passage.

Channel Condition	Return Current (m/s) (V_r)	Shear Stress (Pa) (τ_b)	Erosion per passage (m) (d_s)
Base	1.3	8.5	8.8×10^{-6}
Plan	1.1	6.1	4.6×10^{-6}

The coefficients needed to calculate the impact upon sedimentation are derived from the field sediment data collection. Figure 17 shows the erosion rate compared to the shear stress at push core sta 1 in the bay west of the Houston Ship Channel. From inspection, the critical shear stress for erosion, τ_{ce} (see Partheniades 1962), is about 1.0 Pa.

The erosion rate, K_e, is calculated to be $6.8x10^{-6} \frac{Kg}{m^2 x\ s\ x\ Pa}$ from this figure as the slope of the line between 0.97 Pa and 1.14 Pa. Assume that the dry sediment density, ρ_s, is 500 kg/m^3. The depth of erosion per vessel passage, d_s, is calculated using the following equation.

$$d_s = \frac{1}{\rho_s} \int_0^{t_p} K_e (\tau_b - \tau_{ce}) dt \quad (3)$$

where

τ_b = bed stress
t_p = time of passage

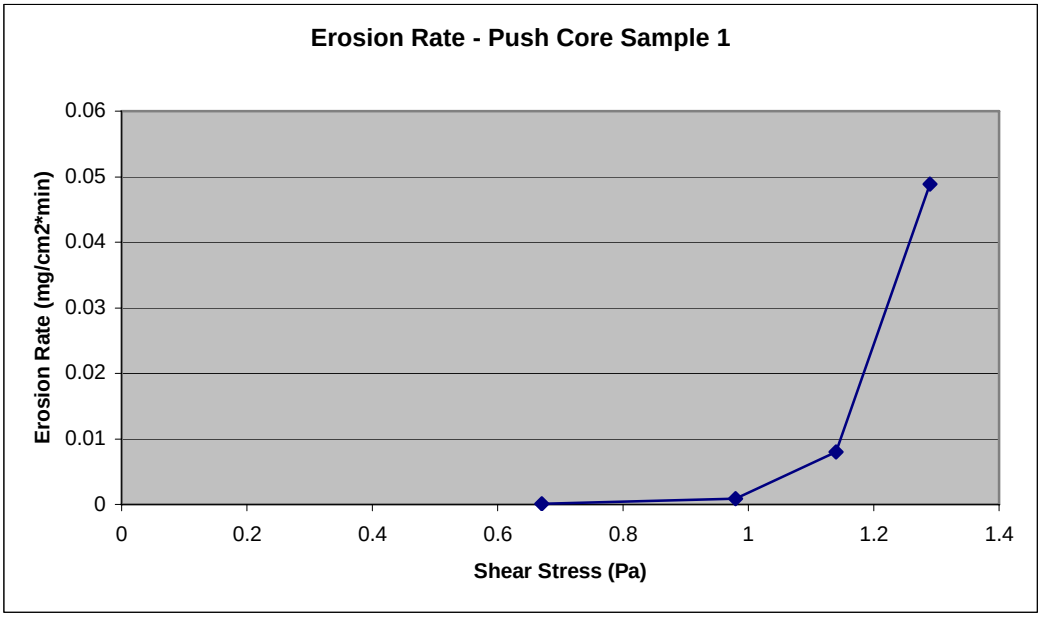

Figure 17. Erosion rate versus shear stress field results.

This time of passage, t_p, is the length of time the bed is subject to the stress. In this case it is assumed to be the length of the vessel divided by the speed of the vessel. All the terms are assumed to be a constant. The results are shown in the last column of Table 4. From the 2004 records of the Port of Houston (Dept. of the Army 2006) there were 4280 passages of vessels with a draft of 30 ft or more in this year. Using 4280 passages in a year the total erosion for base conditions would be about 0.04 meters per year and for the plan condition about 0.02 meters per year. The dredging records suggest that channel deposition in the upper bay is on the order of 0.4 meters per year. This would suggest that the increase in apparent shoaling due to the reduced stress of the return currents associated with the vessel passage is on the order of 5%. This does not include the fact that larger vessels will utilize the larger channel thus making this effect even less. The analysis does not include erosion caused by the ship propeller. It has been noted in the field data section that the center of the channel has maintained its "as built" condition. The channel edges however have shoaled considerably. This is most likely a result of the vessel propeller with some influence from the vessel return currents. Our estimate of the erosion caused by ship passage alone only accounts for about 0.02 meters

of increased deposition annually. Therefore, the difference in vessel erosion in the channel with the two different channel sizes doesn't appear to be large enough to explain the deposition rate shown in the enlarged channel.

5 Numerical Model Simulation and Analysis

This chapter details the model study analysis of the hydrodynamics and a sediment tracer in Galveston Bay, TX. TABS-MDS is the finite element numerical model used for this investigation, which models three-dimensional (3-D) hydrodynamics and salinity as well as suspended sediment transport and bed changes. This model has been widely used by ERDC to model 3-D hydrodynamics and salinity at numerous locations, including Galveston Bay (Berger et al. 1995a,b). Numerical model simulations were performed for both the original 40- x 400-ft (12.2- x 122-m) channel and the 45- x 530-ft (13.7- x 162-m) channel. The enlarged channel dimensions are nominally 45- x 530-ft (13.7- x 162-m); however, actual surveys were used and the depth for the 45-ft- (13.7-m-) deep channel is typically about 49 ft (14.9 m) mlw at the channel centerline. Initial runs were made simulating hydrodynamic effects only in order to determine residual shear stresses on the bed. These stresses give an indication of any changes in the bed due to velocity variations among the two channel configurations. Sediment conditions were then added to the simulations. These runs do not represent a full sediment simulation of the model domain, but rather give an estimate of where suspended sediment travels and settles given the grain characteristics, model hydrodynamics, and wind induced wave effects.

Experimental Conditions

The model conditions use the present low-flow and medium-flow hydrologic eras from the previous investigations. The river inflows for the Trinity River and San Jacinto River were included in the model conditions. The tidal boundary data were from NOS/NOAA sta 877-1510 at Pleasure Pier for the calendar year 1984, which was a typical temperature year. The model boundary, located 26 miles (42 km) offshore, was applied by shifting these data in time by 1.31 hr to match the phase at Pleasure Pier. Periods of less than 3 hr were removed by filtering in order to prevent noise in the results. Wind data from 1984 were obtained from the National Weather Service for Houston Intercontinental Airport. These data were transposed to the bay system after a correlation with field data collected for the prior studies. Gulf boundary salinities are based on 15-year monthly averages for the Gulf and the initial salinity field was taken from the final salinity field produced in the verification runs. For a detailed description of the experimental conditions, see Berger et al. 1995b.

Analysis of Model Currents

This section describes the residual shear stresses in Galveston Bay in and around the Houston Ship Channel for the conditions of the 40-ft- (12.2-m-) deep by 400-ft- (122-m-) wide channel and for the new channel configuration of 45-ft- (13.7-m-) deep by 530-ft- (162-m-) wide. It also estimates a shoaling volume for the two channel configurations. The 40- x 400-ft (12.2- x 122-m) channel is termed the "base" conditions and the 45- x 530-ft (13.7- x 162-m), the “plan” conditions. The 40- x 400-ft (12.2- x 122-m) channel existed in Galveston Bay from the early 1960's into the late 1990's. At that time the channel was enlarged to the plan conditions. The enlarged channel has shown a significant increase in required dredging. Planners need to know if this new increased dredging requirement is a permanent feature or is the shoaling going to return to the earlier channel dredging rates. Typically the dredging rate is elevated while new construction is taking place. This results from leakage from the dredging operation and placement as well as the channel shoulder instability. As a part of that evaluation, the currents from the 3-D model of the bay are analyzed to determine if the currents have changed enough to produce the increase in sedimentation.

An indicator of the average shear stress (the velocity squared) is plotted for a few representative months, made for the near-bed conditions only. A location map for use in this chapter is shown in Figure 18.

Monthly Shear Residuals

These residual shear stresses are given by month. The shear stress values indicate the direction that material in periodic contact with the bed would tend to move. They also reflect the direction that suspended sediment moves and are offered as a means to understand the major hydrodynamic features of the bay sediment movement before launching a full sediment model.

These shear residuals are actually the mean velocity squared for each month. This is calculated as follows:

$$\overline{\mathbf{S}} \equiv \frac{\int_0^T \left(\mathrm{u}(\mathrm{t})\mathbf{i} + v(t)\mathbf{j}\right)\left|\mathbf{V}(t)\right| dt}{T} \tag{4}$$

where:

$$\mathbf{V} \equiv u(t)\mathbf{i} + v(t)\mathbf{j}$$

T = time period over which the residual is being evaluated.

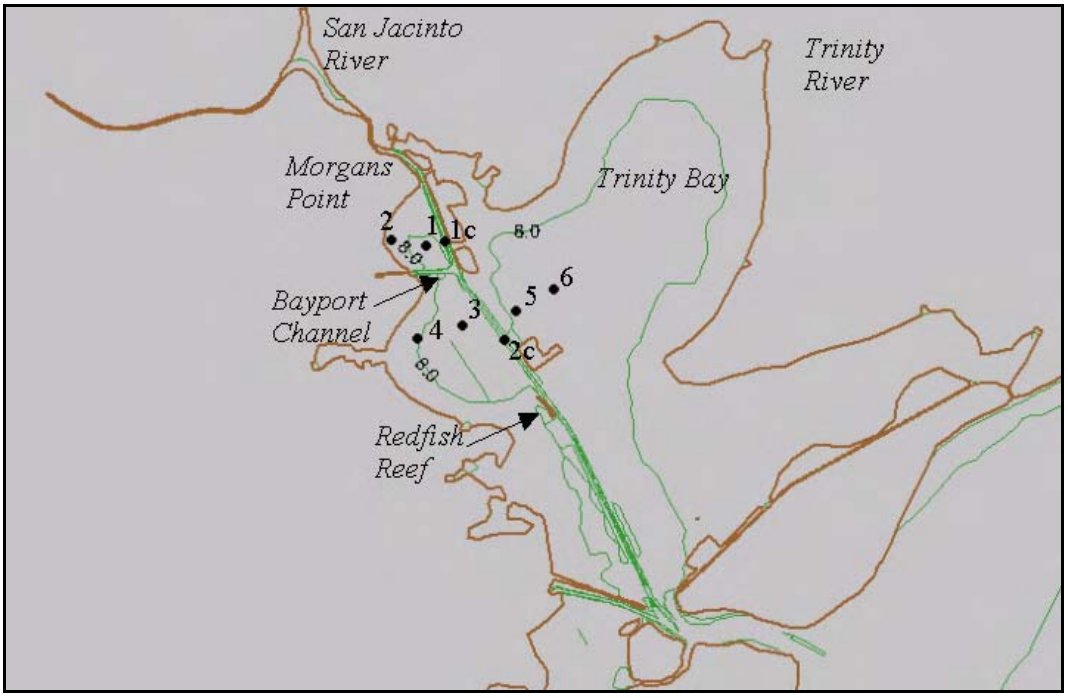

Figure 18. Location map of Galveston Bay, showing depth contours and velocity point data locations.

The runs used in the analysis were yearlong simulations. However, the first few months are used to let the system adjust from initial conditions. The salinity is slower to acclimate than are the water-surface elevations and currents. Allowing the first 3 months for this spin-up period, and since the months of November and December are much like October, only April through October are included. Figures 19 through 32 contain the midbay residual shear results and Figures 33 through 46 show those for the upper bay.

First consider the midbay shear residual for the 40- x 400-ft (12.2- x 122-m) channel in Figures 19-25. April shows a strong flood residual shear. This weakens in May, but is still flood-oriented. June and July have strong ebb residual shear down to about Redfish Reef, where the residual shear is very small. One might expect sediment accumulation in this region, at this time. August through October show a return to flood-directed shear.

The midbay shear residual for the 45- x 530-ft (13.7- x 162-m) channel is shown in Figures 26-32. All months show flood oriented shear residuals. However, they are weak in June and are strong in April, September, and October. There is also some noticeable shear shown in the shallows during September and October around the midbay marsh site.

In the upper bay, the shear residual for the 40- x 400-ft (12.2- x 122-m) channel is shown in Figures 33-39. The April pattern is for a strong flood residual in the channel, except near the Bayport Channel flare where the residual is essentially zero. The shallows near the channel tend to have an ebb residual shear. The May pattern is a weak version of April. June and July have ebb residual shear in the channel. There is also a flood shear residual on the western edge of the bay in the shallows. In the subsequent months the pattern returns to that of April, though weakly in August.

The upper bay shear residual for the 45- x 530-ft (13.7- x 162-m) channel is shown in Figures 40-46. The April pattern shows a strong flood residual in the channel, a dead area near the Bayport Channel flare, and an ebb residual in the shallows near the channel. This pattern is similar for the other months, but is weak during June and strengthens in later months.

Figure 47 shows the total freshwater inflow to Galveston Bay in these model tests. Figure 48 shows the salinity used at the Gulf boundary during these runs. A more in-depth explanation for these particular boundary conditions is found in Berger et al. (1995b). This is a simulated low freshwater flow year. Therefore, the saltwater is not being pushed out of the bay. In fact, the salinity in the upper Galveston Bay is around 15 ppt during the June-July period for the 40- x 400-ft (12.2- x 122-m) channel.

What appears to actually be the cause for the difference of the June and July shear directions for both the channel and the shallows is the drop in Gulf salinity to a minimum at mid-May. This drop in salinity results in an evacuation of saline water from the bay. The salt water is retreating from the deeper areas, such as the channel. When this salt water is exiting the bay, it is being replaced with fresher water moving upland in the shallows. This is reversed from the normal pattern of ebb directed shears in the shallows and flood directed net shears in the channel.

Individual Shear Locations

The results at eight individual locations throughout the bay and channel are shown in Figures 49-72. Locations 1 through 6 are distributed in the

upper bay. Locations 1C and 2C are in the channel. Each figure shows the percentage of time for which the velocity squared is exceeded. While the solutions were calculated over a year, the months of April, June, and October were used as indicators and they are shown in these figures. For the months of April and June the currents were generally reduced as a result of the channel enlargement. This is particularly true in the channel. It is also noted that at the stations farther from the channel (Points 2, 4, and 6) the reduction in currents is more than the near channel stations (Points 1, 3, and 5). It is important to note that for April and June, the near-bed channel currents have been reduced. This could lead to increased deposition. For all points, the October currents did not vary greatly between the two channel configurations.

Generally, the Houston Ship Channel within Galveston Bay is flood-directed shear. However, for the base conditions in the months of June and July, the shear is ebb-directed in the northern portion of the bay channel. This period of ebb-dominated shear is likely due to the drop in salinity in the model ocean. The dense water is then tending to evacuate the system. The period of low salinity at the Gulf of Mexico is due to the freshwater currents from the Atchafalaya and Mississippi Rivers. For the other months and for the plan channel the bed shear is flood-directed. In June and July the plan condition shears are flood-directed, but much less strongly.

The area around the junction of the Bayport Channel and the Houston Ship Channel shows a disrupted shear pattern. The shear is low in the flare for the Bayport Channel but also in the Houston Ship Channel in that location. This does not appear when the shear is ebb-directed, but it does whenever the shear is flood-directed. There is a bend in the Houston Ship Channel just south of this junction that may be the cause.

The shear at several individual locations is presented. Of particular interest are two channel stations that show that the enlarged channel results in reduced shear. This reduction in shear should result in an increase in deposition.

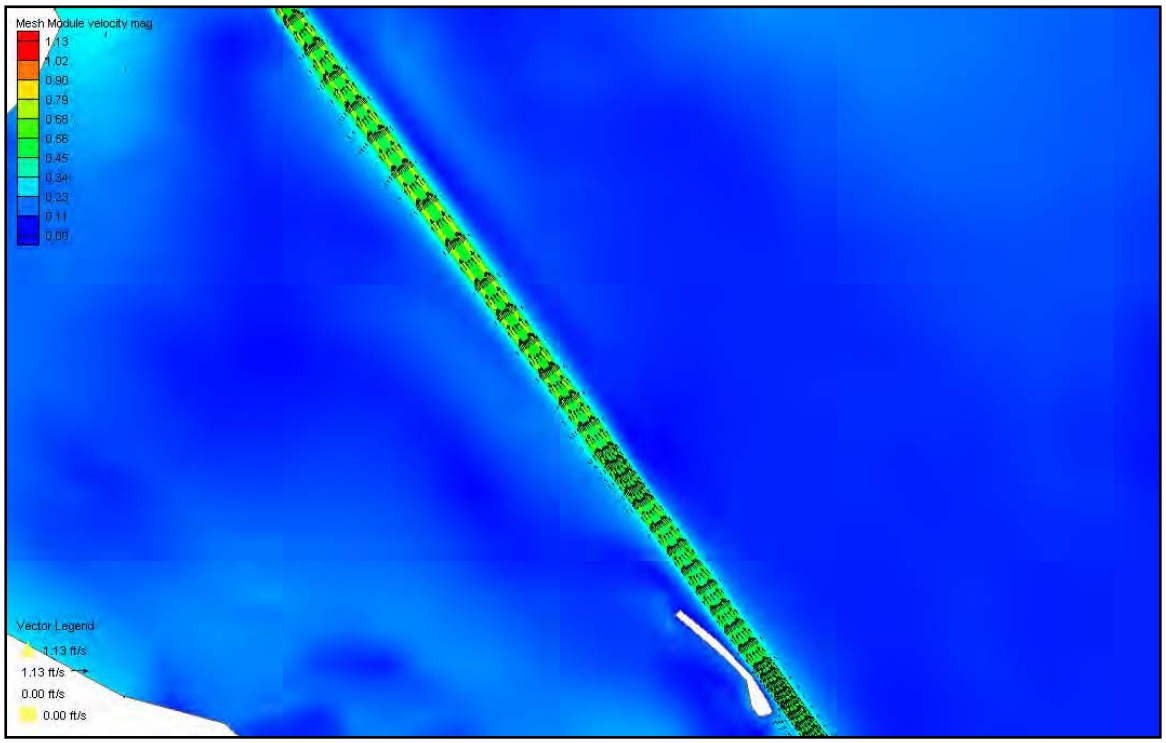

Figure 19. April, midbay, bottom depth, 40X400 channel, residual shear.

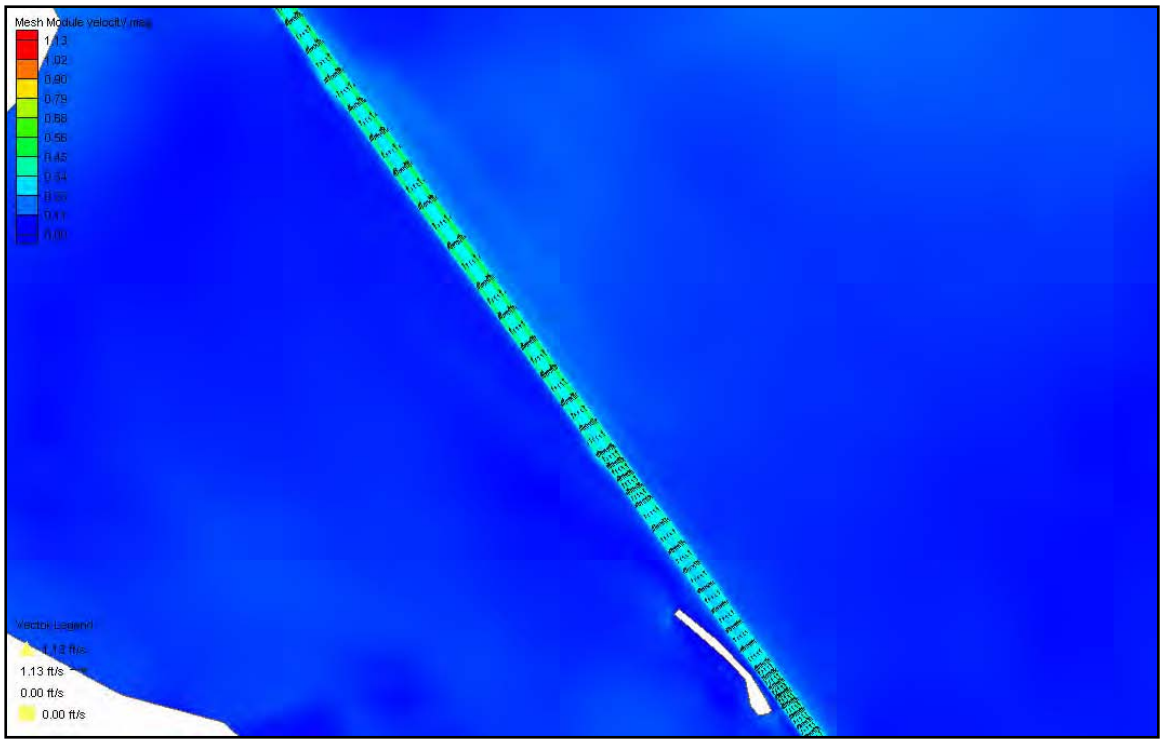

Figure 20. May, midbay, bottom depth, 40X400 channel, residual shear.

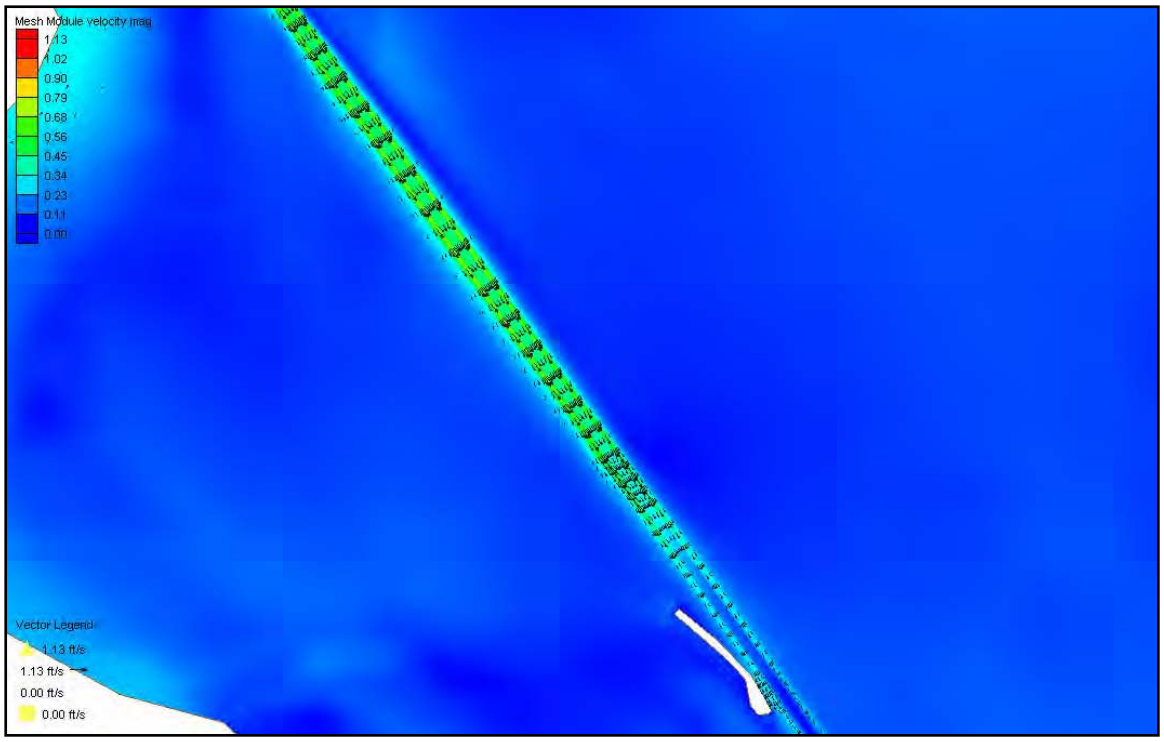

Figure 21. June, midbay, bottom depth, 40X400 channel, residual shear.

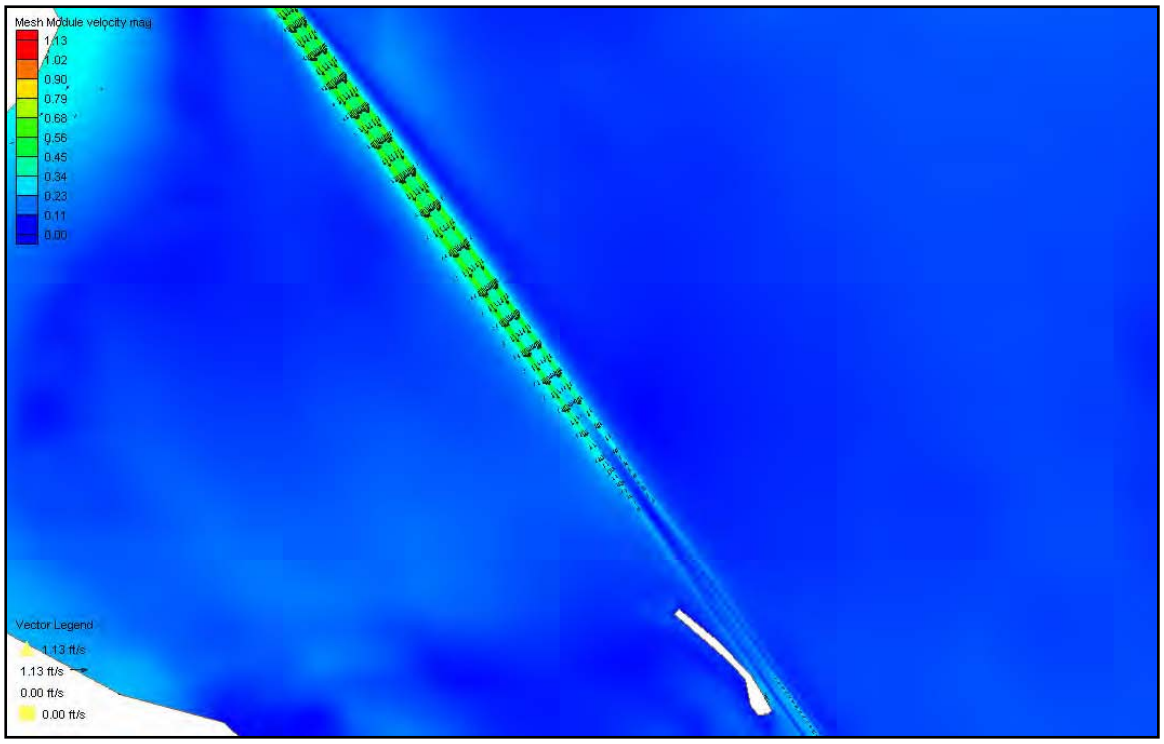

Figure 22. July, midbay, bottom depth, 40X400 channel, residual shear.

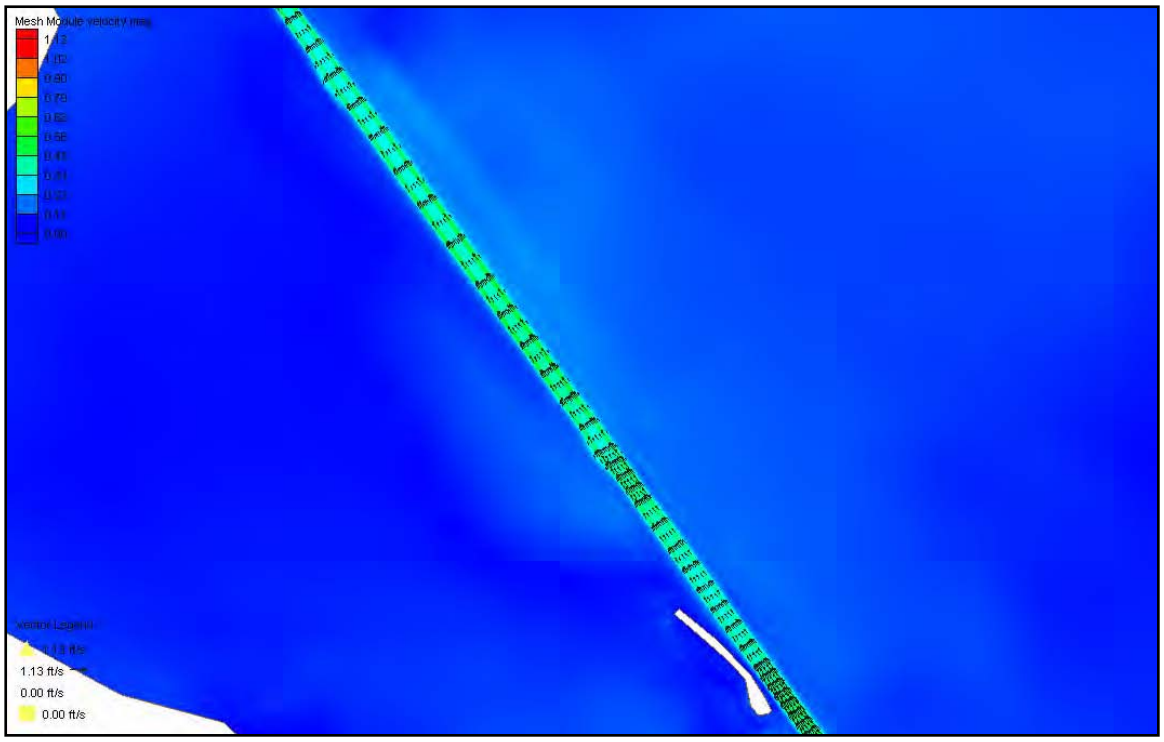

Figure 23. August, midbay, bottom depth, 40X400 channel, residual shear.

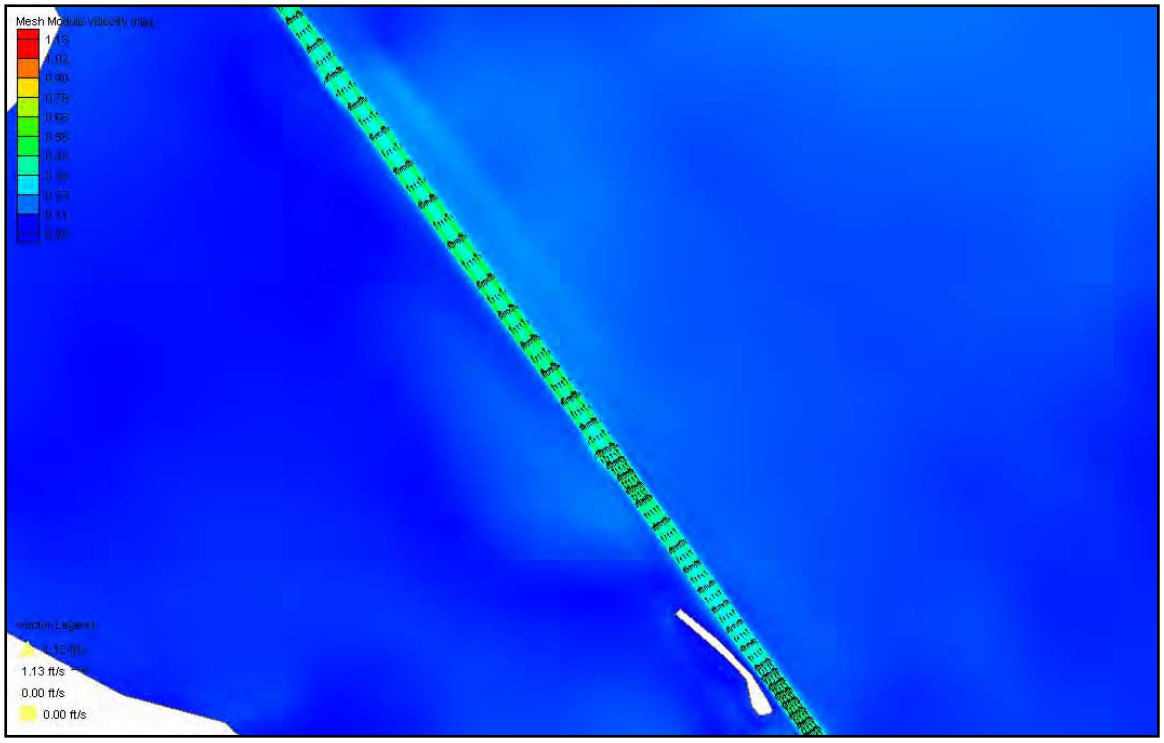

Figure 24. September, midbay, bottom depth, 40X400 channel, residual shear.

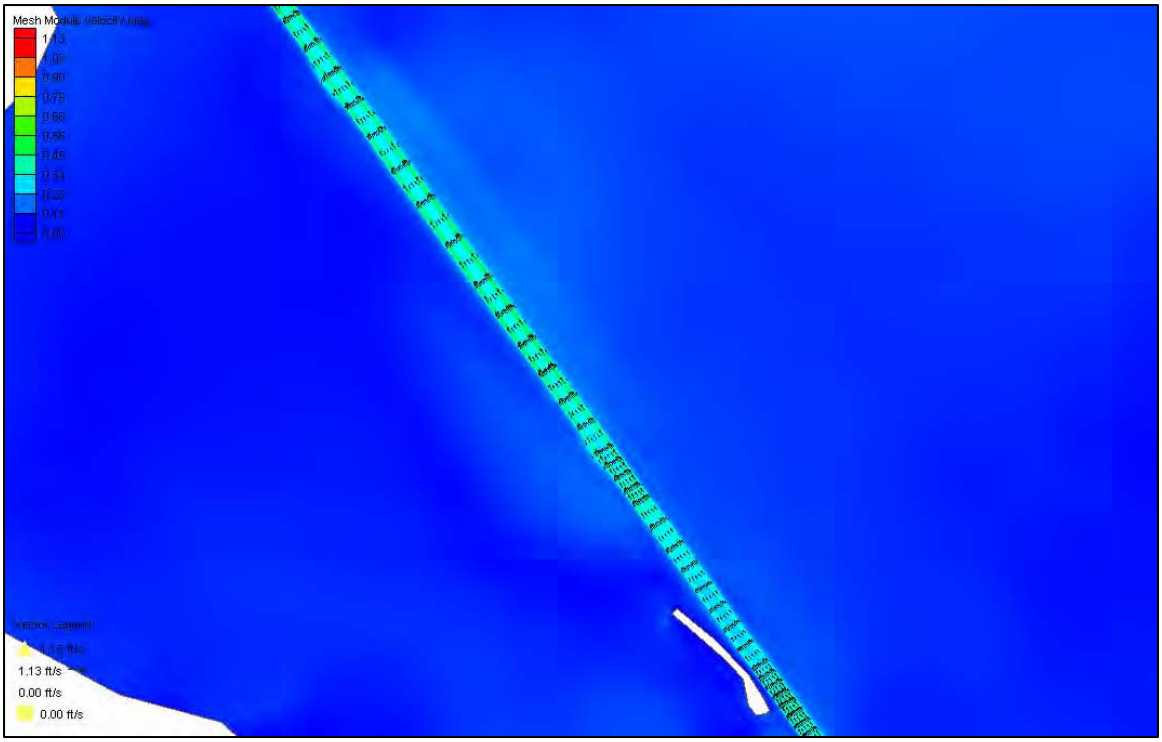

Figure 25. October, midbay, bottom depth, 40X400 channel, residual shear.

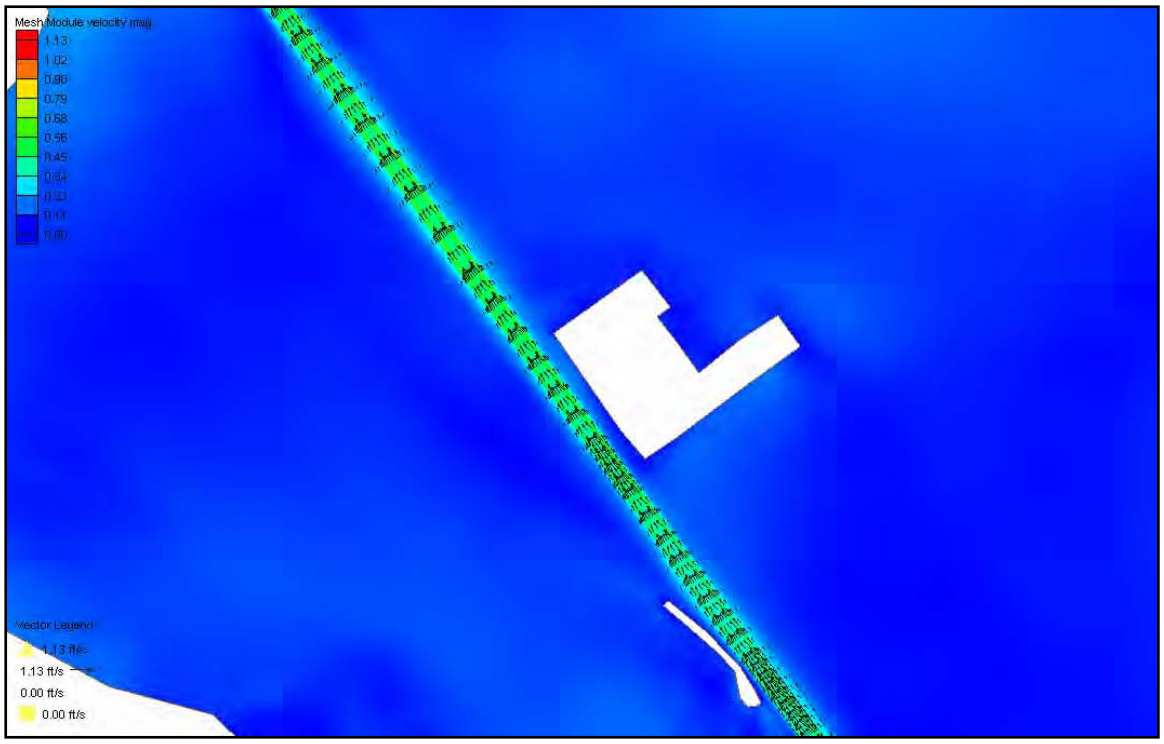

Figure 26. April, midbay, bottom depth, 45X530 channel, residual shear.

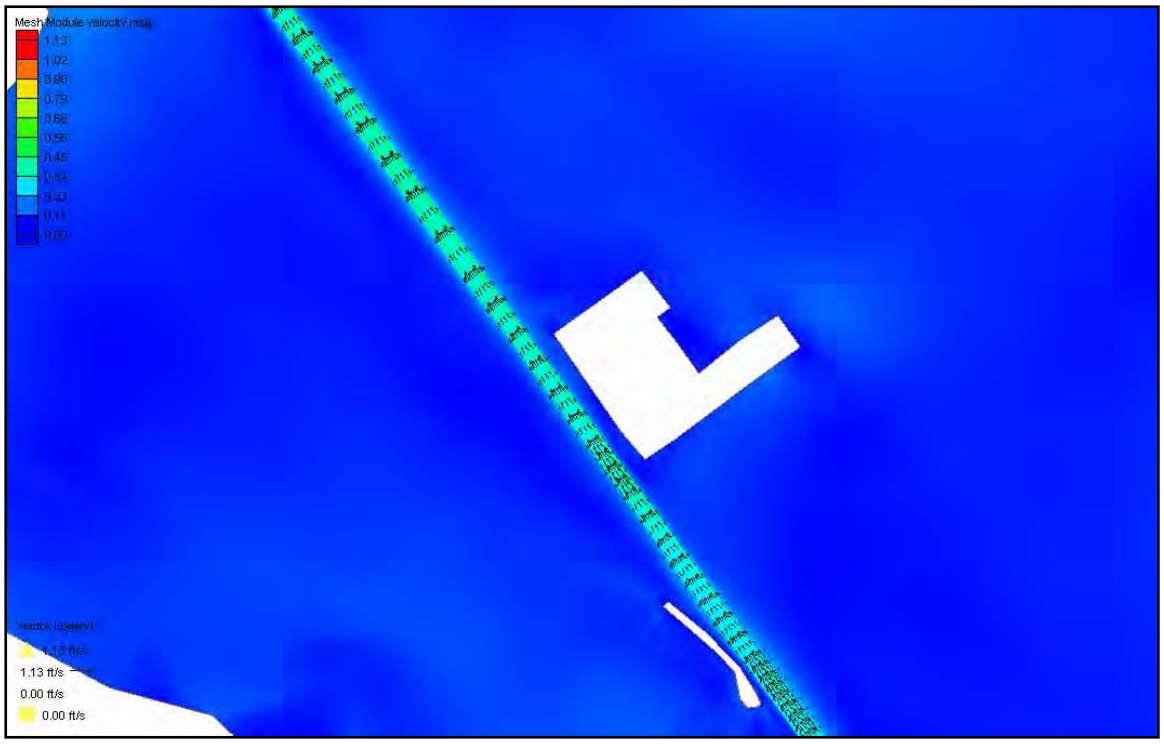

Figure 27. May, midbay, bottom depth, 45X530 channel, residual shear.

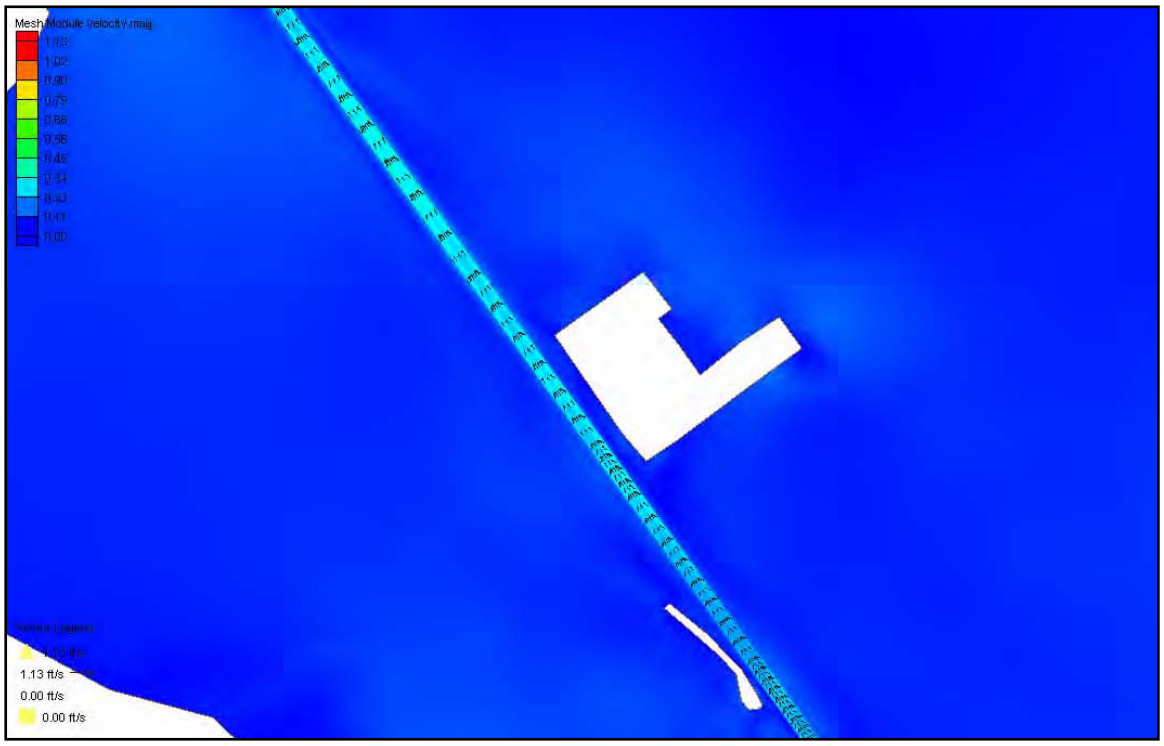

Figure 28. June, midbay, bottom depth, 45X530 channel, residual shear.

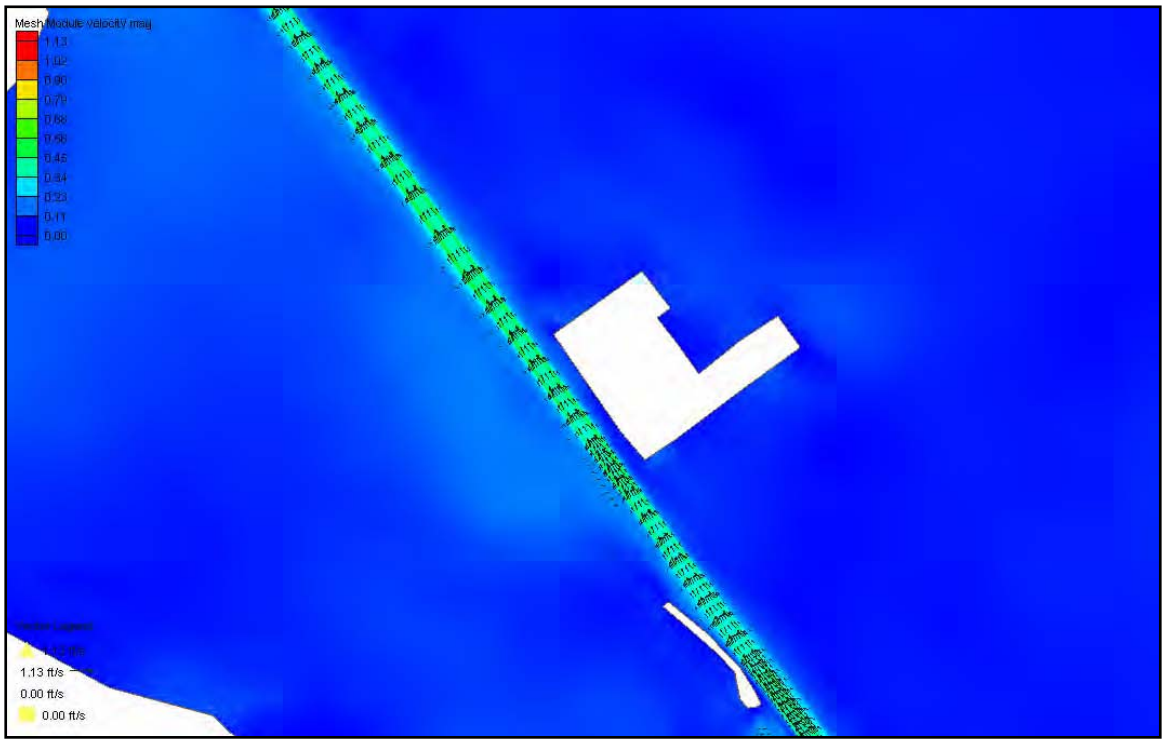

Figure 29. July, midbay, bottom depth, 45X530 channel, residual shear.

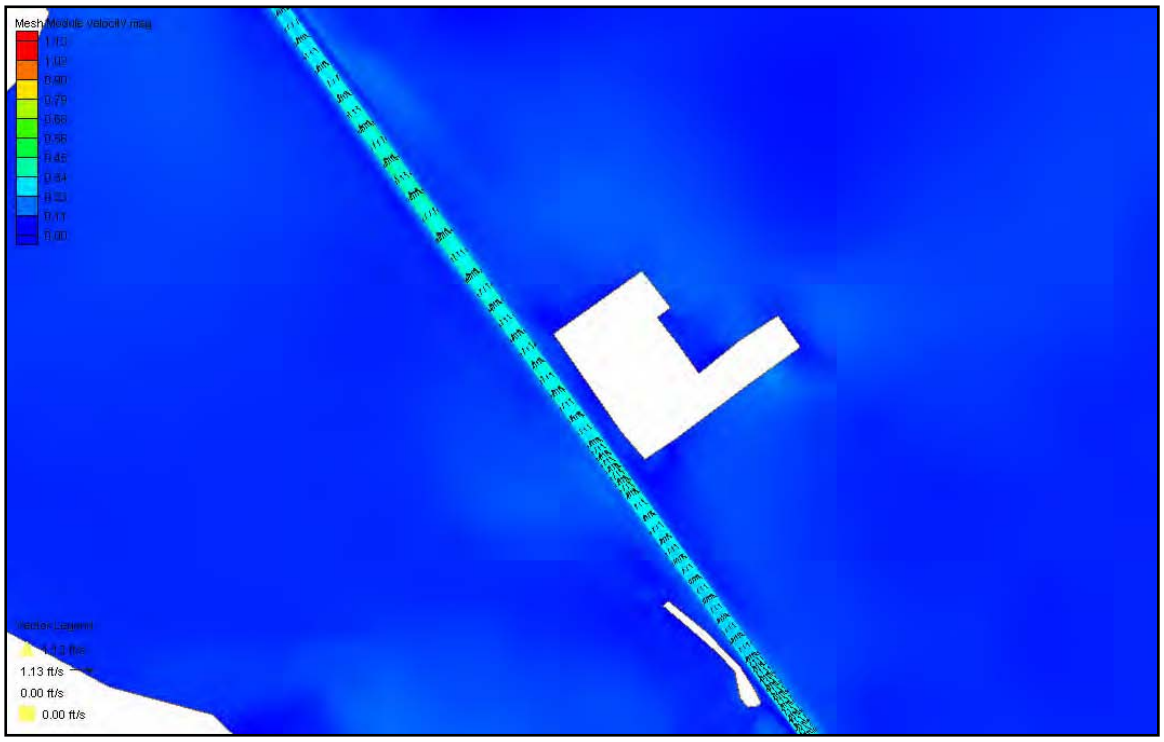

Figure 30. August, midbay, bottom depth, 45X530 channel, residual shear.

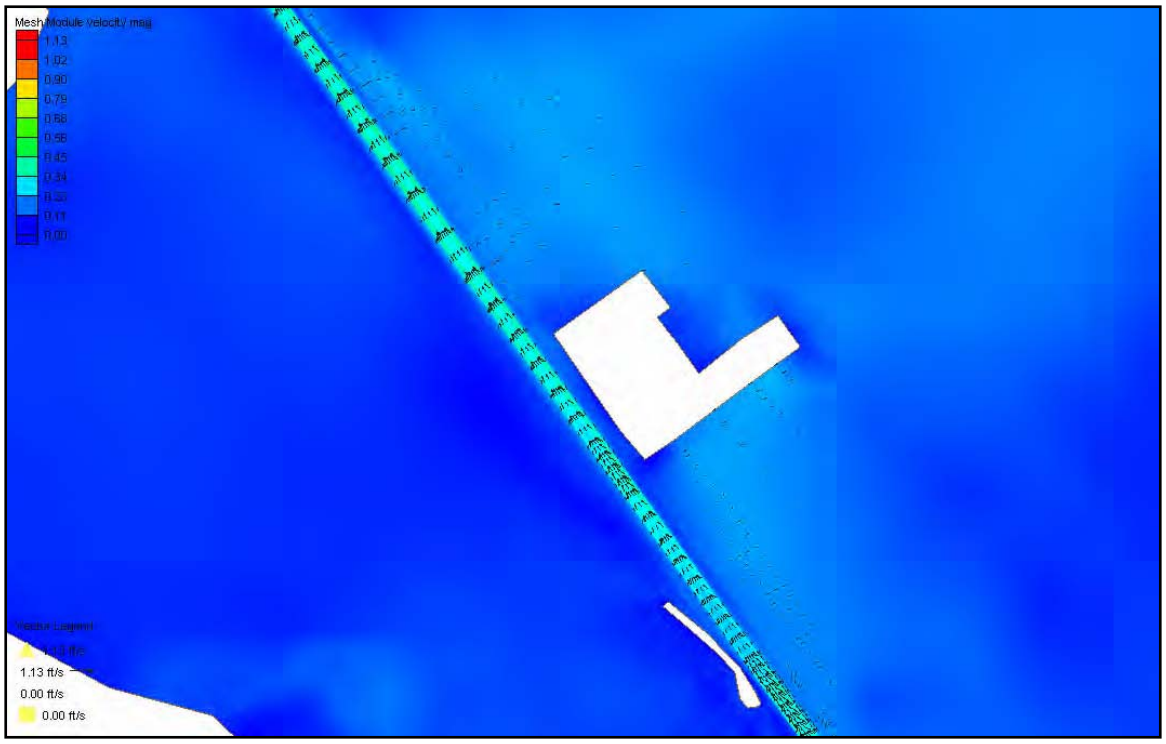

Figure 31. September, midbay, bottom depth, 45X530 channel, residual shear.

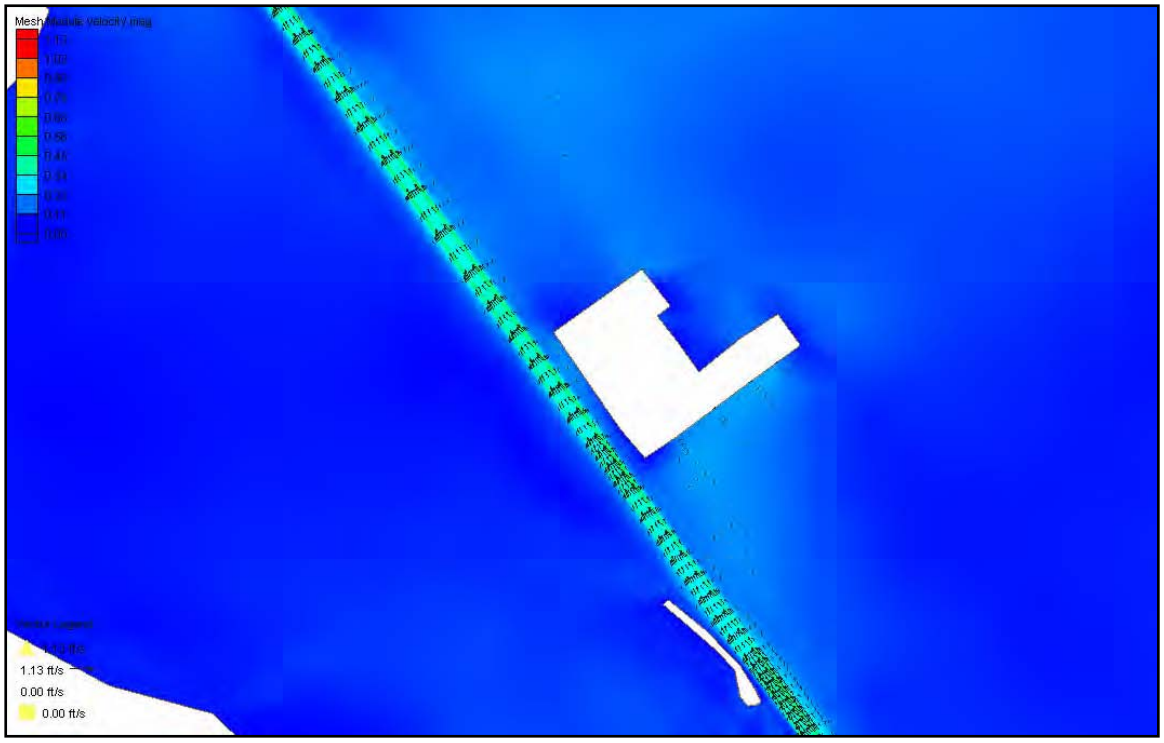

Figure 32. October, midbay, bottom depth, 45X530 channel, residual shear.

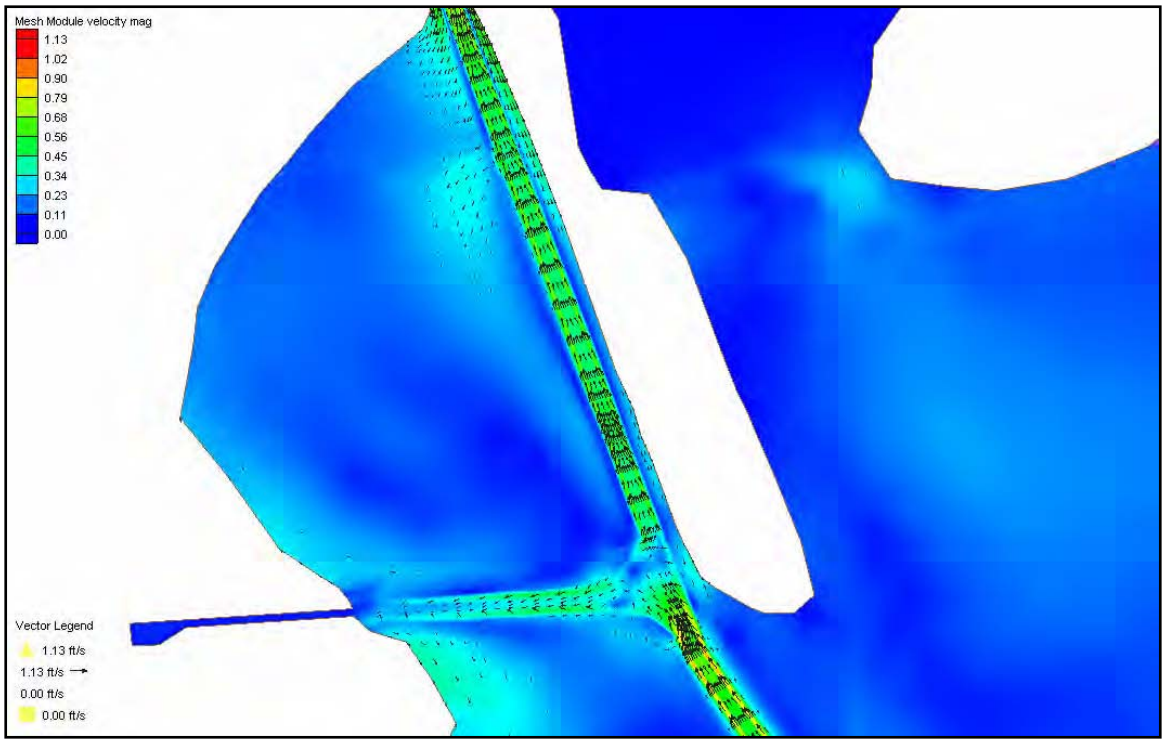

Figure 33. April, upper bay, bottom depth, 40X400 channel, residual shear.

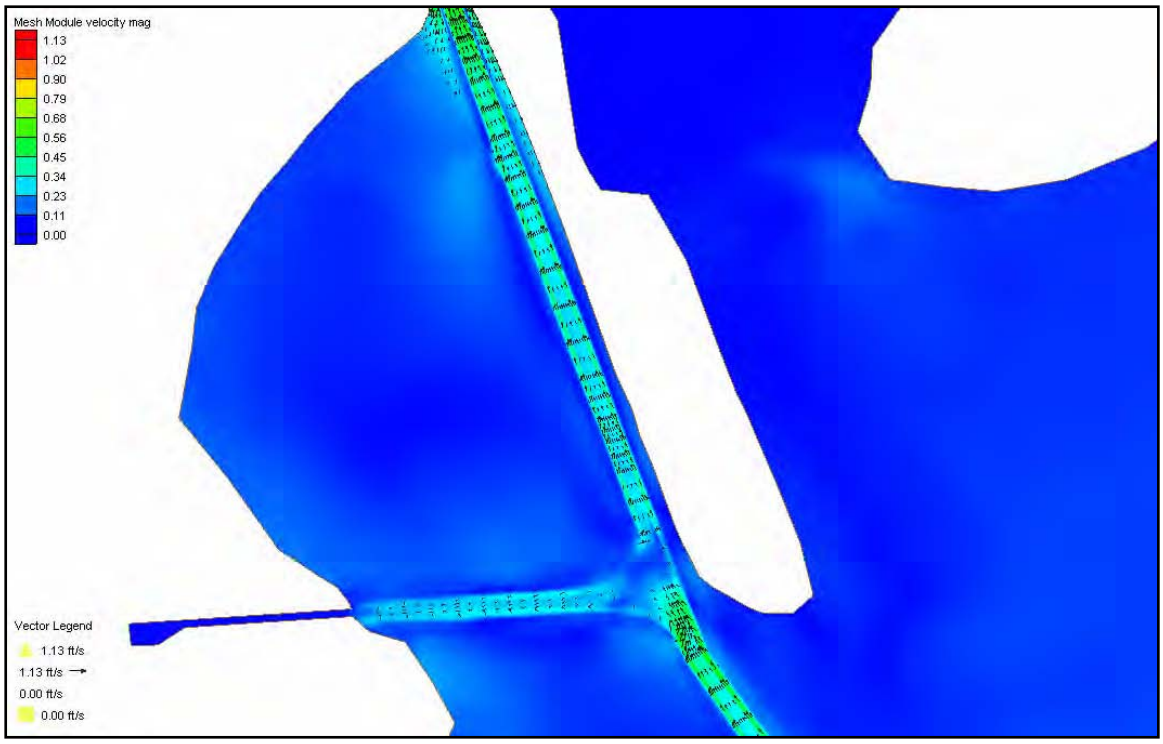

Figure 34. May, upper bay, bottom depth, 40X400 channel, residual shear.

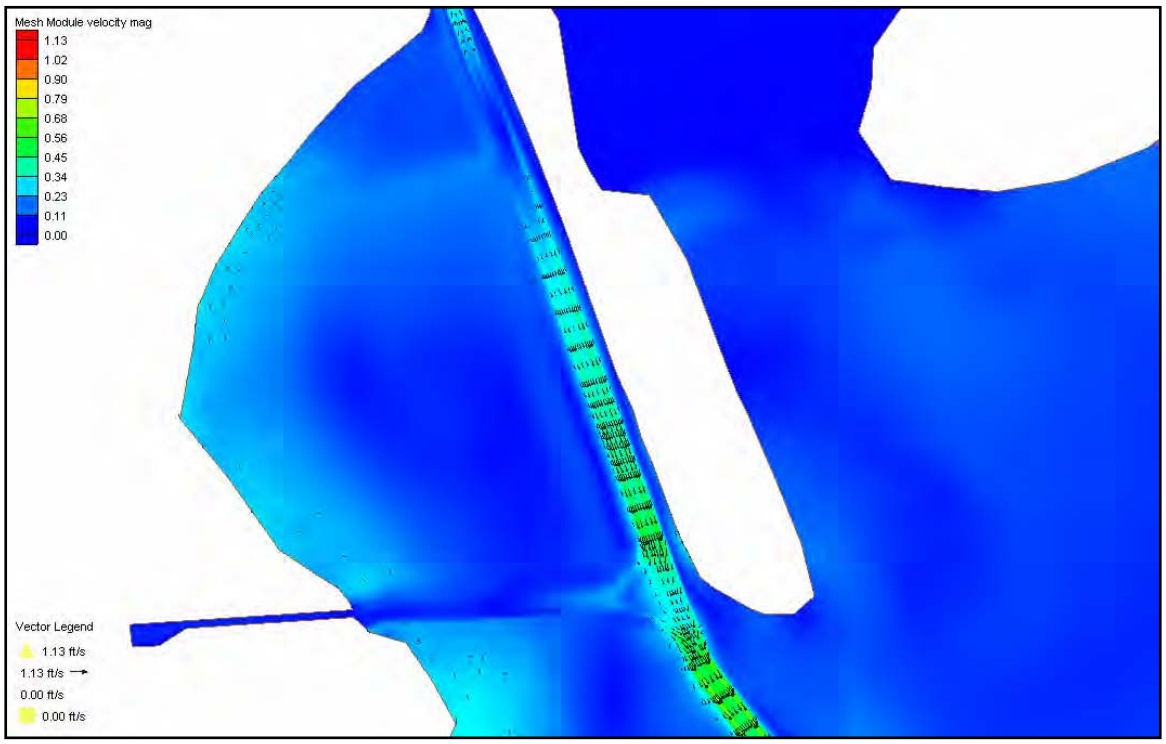

Figure 35. June, upper bay, bottom depth, 40X400 channel, residual shear.

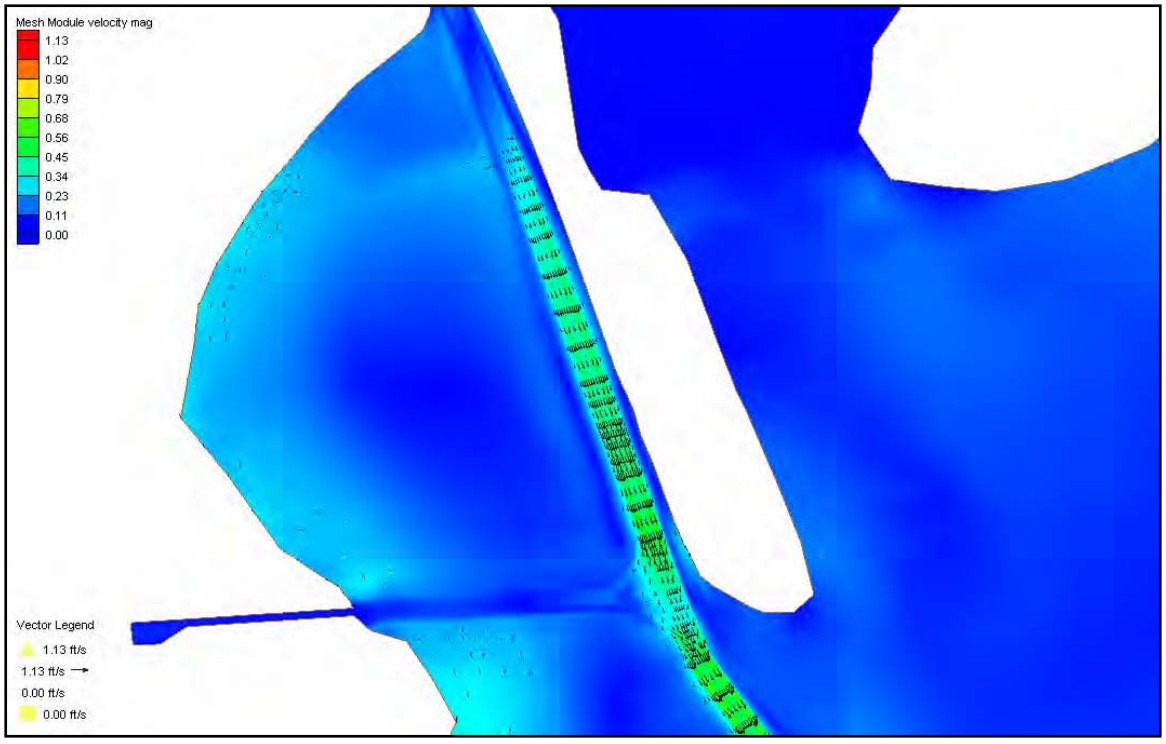

Figure 36. July, upper bay, bottom depth, 40X400 channel, residual shear.

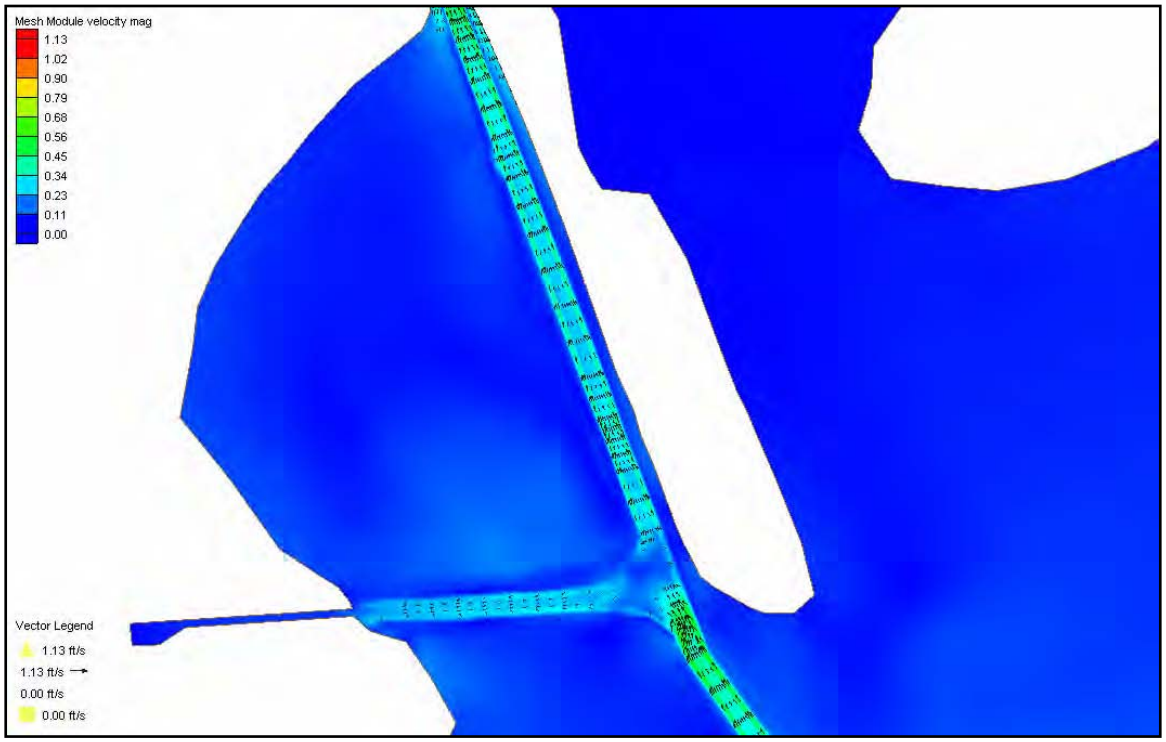

Figure 37. August, upper bay, bottom depth, 40X400 channel, residual shear.

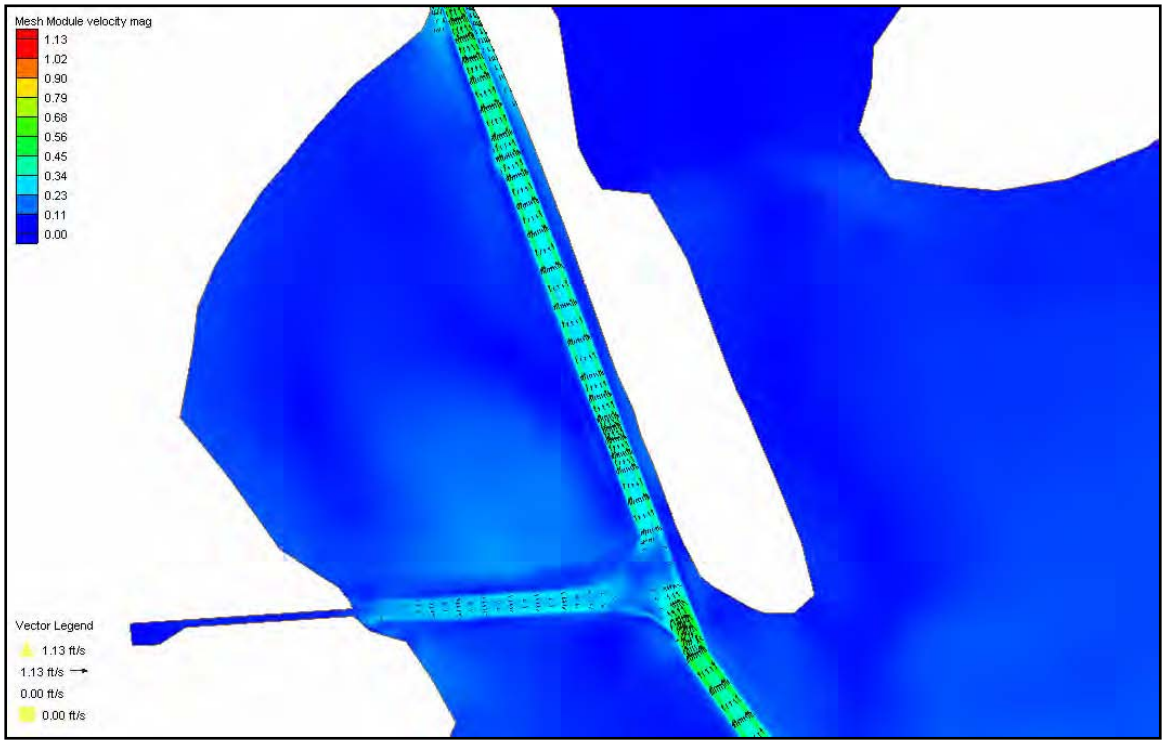

Figure 38. September, upper bay, bottom depth, 40X400 channel, residual shear.

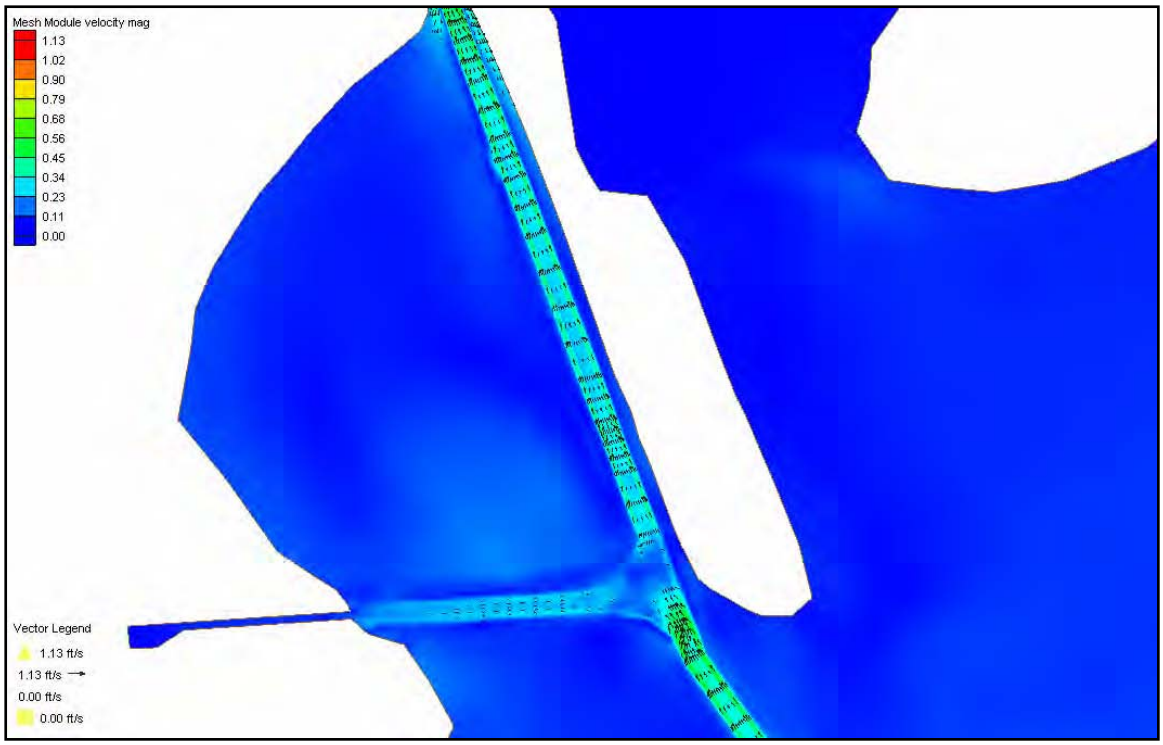

Figure 39. October, upper bay, bottom depth, 40X400 channel, residual shear.

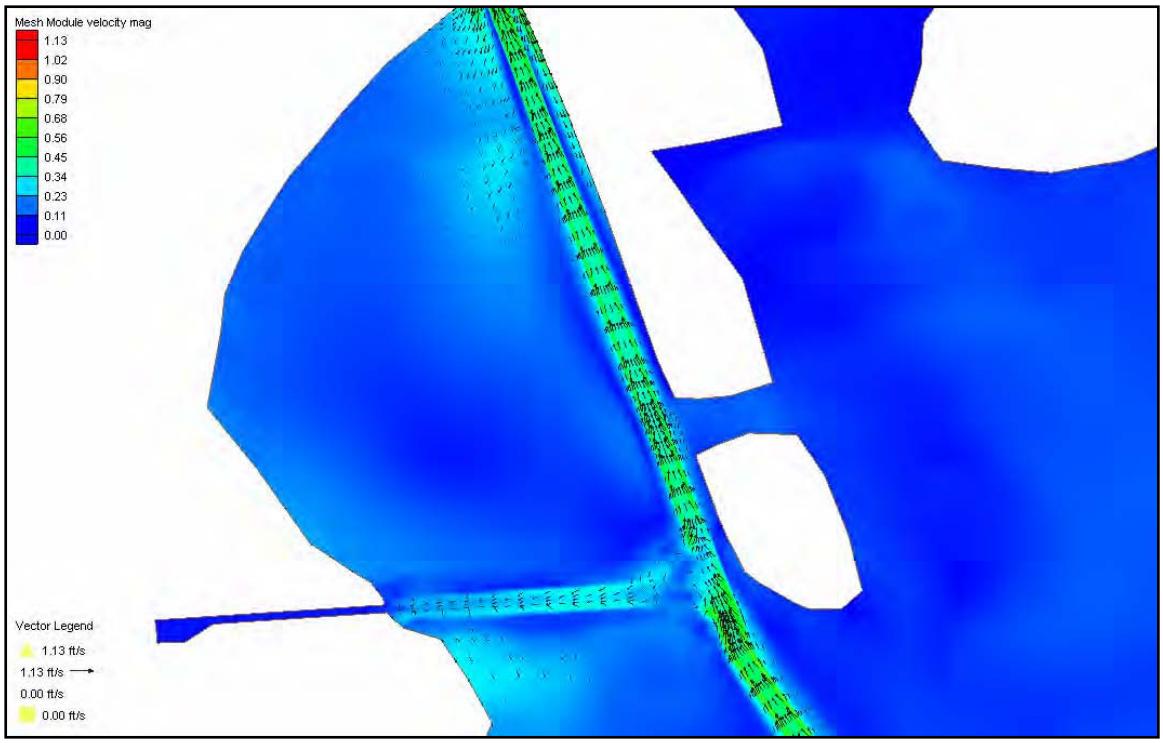

Figure 40. April, upper bay, bottom depth, 45X530 channel, residual shear.

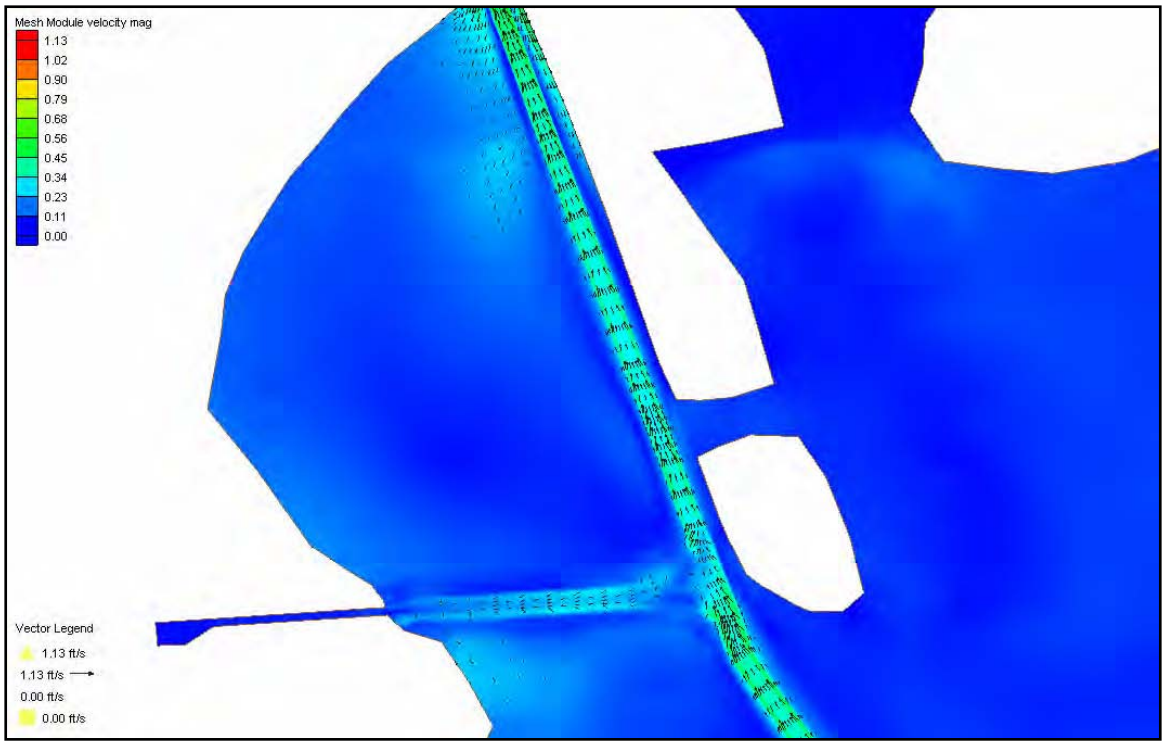

Figure 41. May, upper bay, bottom depth, 45X530 channel, residual shear.

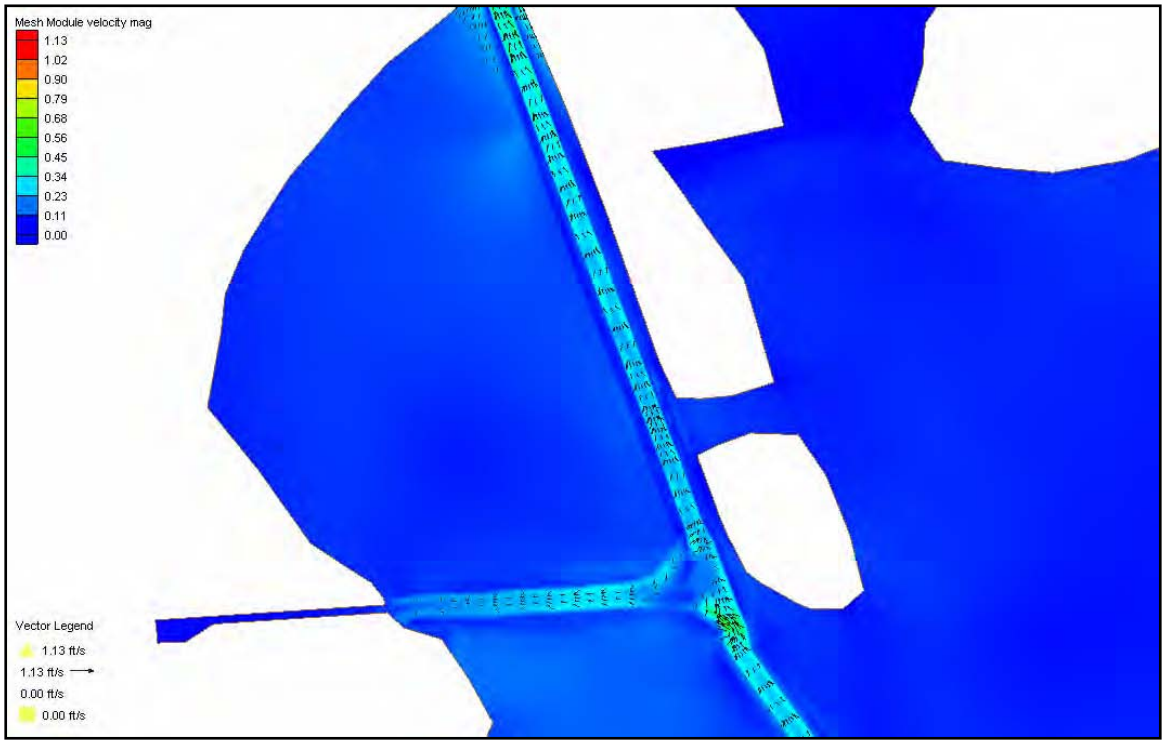

Figure 42. June, upper bay, bottom depth, 45X530 channel, residual shear.

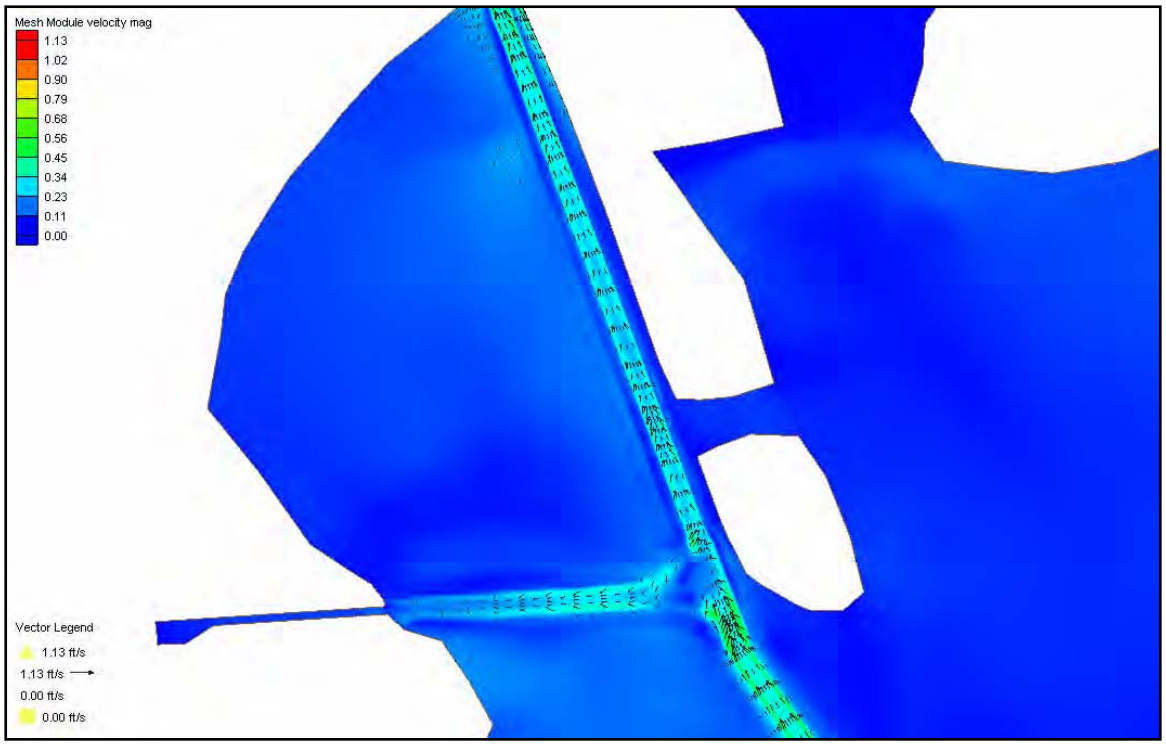

Figure 43. July, upper bay, bottom depth, 45X530 channel, residual shear.

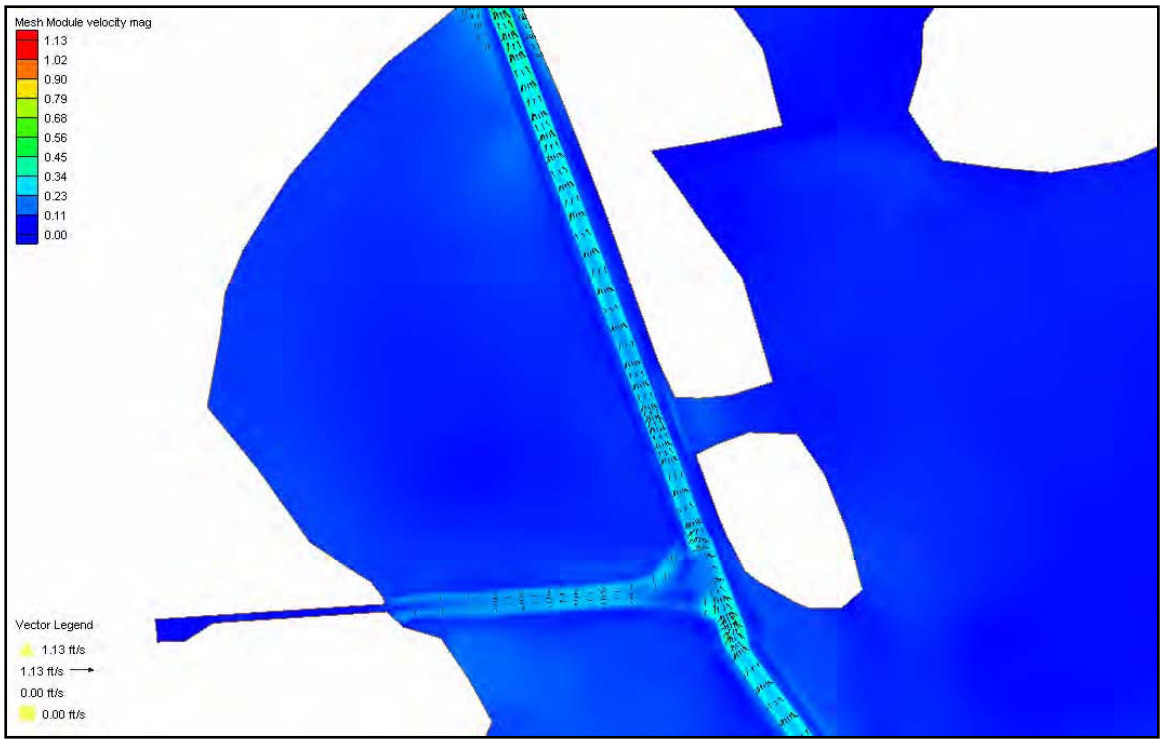

Figure 44. August, upper bay, bottom depth, 45X530 channel, residual shear.

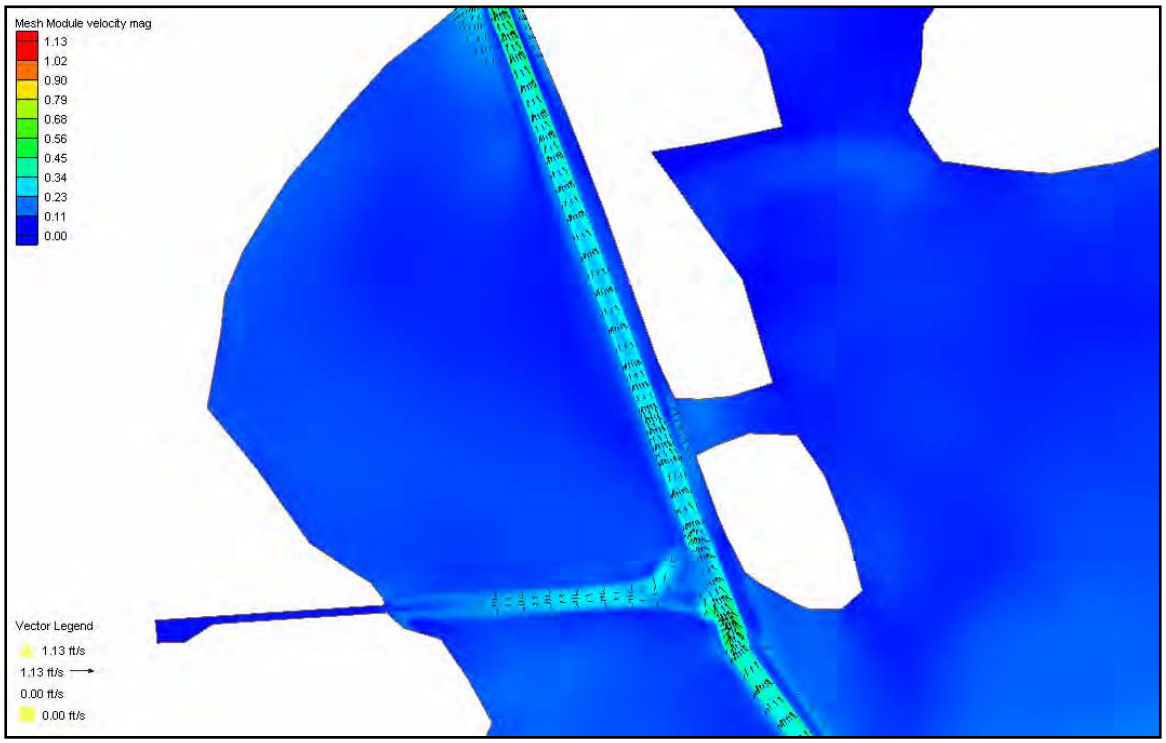

Figure 45. September, upper bay, bottom depth, 45X530 channel, residual shear.

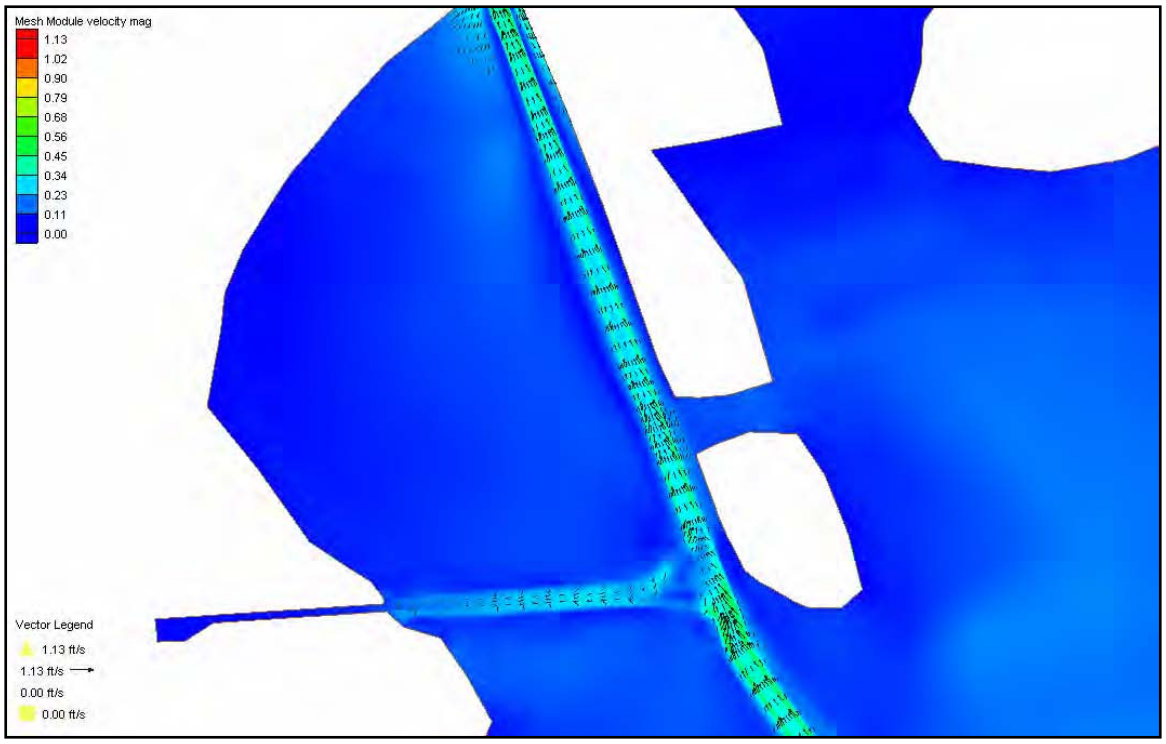

Figure 46. October, upper bay, bottom depth, 45X530 channel, residual shear.

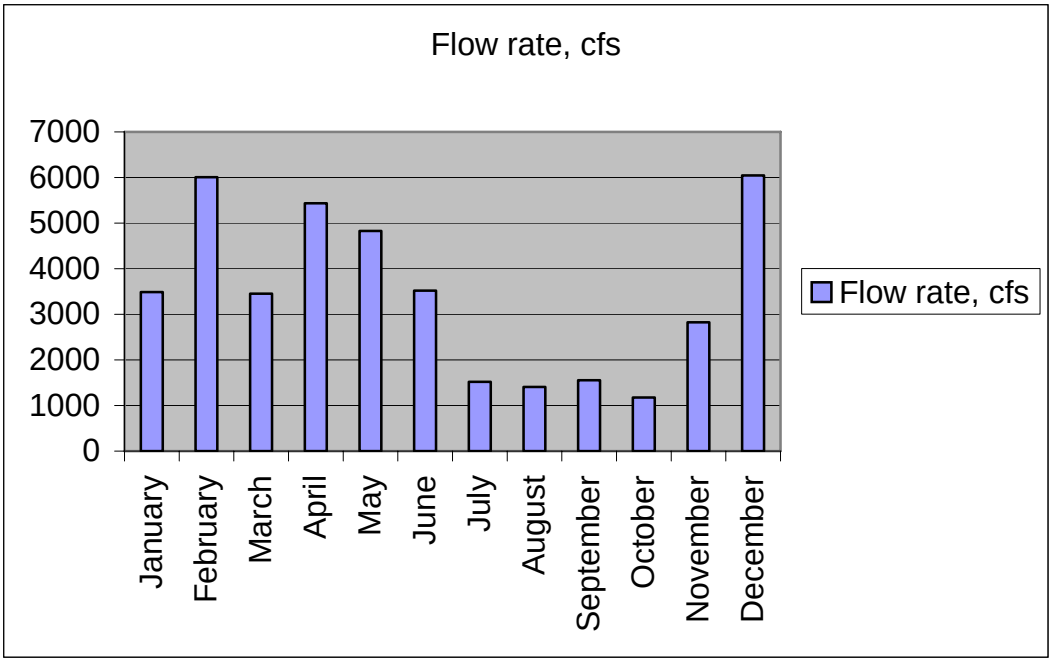

Figure 47. Flow rate in combined Trinity and San Jacinto rivers for low flow, 1990 hydrology year.

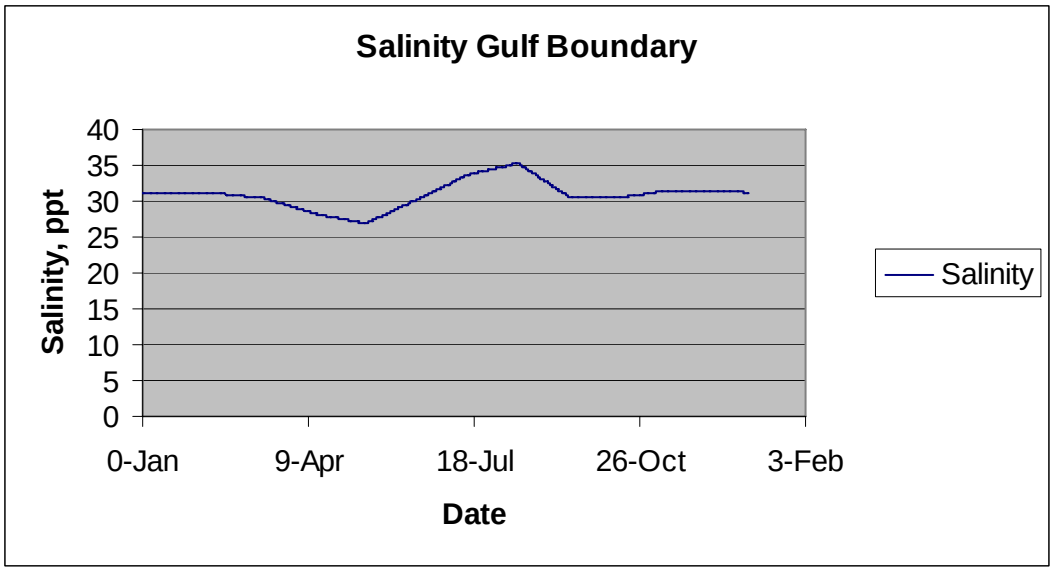

Figure 48. Salinity used for Gulf boundary in model simulations.

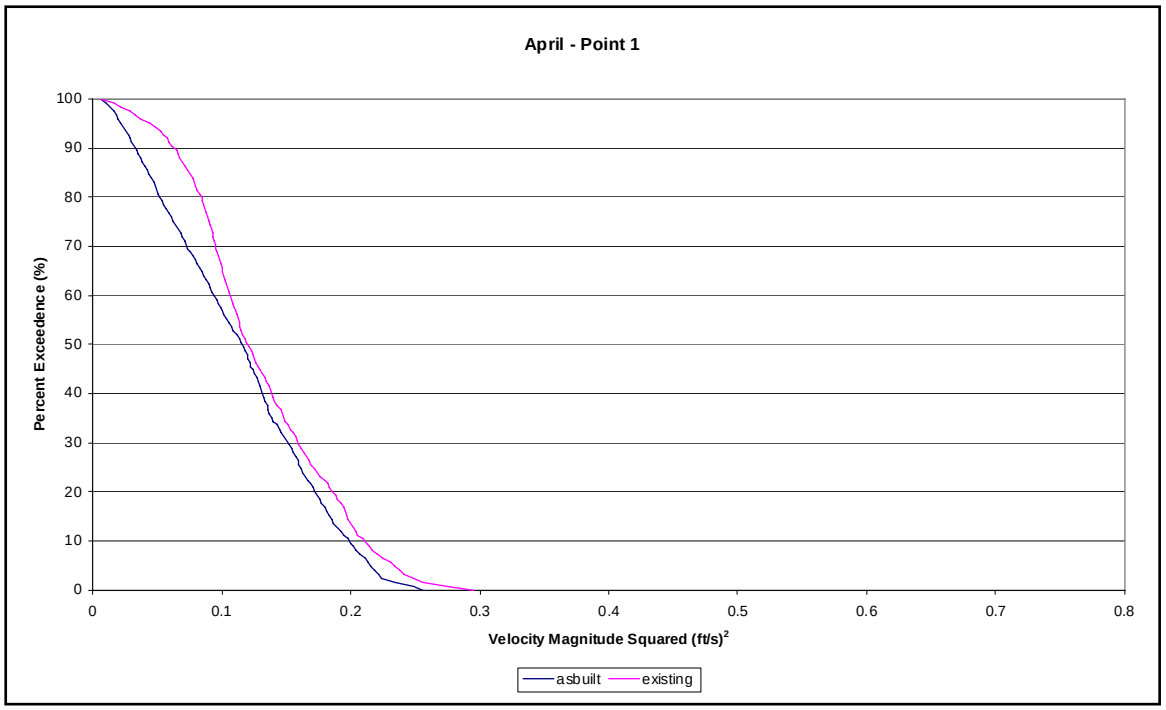

Figure 49. April velocity squared exceedance for Point 1.

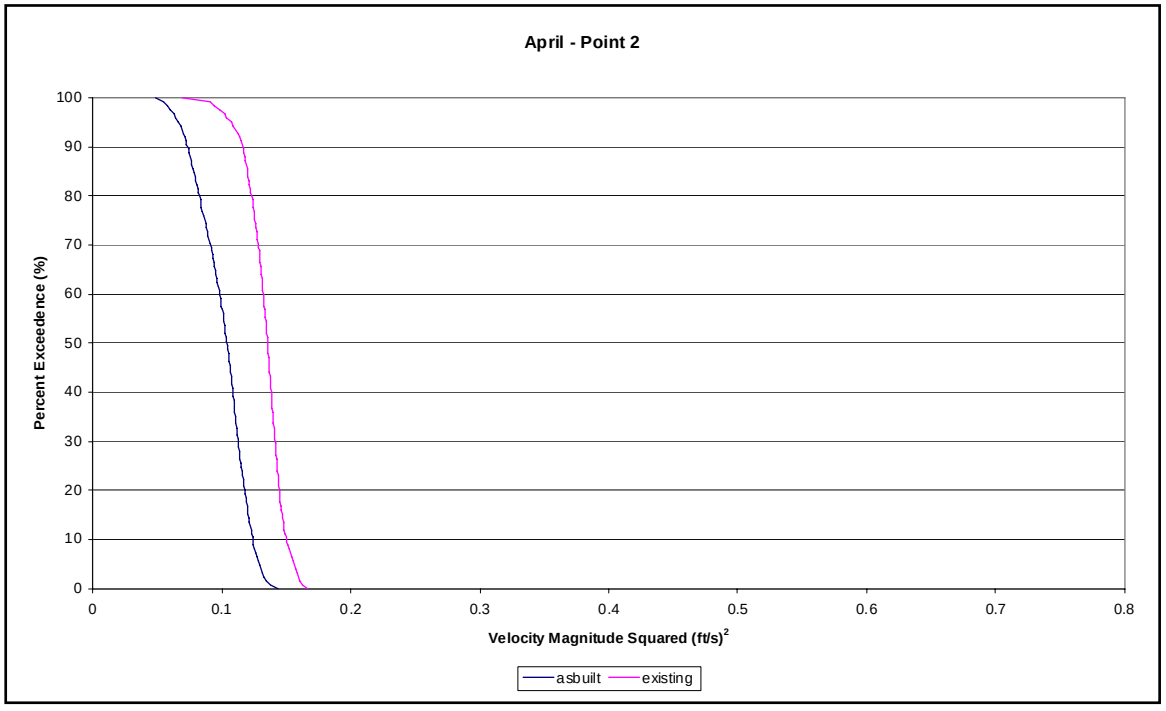

Figure 50. April velocity squared exceedance for Point 2.

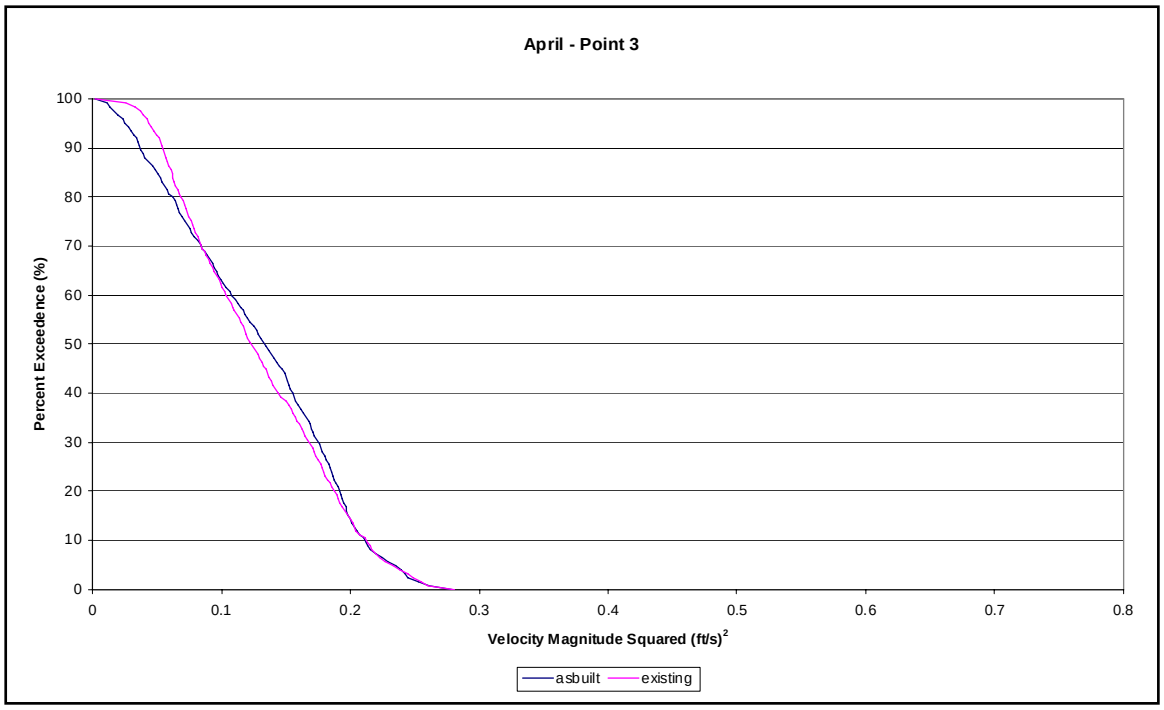

Figure 51. April velocity squared exceedance for Point 3.

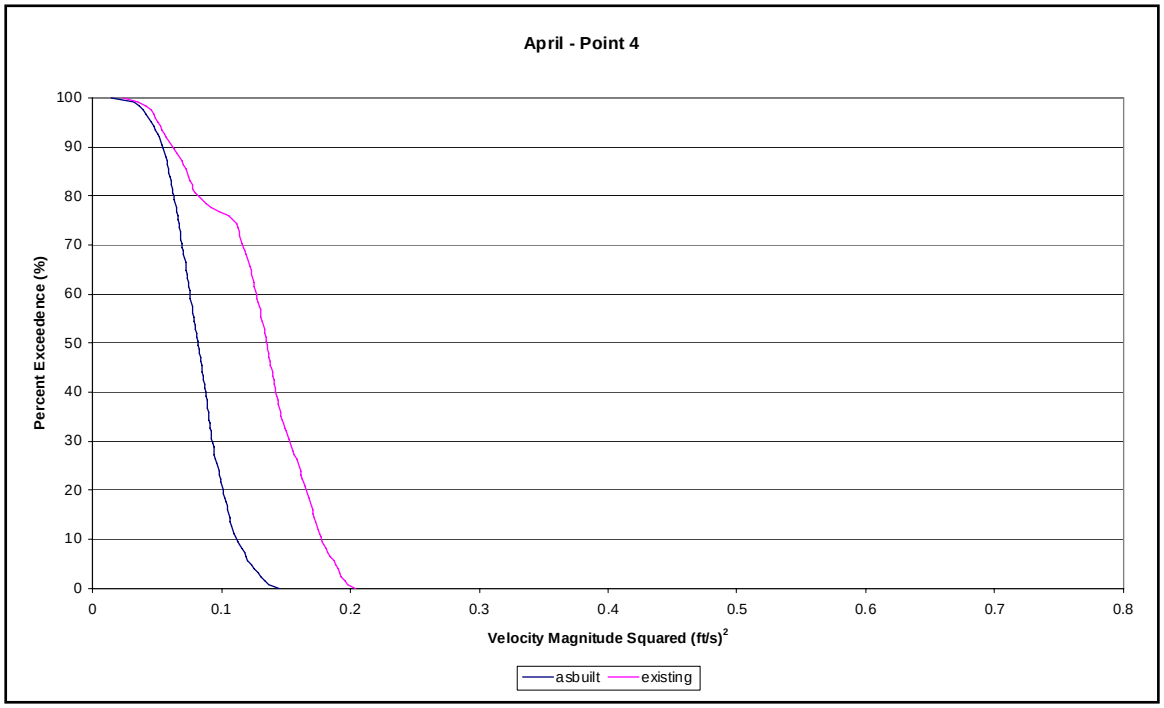

Figure 52. April velocity squared exceedance for Point 4.

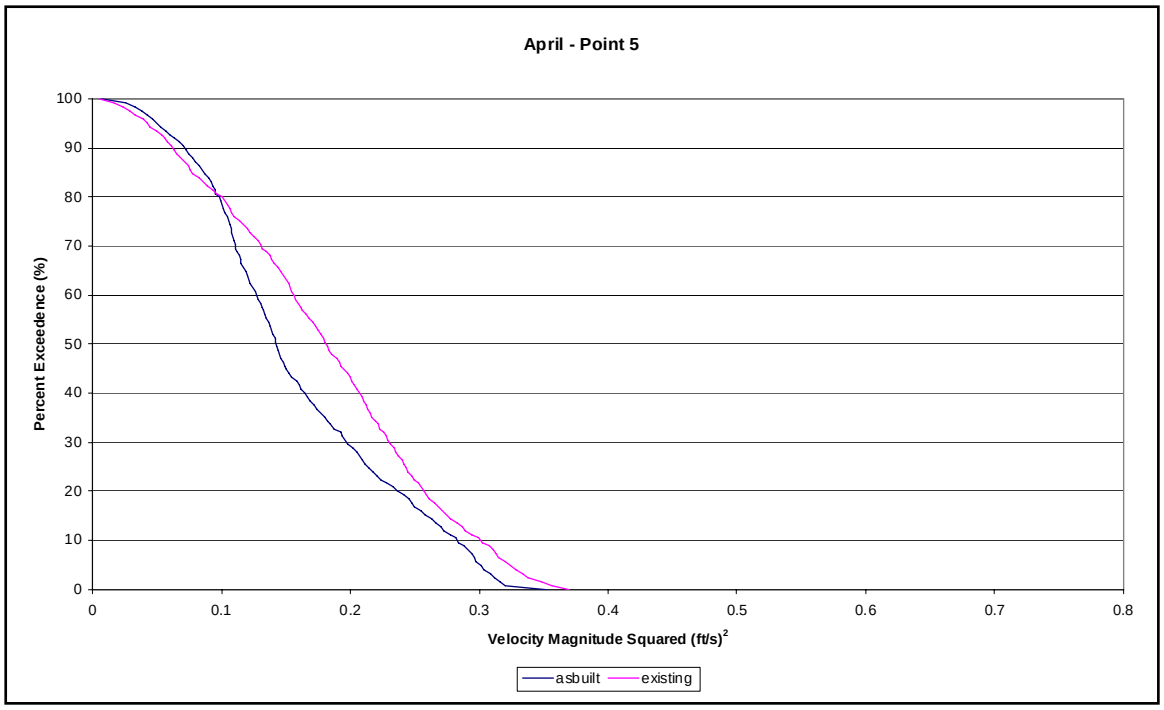

Figure 53. April velocity squared exceedance for Point 5.

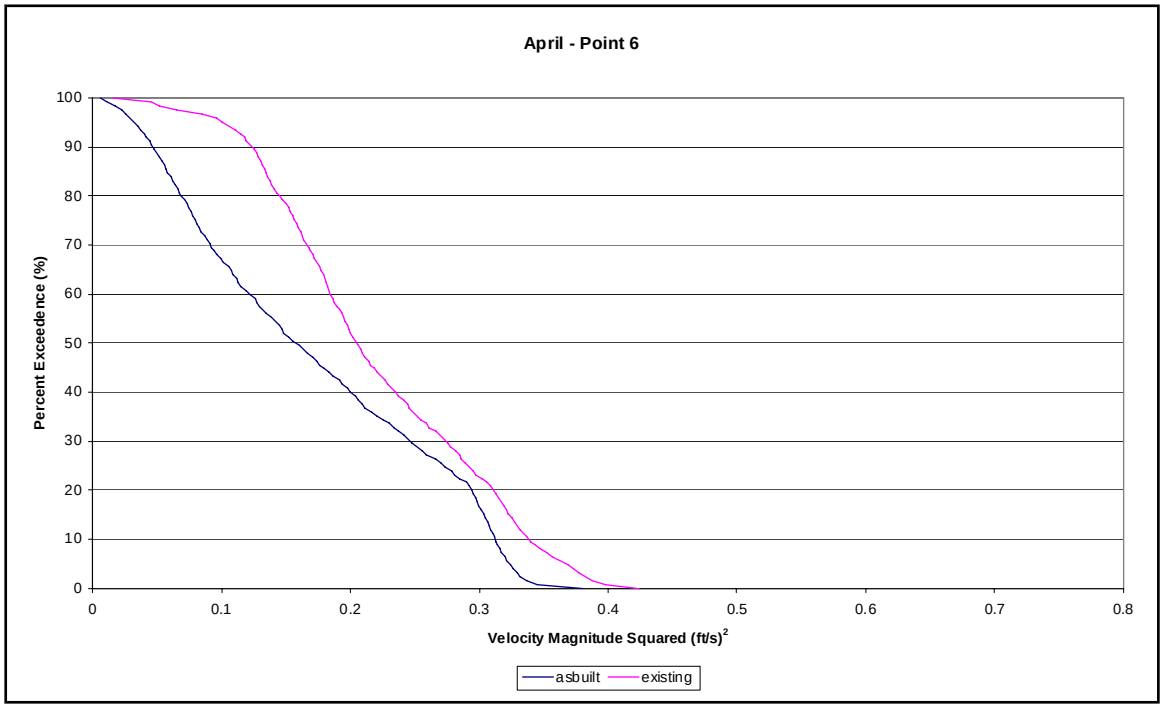

Figure 54. April velocity squared exceedance for Point 6.

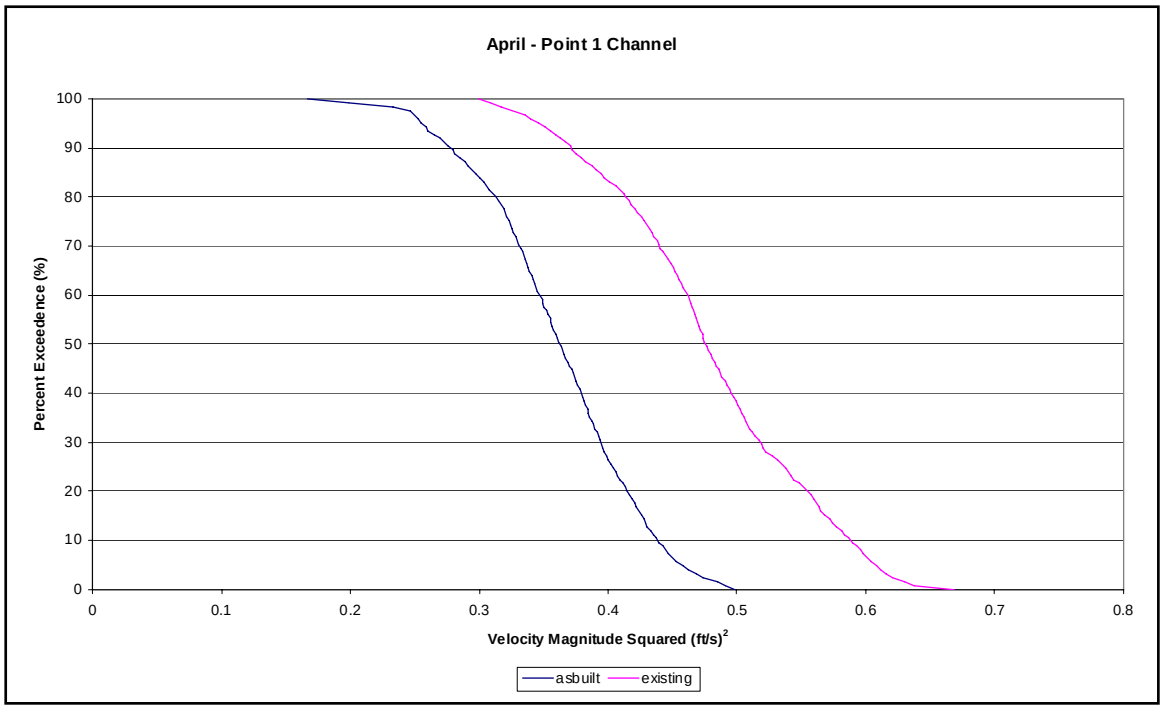

Figure 55. April velocity squared for Point 1C.

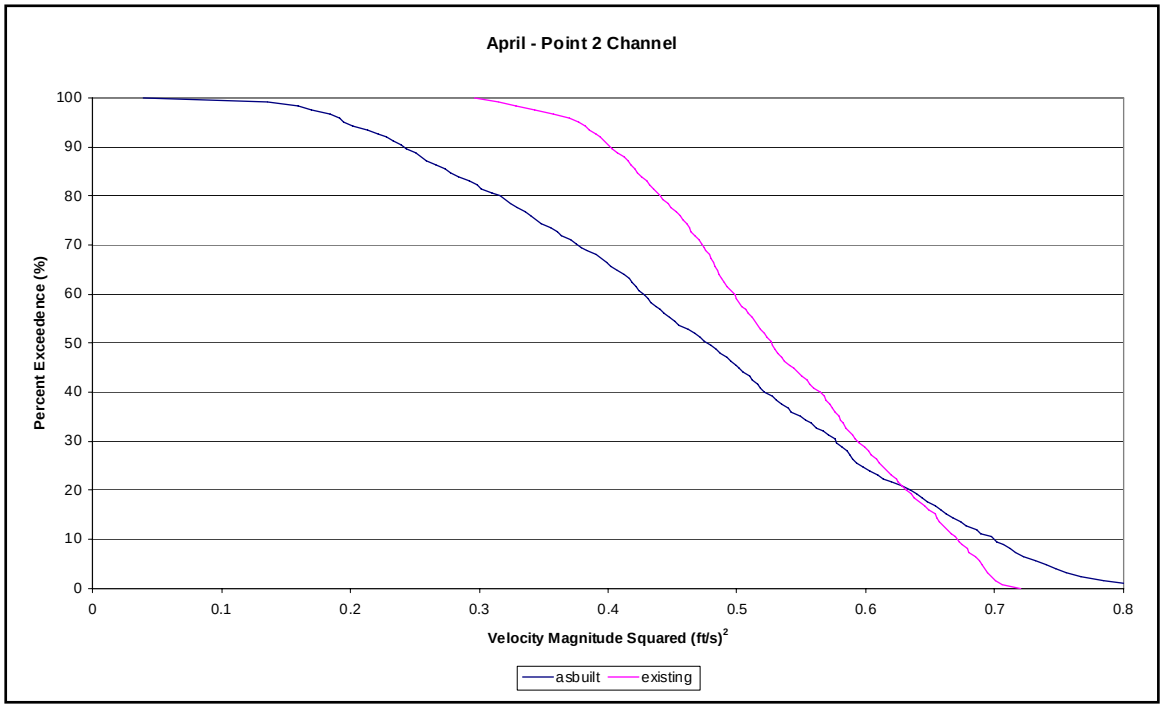

Figure 56. April velocity squared for Point 2C.

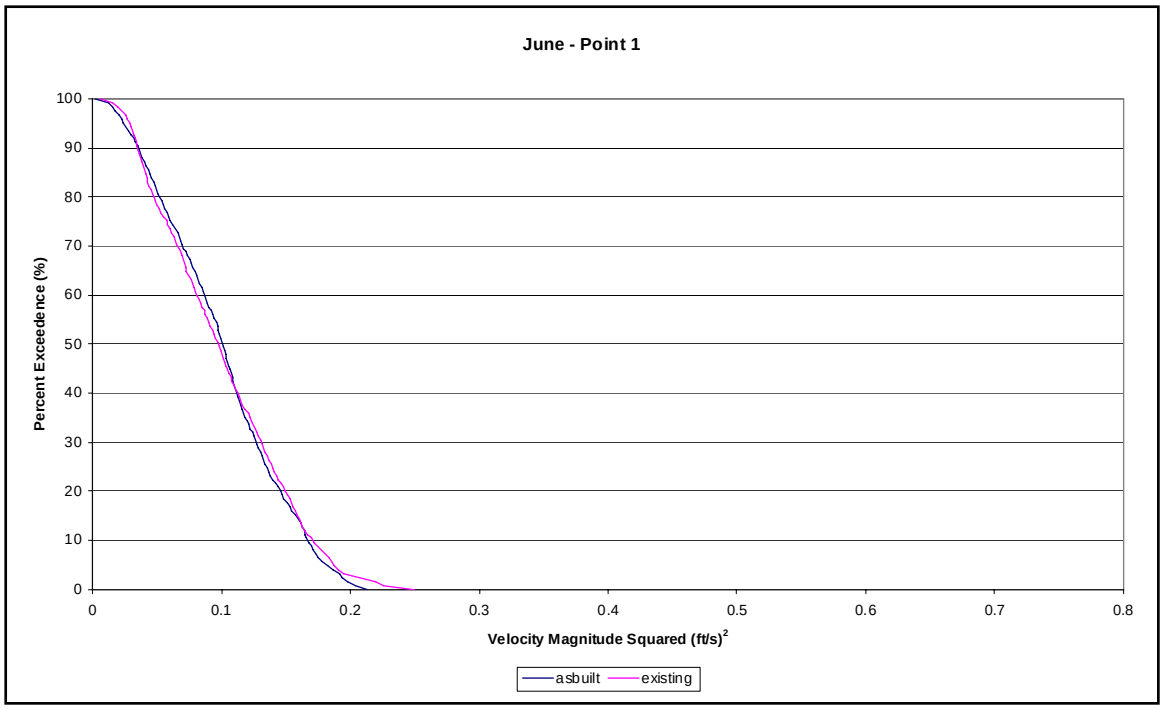

Figure 57. June velocity squared exceedance for Point 1.

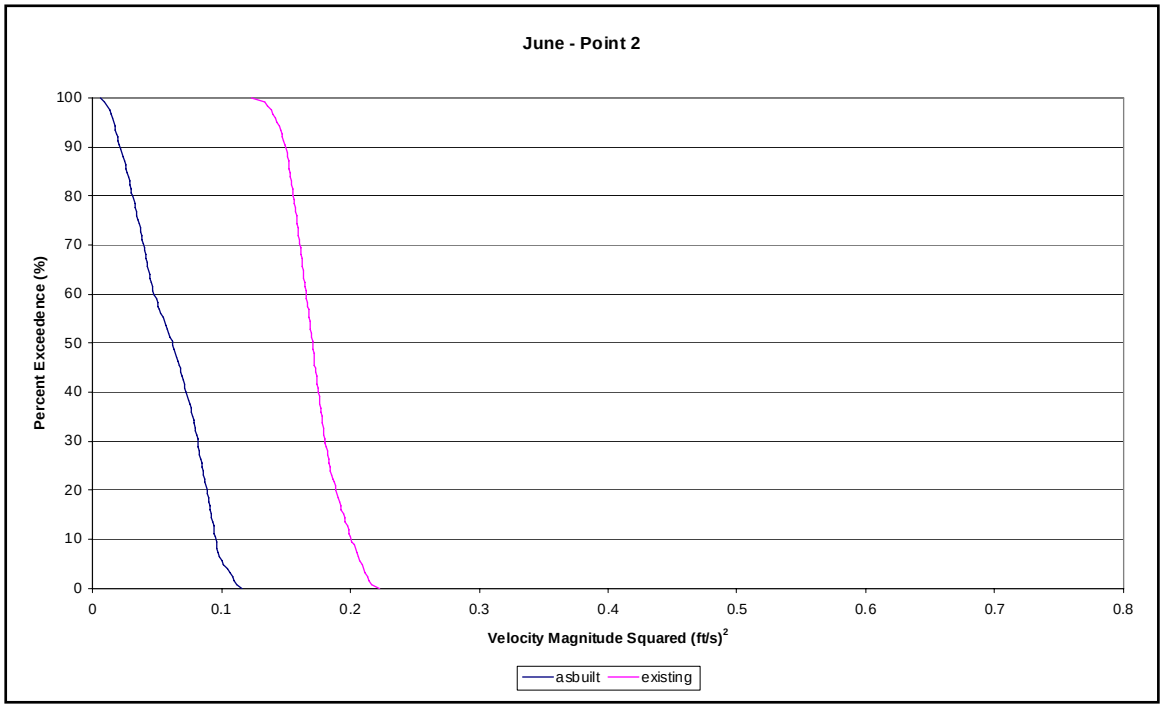

Figure 58. June velocity squared exceedance for Point 2.

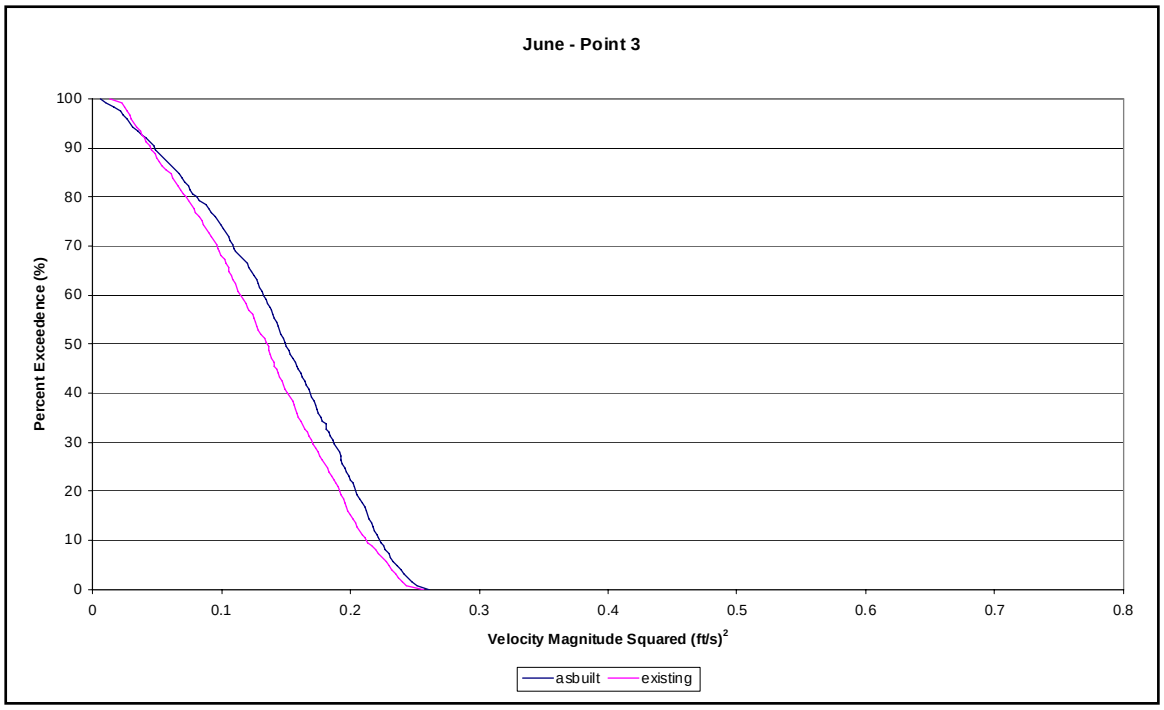

Figure 59. June velocity squared exceedance for Point 3.

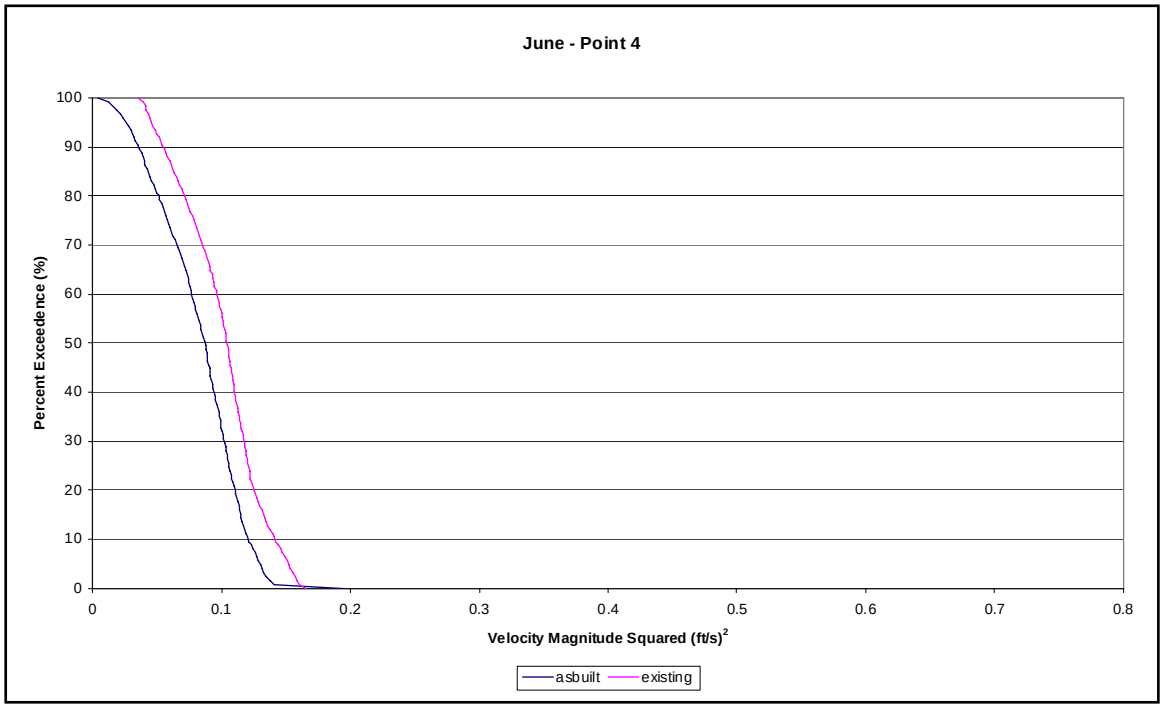

Figure 60. June velocity squared exceedance for Point 4.

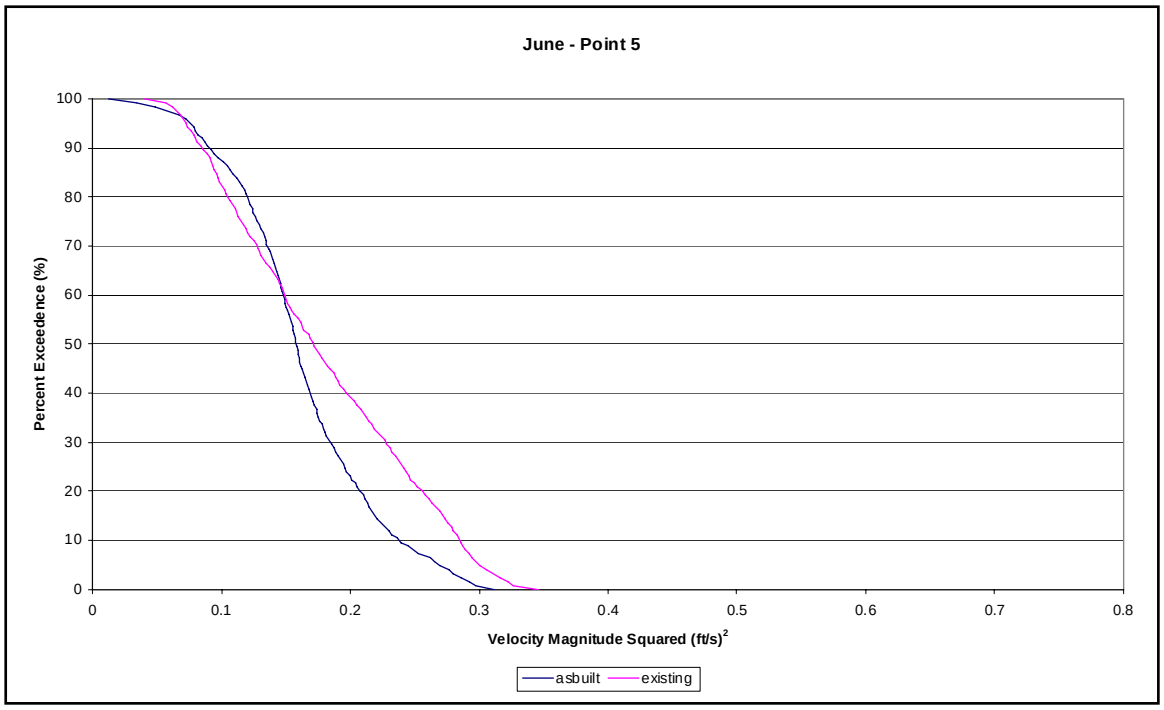

Figure 61. June velocity squared exceedance for Point 5.

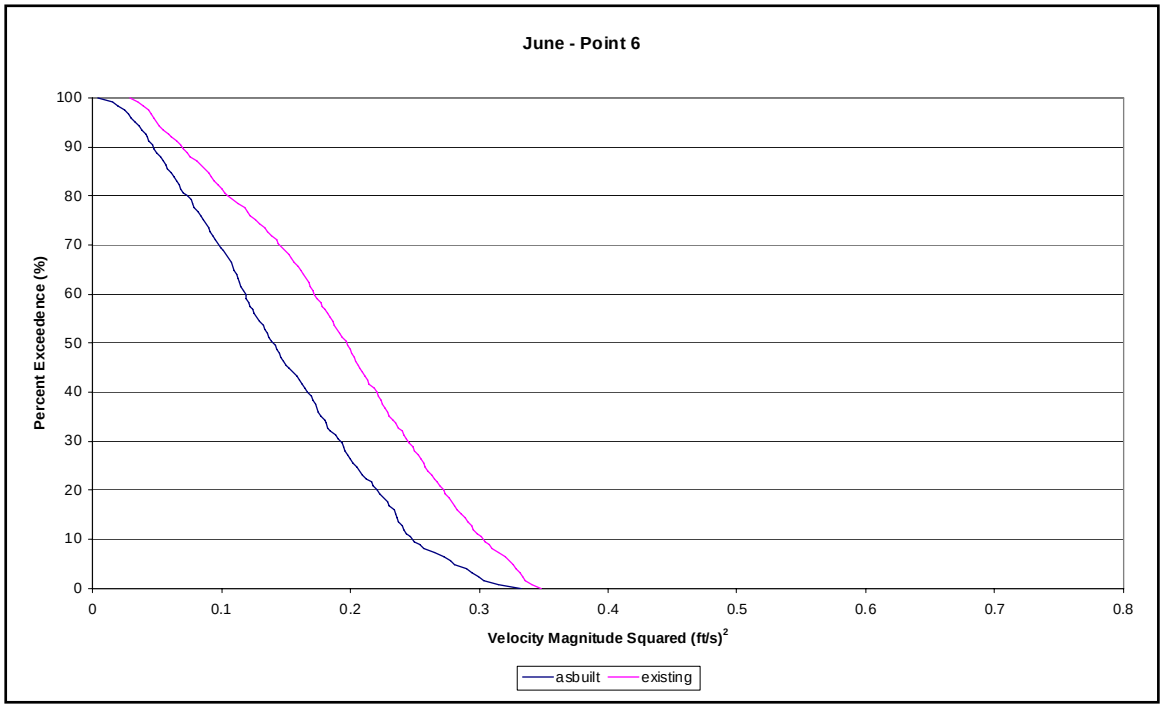

Figure 62. June velocity squared exceedance for Point 6.

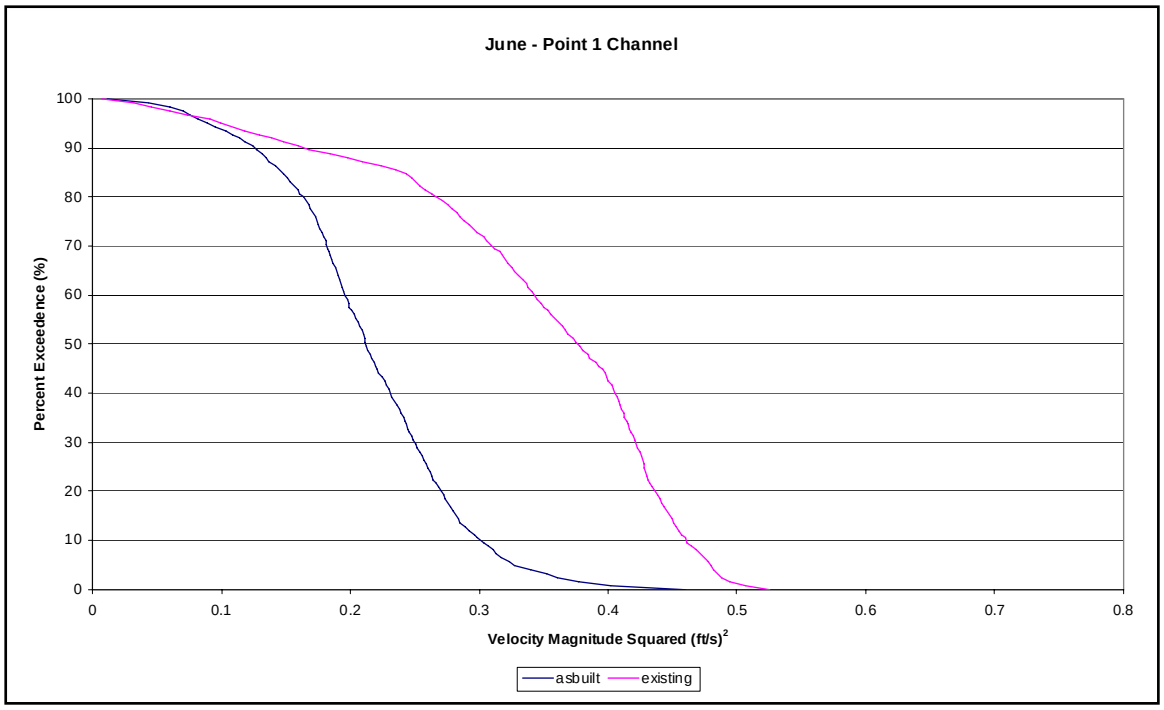

Figure 63. June velocity squared exceedance for Point 1C.

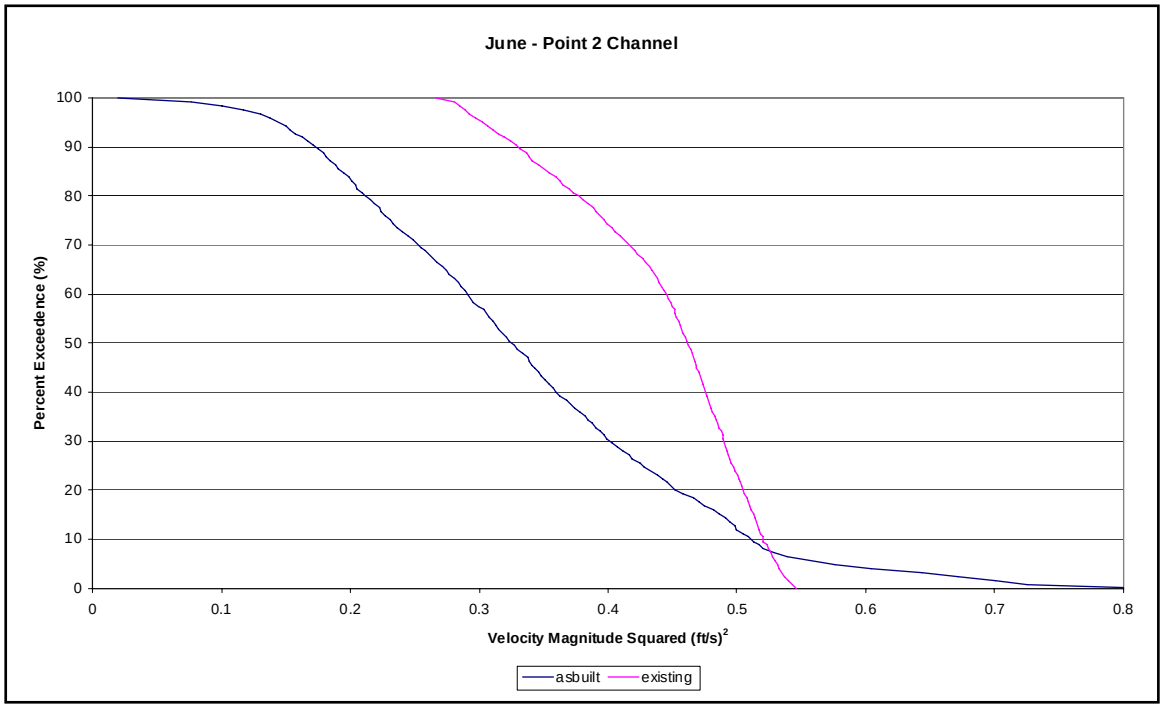

Figure 64. June velocity squared exceedance for Point 2C.

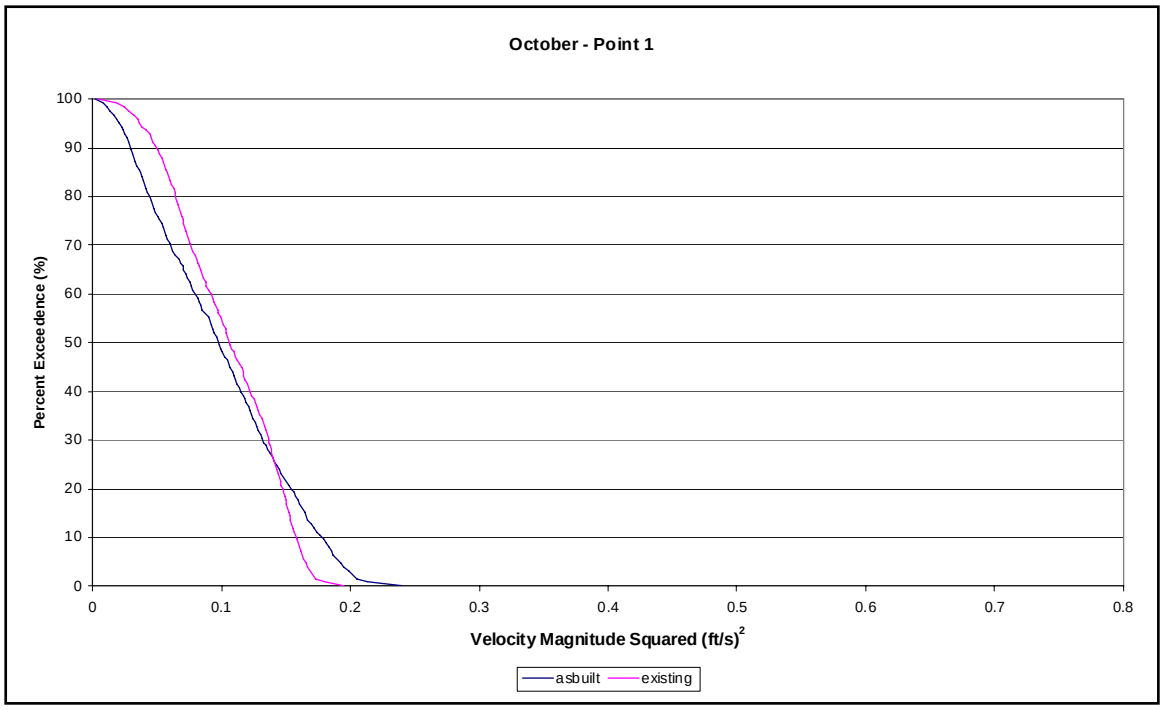

Figure 65. October velocity exceedance for Point 1.

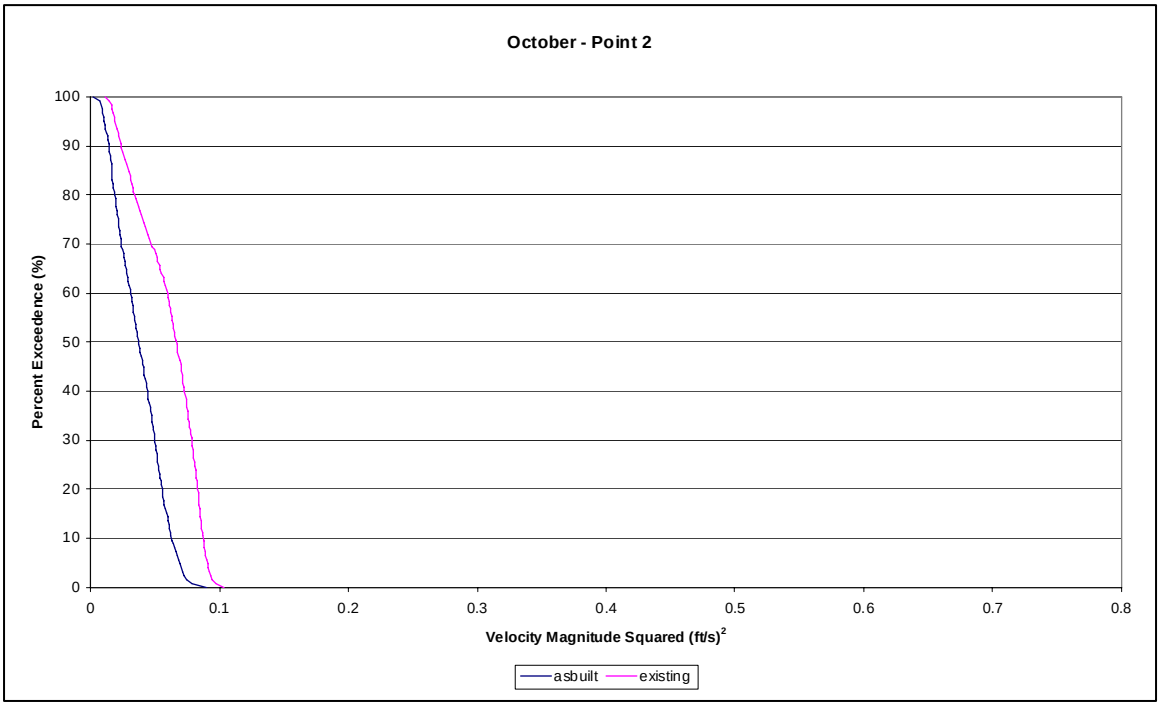

Figure 66. October velocity exceedance for Point 2.

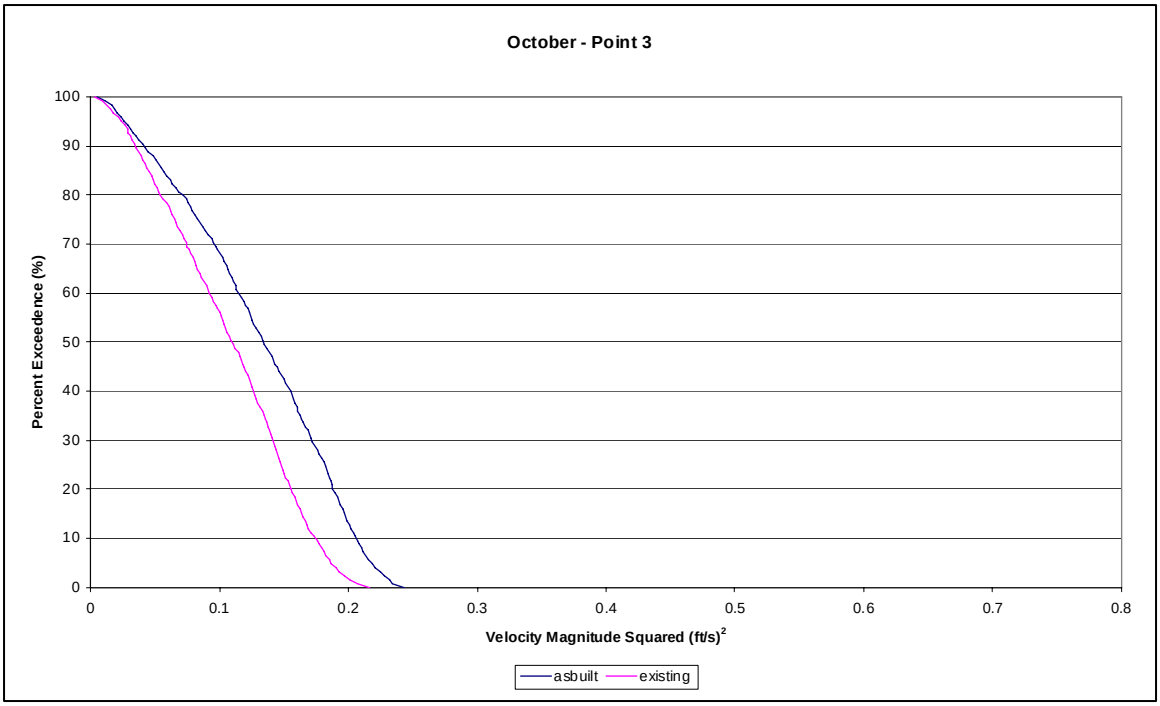

Figure 67. October velocity squared exceedance for Point 3.

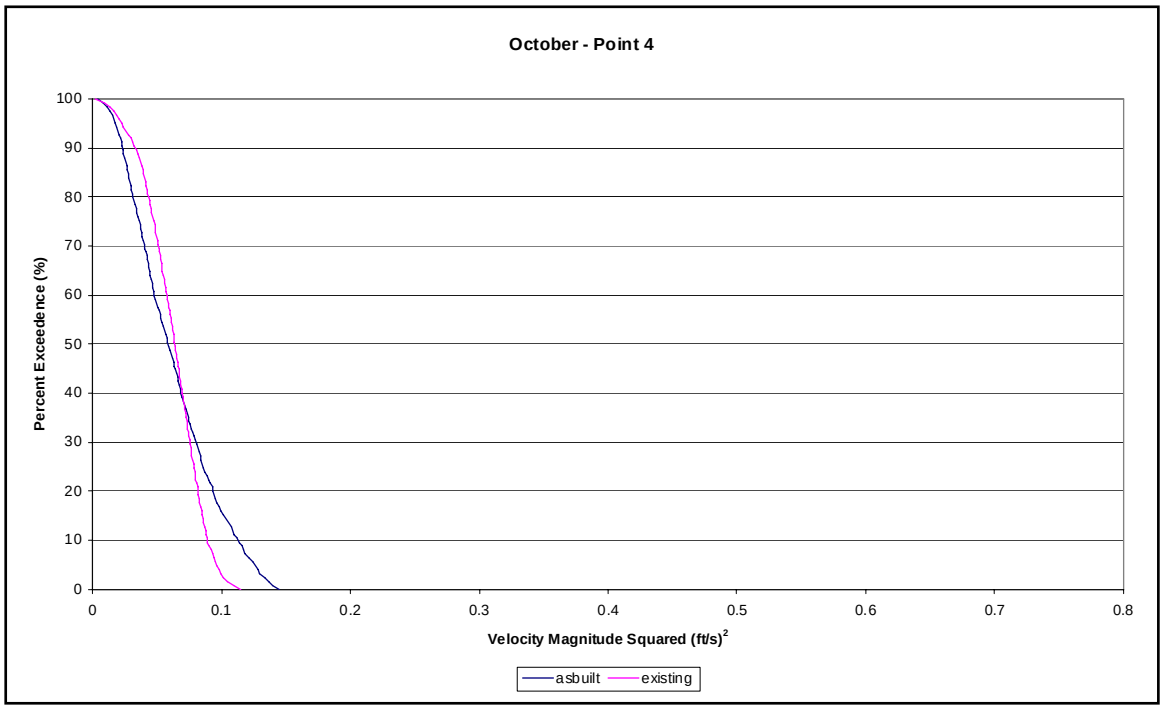

Figure 68. October velocity squared exceedance for Point 4.

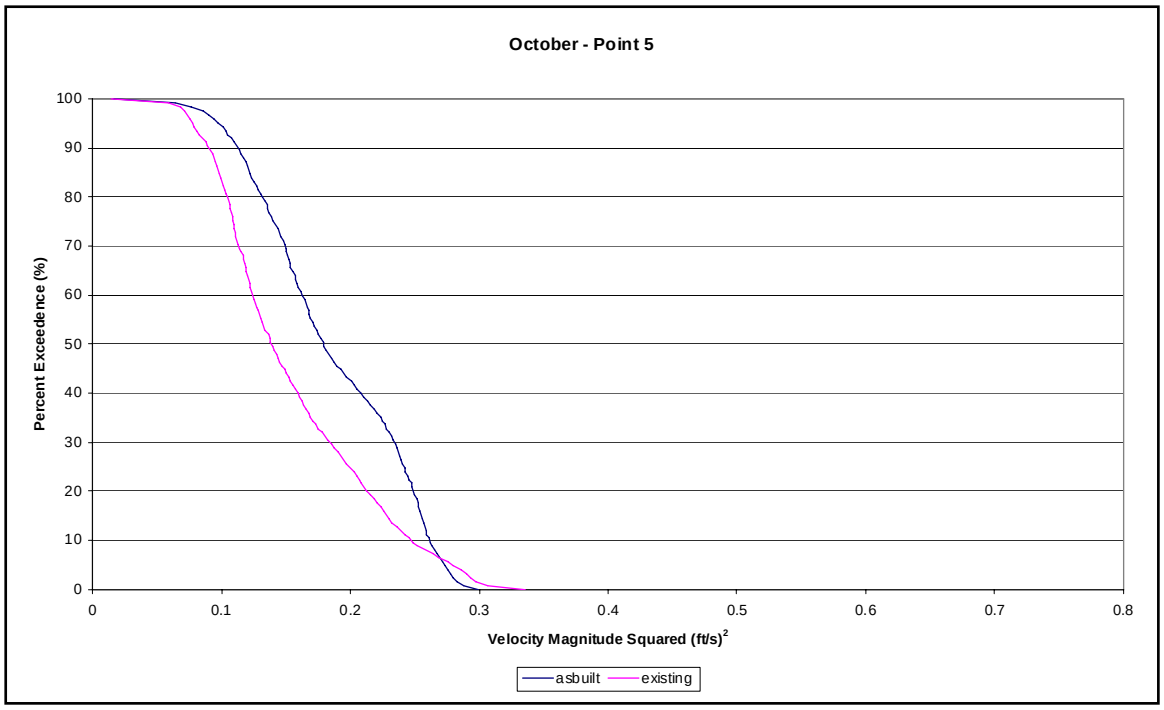

Figure 69. October velocity squared exceedance for Point 5.

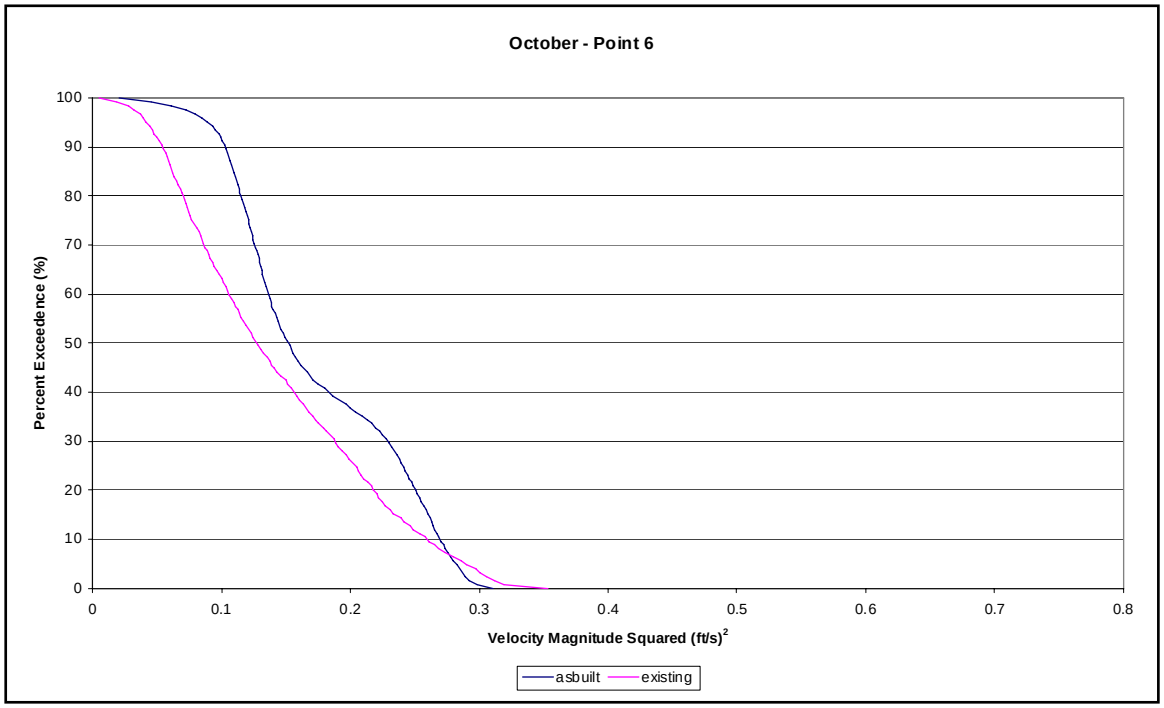

Figure 70. October velocity squared exceedance for Point 6.

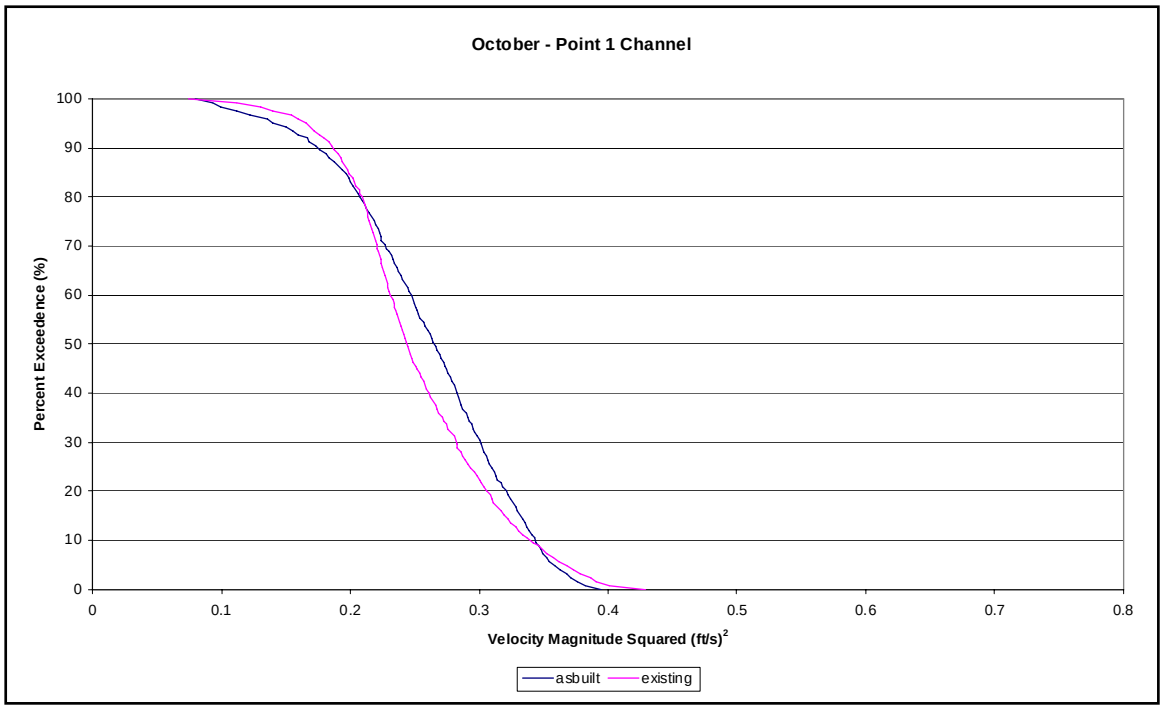

Figure 71. October velocity squared exceedance for Point 1C.

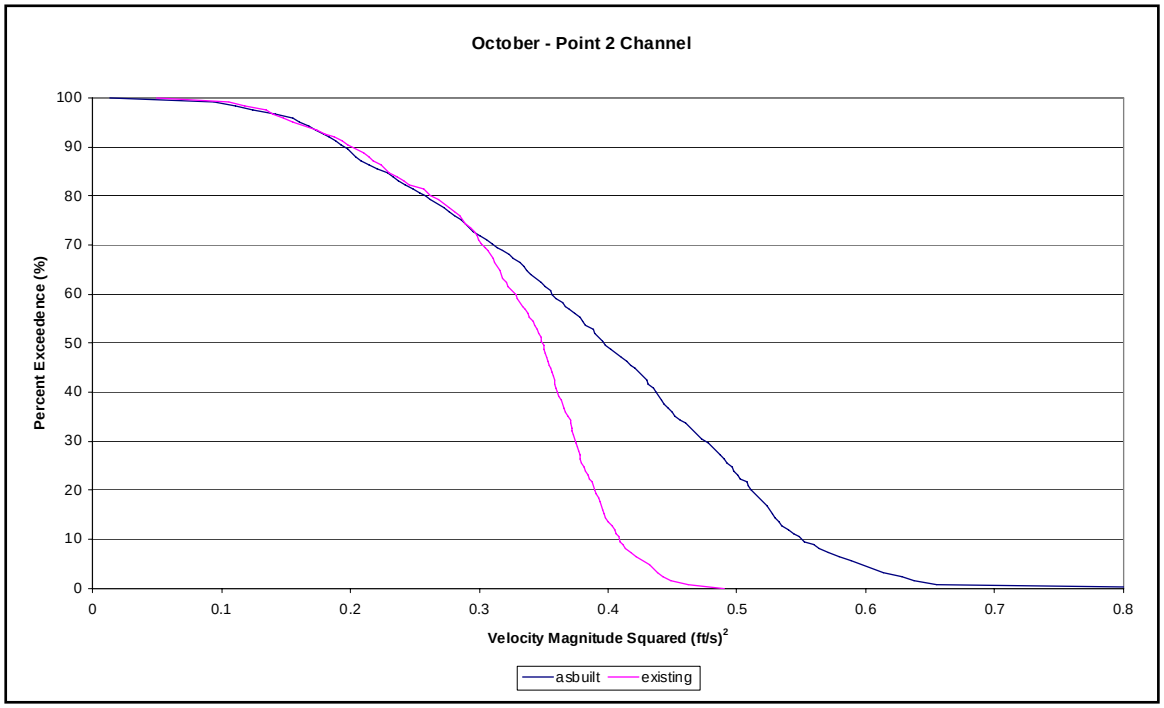

Figure 72. October velocity squared exceedance for Point 2C.

Sediment Estimates based upon Hydrodynamic Model

As a preliminary effort the shears obtained from the hydrodynamic model are used to estimate the shoaling rate in the channel. This part of the report was done before the sediment model was in operation and was used to provide a quick estimate. This is followed up in the next chapter with the sediment model, at which time some of the parameters used in this section may be modified. A rough estimate of the shoaling rate during April can be made using values from the field data and other bounding estimates. This estimate will allow us to more precisely define the critical shear stress for deposition. This, in turn, will be used by the model to calculate the deposition rate change caused by the channel enlargement. April in the field is typically a high shoaling period. An estimate for the coefficient of friction is $C_f = 0.091$ in the equation $\tau = \frac{1}{2}\rho C_f V^2$. This estimate comes from the Manning coefficient used in the model run of 0.033 for the channel. This friction is based on the bottom velocity and so the Manning coefficient is higher than when using the mean velocity. The velocity-squared is in feet per second and shear stress is calculated in Pascals (Pa). The rate of deposition can be estimated as

$$d = V_s P C_B \quad \text{(Krone 1962)} \tag{5}$$

where:

V_s = settling velocity

$P = 1 - \frac{\tau}{\tau_{cd}}$ = probability. That reduces the settling velocity to an effective settling velocity; if $\tau > \tau_{cd}, P = 0$

C_B = bed concentration.

The estimates of the shear exceedance for locations 1C and 2C are shown in Figures 55 and 56, respectively. The following estimated parameters were found using representative values from the collected field data of August 2004.

C_B = 200 mg/L (0.2 kg/m^3)
V_s = 0.5 mm/s (0.0005 m/s)

Other estimated parameters are as follows:

S_s = 2.65 is the grain specific gravity commonly used value
Dry sediment density = 500 kg/m^3
Critical shear stress for deposition $\tau_{cd} \approx 0.5$ Pa.

These final two parameters were suggested by Teeter (2005). The dry sediment density is for fresh deposits. Over time, the deposit will consolidate and the density will increase. The field data found that the critical shear stress for erosion in the bay was about 1.0 to 1.2 Pa. This would be the upper limit for τ_{cd}. Also samples in this area of the channel contained fine sand and medium to coarse silts (along with some clay). This suggests a value of approximately 0.5 Pa. Values of 0.25, 0.5, and 0.75 were used in the calculations simply to test sensitivity.

Tables 5 and 6 contain estimates of deposition for April for Point 1C and 2C, respectively. The first major heading is "Probability" which is the integral of the instantaneous probability over the month. The second major heading is the deposition rate in meters/month. And the final major heading is the volume deposition per meter of channel length. This column is found by multiplying the deposition by the channel width. This width is 400 ft (122 m) for the base conditions.

The different critical shear stresses give typical depth deposit rates for the base conditions between 0.10 and 0.38 m/month for Point 1C and between 0.06 and 0.36 for Point 2C. The lower limit of deposition is for $\tau_{cd} =$ 0.25 Pa. The deposition amounts for this critical shear stress for deposition are too small and the relative size of deposition at the two points is strongly weighted toward Point 1C. The actual dredging records show that the two points have similar shoaling rates. For the critical shear stress for deposition of 0.5 and 0.75 Pa, the distribution is more even and the rate is more like what has been observed in the field. Therefore, the results for 0.5 Pa are probably the most reliable and will be used in subsequent calculations.

Table 5. Estimates of shoaling rate around Point 1C.

Point 1C			
April			
τ_{cd}, Pa	Probability	Deposition Rate, m/month	Volume (m^3) per meter length
	Base	Base	Base
0.25	0.18	0.10	12
0.50	0.59	0.31	38

0.75	0.73	0.38	46

Table 6. Estimates of shoaling rate around Point 2C.

Point 2C			
April			
τ_{cd} Pa	Probability	Deposition Rate, m/month	Volume (m^3) per meter length
	Base	Base	Base
0.25	0.12	0.06	8
0.50	0.54	0.28	34
0.75	0.69	0.36	44

Sediment Model Results

This chapter utilizes a sediment model in which a tracer sediment, that can settle and erode based upon the shear stress, is introduced to the system to estimate the impact of the channel enlargement. In this chapter the sediment model is used in an unvalidated state. The next study (Phase 2) will validate the model and use it to evaluate alternatives to reduce the required channel maintenance. This chapter is a follow on of the previous chapters. These chapters were provided to the sponsor as they were completed to provide estimates as early as possible. The adjustment period in this model began with the parameters developed in the prior chapters but in order to behave more like the system these were adjusted as needed. This model study made no attempt to introduce the sediment via the rivers or attempt to match quantities of shoaling. Here the model used a tracer sediment introduced along the channel. The ultimate deposition distribution is compared with the field distribution. This sediment tracer is then introduced over the same area with the enlarged channel condition. The change in deposition distribution and amount is then compared with the base (40X400 ft) channel condition.

Hydrodynamic and salinity coupled runs were made using the "Present" low-flow and medium-flow hydrologic eras from a prior study as described earlier (see Berger et al. 1995b). The effects of wind waves on the sediment movement were included in the TABS-MDS simulations. The wind was applied using the same speeds and directions as in the hydrodynamic simulations. These runs were made from January through June. A single grain size sediment was “rained” into the model along the channel region for both configurations. An identical sediment load was added to both

domains over the same areas. The sediment, with a concentration of 1 kg/m^3, was introduced for 3 days at a rate of 0.01 m/s over the area shown in Figure 73. The sediment was modeled for April, May, and June separately with grain and bed characteristics determined from the field data collection. The bed was defined such that the only sediment available for erosion was that which entered during the run. Each run was started 10 hours prior to midnight on the first of the month in order to allow the model to spin up before introducing the sediment. The characteristics of the sediment used in the model are provided in Table 7.

Table 7. Sediment characteristics

Sediment Characteristics	
Density	1.565 g/cm^3
Erosion Rate	0.0000346 kg/m^2*sec
Critical Shear for Erosion	1.336 Pa
Critical Shear for Deposition (τ_{cd})*	0.5 Pa
Settling Velocity (V_s)*	0.5 mm/sec
* denotes variables modified for sensitivity analysis	

The ratios of the volumetric change in shoaling along the channel reach between the two configurations for both the low-flow and medium-flow are given in Table 8. These are given separately for each of the three months simulated.

Table 8. Shoaling volume ratios for low and medium flows.

Shoaling Volume Ratio (Plan/Base)			
Flow Condition	April	May	June
Low	1.28	1.19	1.17
Medium	1.34	1.18	1.07

The increase in volume of deposition in the channel ranged from 7% in June for the medium flow event to 34% in April for the same flow condition. Given the limitations of these sediment simulations, the predicted increase in shoaling within the enlarged channel could conservatively be predicted to range from 20-30 percent.

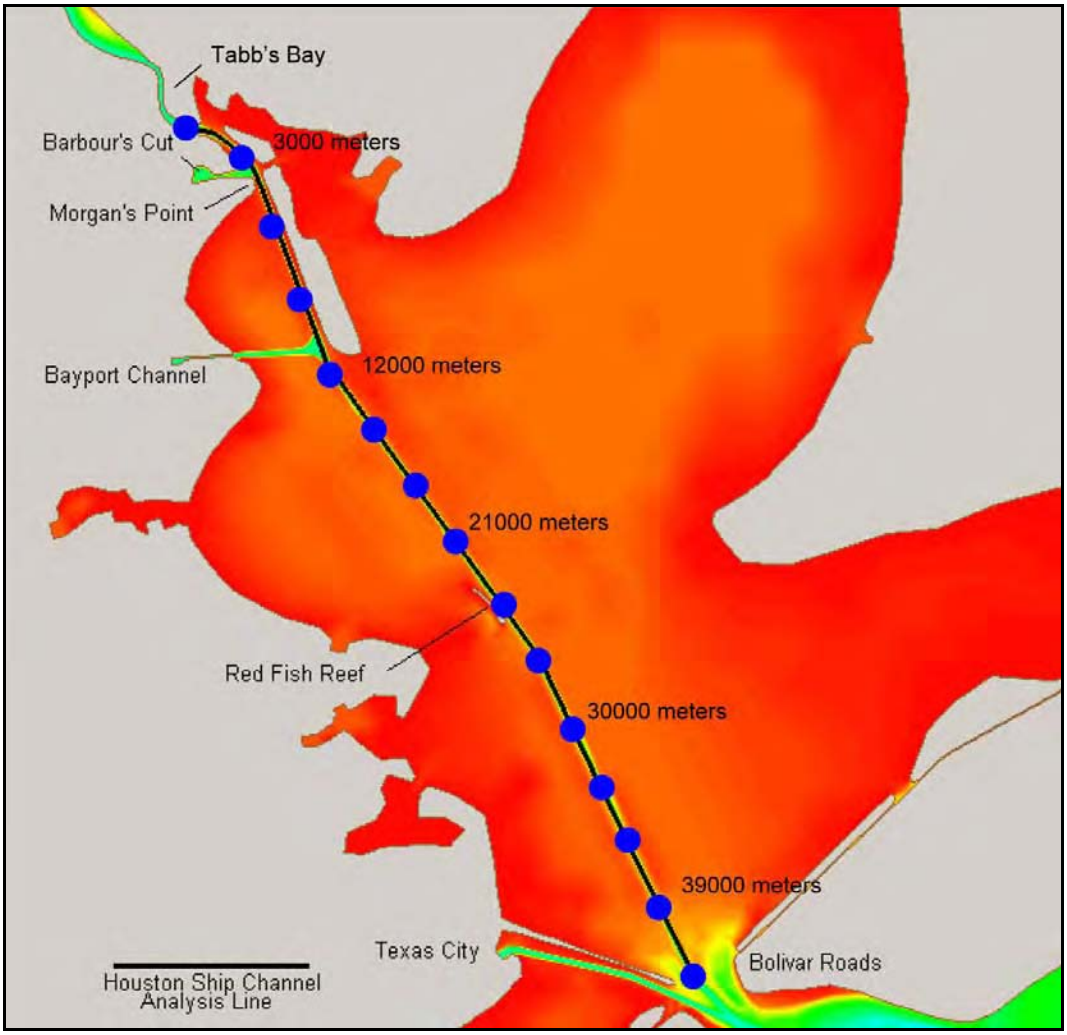

Figure 73. 40- X 400-ft channel configuration and location map, blue dots are 3,000-m increments from 0 at Tabb's Bay to 42,000 m at Bolivar Roads.

Figures 74-76 show the change in distribution between the base condition and the plan (enlarged channel) condition for the low-flow and medium-flow hydrology. These figures only consider the Houston Ship Channel and do not account for any shoaling outside of the channel. The distribution plots are given in 3,281-ft (1,000-m) increments that can be referenced using the 9,842.5-ft (3,000-m) markers (blue dots) in Figure 73. Generally, the distribution has shifted to show more shoaling toward the upland regions. In April there is also a shift toward the Red Fish Reef channel region.

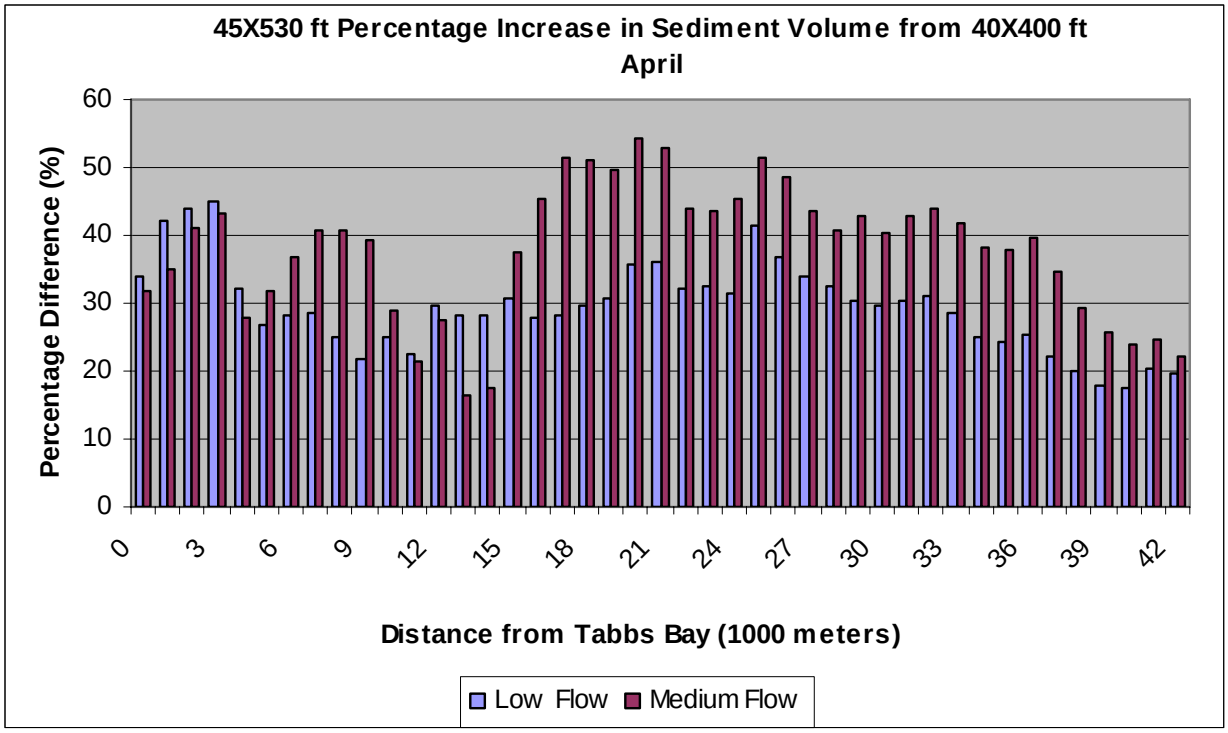

Figure 74. Percentage increase in shoaling for enlarged channel for April.

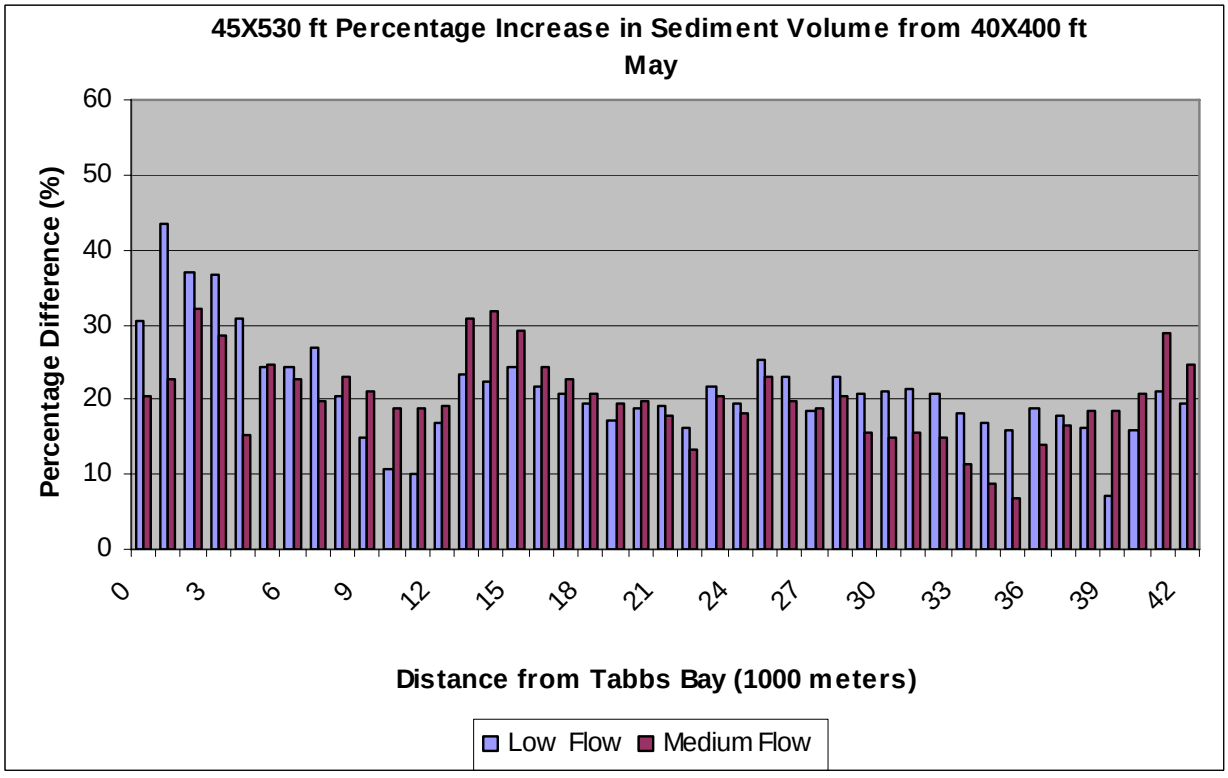

Figure 75. Percentage increase in shoaling for enlarged channel for May.

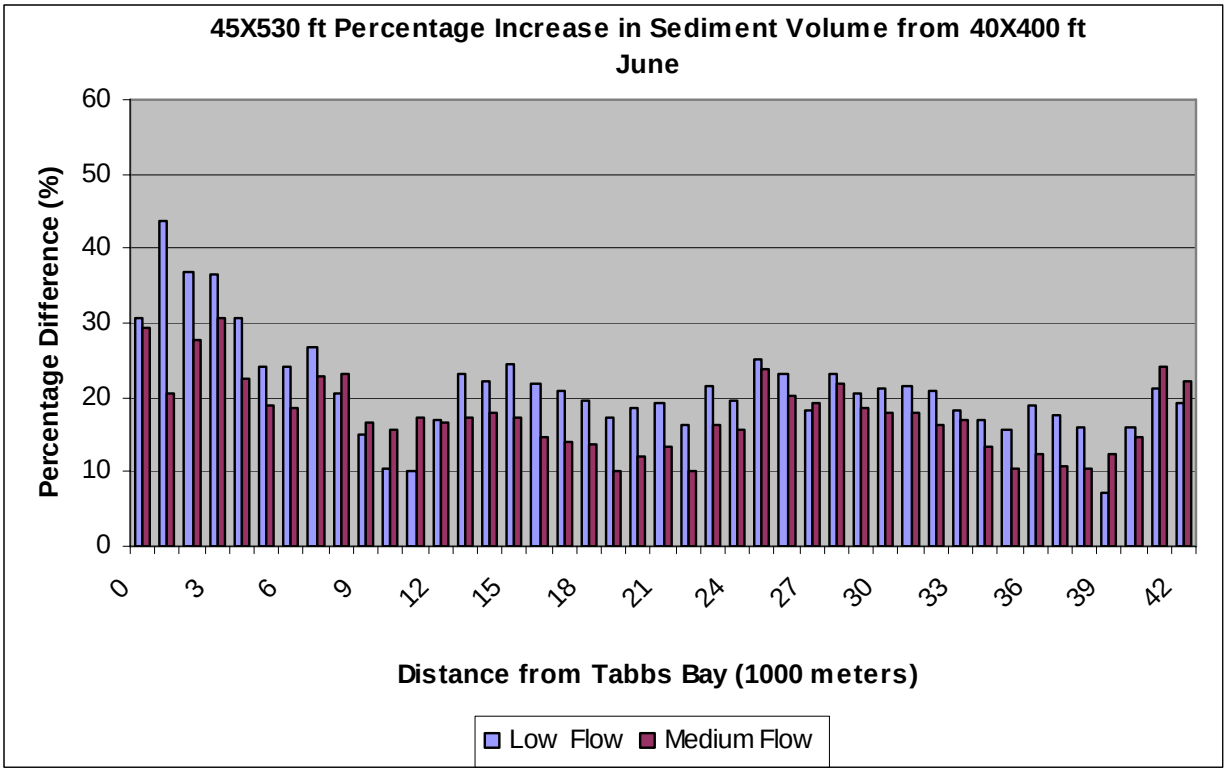

Figure 76. Percentage increase in shoaling for enlarged channel for June.

Sensitivity analyses were performed to determine which variables affected the shoaling results given by the sediment simulations. The settling velocity (V_s) and critical shear stress for deposition (τ_{cd}) were varied as a means to influence the time particles remained in the water column. The domain is generally a depositional one and so the critical shear stress for erosion has little effect. Lowering the critical shear stress for deposition will allow the sediment to deposit at lower velocities. Lowering the settling velocity will keep the sediment in suspension longer and allow it to move further throughout the system. So by lowering both of these values independently, the possibility of high and low deposition throughout the length of the channel will be included in the sensitivity analyses. Both of these values were varied from a magnitude of 0.5 to 0.1 in order to determine the impact of extreme variation in these parameters. These variations did show a change in the volume of the deposited sediment within the channel among the configurations; however, this change was not large and the distribution of the sediment did not vary. The wind wave effects were included and removed as well. In this case, the wind waves would only be able to reintroduce sediment that had fallen in the shallows during the simulation since the initial state of the model was to have no sediment on the bed. Tables 9-16 give the ratios by which the shoaling volume

changed for the base and sensitivity runs for both flow conditions within the channel from Tabb's Bay to Bolivar Roads, within the channel along Atkinson Island, in the Bayport Flare and Channel, and in Barbour's Cut. The Bayport and Barbour's Cut channels were not enlarged in this study. The effects of enlargement are only from the Houston Ship Channel. The original conclusion of a 20 to 30% increase seems reasonable even considering the impact of this sensitivity.

Table 9. Shoaling volume ratios for channel and low flow.

Low Flow Hydrology				Channel Only
Change Factor		April	May	June
40 X 400	Base	1.28	1.19	1.17
vs	τ_{cd} = 0.1 Pa	1.34	1.02	0.99
45 X 530	V_s = 0.1 mm/s	1.22	1.21	1.23

Table 10. Shoaling volume ratios for channel and medium flow.

Medium Flow Hydrology				Channel Only
Change Factor		April	May	June
40 X 400	Base	1.34	1.18	1.07
vs	τ_{cd} = 0.1 Pa	1.54	0.99	0.91
45 X 530	V_s = 0.1 mm/s	1.31	1.21	1.19

Table 11. Shoaling volume ratios for Atkinson Island and low flow.

Low Flow Hydrology				Atkinson Island
Change Factor		April	May	June
40 X 400	Base	1.26	1.20	1.20
vs	τ_{cd} = 0.1 Pa	1.24	1.10	1.04
45 X 530	V_s = 0.1 mm/s	1.12	1.18	1.27

Table 12. Shoaling volume ratios for Atkinson Island and medium-flow.

Medium Flow Hydrology				Atkinson Island
Change Factor		April	May	June
40 X 400	Base	1.36	1.22	1.19
vs	τ_{cd} = 0.1 Pa	1.56	1.11	0.98
45 X 530	V_s = 0.1 mm/s	1.24	1.26	1.16

Table 13. Shoaling volume ratios for Bayport Channel and Flare and low flow.

Low Flow Hydrology				Bayport Flare
Change Factor		April	May	June
40 X 400	Base	1.08	0.99	1.07
vs	τ_{cd} = 0.1 Pa	1.09	0.94	1.07
45 X 530	V_s = 0.1 mm/s	0.93	1.13	1.21

Table 14. Shoaling volume ratios for Bayport Channel and Flare and medium flow.

Medium Flow Hydrology				Bayport Flare
Change Factor		April	May	June
40 X 400	Base	1.01	1.05	1.00
vs	τ_{cd} = 0.1 Pa	0.96	1.02	0.92
45 X 530	V_s = 0.1 mm/s	1.01	1.12	1.04

Table 15. Shoaling volume ratios for Barbour's Cut and low flow.

Low Flow Hydrology				Barbour's Cut
Change Factor		April	May	June
40 X 400	Base	0.98	0.99	1.04
vs	τ_{cd} = 0.1 Pa	1.00	1.01	1.05
45 X 530	V_s = 0.1 mm/s	0.95	0.97	1.08

Table 16. Shoaling volume ratios for Barbour's Cut and medium flow.

Medium Flow Hydrology				Barbour's Cut
Change Factor		April	May	June
40 X 400	Base	1.19	1.02	1.18
vs	τ_{cd} = 0.1 Pa	1.21	1.03	1.21
45 X 530	V_s = 0.1 mm/s	1.27	1.07	1.44

6 Summary and Conclusions

This report analyzes the likely causes of an increase in channel sedimentation due to the enlargement. It has been noted that a large increase has occurred since the enlarged channel has been in place and the question is whether or not this is a permanent increase or will the sedimentation rate drop back to more typical levels. This investigation takes place and is reported in stages. As each stage was completed the results were reported to the sponsor. This report is a compilation of each of these interim reports.

Dredging Analysis

The historic dredging records indicate that the shoaling rate was higher in the upper half of the bay channel than in the lower bay channel for the 40- x 400-ft (12.2- x 122-m) condition (this is in the region north of Redfish Reef and along Atkinson Island). In this upper reach, the sedimentation dredging volume decline is moderately steady throughout the 34 years of this channel configuration. In the lower bay, there was no strong trend over this period. Analysis of the freshwater flow to the system for the Trinity and San Jacinto rivers appears to show a slight increase in flow over this time period. However there is not a strong relationship shown between the long-term decline in required dredging and the freshwater inflow to the system.

It is possible that the channel stabilized over time causing less sediment to erode from its banks. Perhaps dredging practices improved so that less dredged material was allowed to reenter the channel. Another possibility is that the ship traffic has increased substantially over this time period. This increase would have an impact on the dredging since the vessels tend to cause resuspension of the bed material meaning that less sediment would remain on the bed. Also, a possibility for the drop in dredging over this period is the change in the sediment load from upstream sources to the bay. Ward and Armstrong (1993) found that the suspended solids in the upper Houston Ship Channel had dropped to one third of that from 25 years earlier. They attribute this reduction to improved waste treatment, altered land use, and impoundments on the principal rivers. Solis et. al. (1994) found that the Trinity River gauge at Romayor, TX (USGS gauge 08066500 located approximately 46 miles (74 km) upstream from the river's entrance to the bay) shows a significant reduction in downstream sediment inputs after the completion of Lake Livingston in 1968. There

actually is a decline in total suspended sediment throughout most of the bay.

Field Data

The sediment field data collection revealed finer sediments in the bed of the channel and at a considerable distance to the west, and also to the east beyond Atkinson Island. In the shallows near the channel the bed material was firmer, containing more sands. The area east of the channel (toward Atkinson Island) contained coarser material than to the west, which is likely a result of exposure to the waves caused by vessel traffic. The western edge of Atkinson Island contained sand and shells. Moving around the island to areas more protected, the bed material returned to finer sediments. What had previously been islands near the barge mooring basin had eroded to about a 6-ft (1.8-m) depth, which was also the approximate depth of the former disposal area just south of Atkinson Island. The bed material, which was quite firm, contained progressively more fines as one moved to the west of the channel out into the bay. This distance was greater than the effect of the vessels. It was consistent with the natural deposition pattern of a river flowing into a bay. The currents slowed down and the coarser materials settled first. Within the channel (in the region around Atkinson Island) the bed material became finer moving upland. The currents were small and the net drift near the bed was shown to be upland. So this sediment gradation was consistent with the net drift in the channel. In general, the suspended sediment concentrations were low during the survey. Retrieving samples behind vessels did not necessarily result in high concentrations. The highest measurements occurred behind a vessel that was toward the edge of the channel.

Vessel Effects

A vessel moving in the channel causes a depression in the water surface and return currents moving from the bow to the stern. The wavelength of this depression is roughly that of the vessel length. Generally this is much greater than the depth of the waterway. In this case, the wave is considered a long wave and travels at a speed of about $\left(gh\right)^{1/2}$. This speed is called the wave celerity. This depression wave moves away from the vessel. The speed of the wave is calculated using the local depth. If the vessel speed is less than the wave celerity, then the vessel impact may be felt ahead of the arrival of the vessel. Although it will be a diminished effect. If the vessel is traveling in the channel more quickly than the wave speed in the shallows, then the drawdown will arrive after the vessel. In this case

a bore can be formed. With a channel that is parallel to the shoreline (as is the case with the Houston Ship Channel) this drawdown is reflected at the shoreline and by the deeper water forming a series of bores perpendicular to the shore. The breaking wave, or bore, can cause high shear stresses and erosion.

This effect is apparent in the field sediment data that shows the grain sizes on the Atkinson Island side of the channel to be larger than on the opposite channel side. (The shoreline in places has been artificially armored as well.) This bed material is now coarser than the usual material found in channel deposits. The increased vessel speed associated with the channel enlargement does contribute to increased channel deposition. However, there have been problems with erosion of the islands along the Houston Ship Channel for some time before the channel enlargement.

A vessel moving in the channel will cause significant return currents that can cause erosion of the freshly deposited sediment. It was estimated that the return currents should decrease in the enlarged channel even though the vessel speed increases. Even so, the amount of erosion due to the vessels over a year was small compared to the annual deposition. It does not appear that at this point the decrease in direct erosion due to the vessel could be responsible for a large increase in deposition as noted in the dredging requirements.

Hydrodynamic and Sediment Model

Generally the Houston Ship Channel within Galveston Bay is flood-directed bed shear. However, for the base conditions in the months of June and July the shear is ebb-directed in the northern portion of the bay channel. This period of ebb-dominated shear is likely due to the drop in salinity in the ocean just before this time. The dense water is then tending to evacuate the system. The period of low salinity at the Gulf of Mexico is due to the freshwater currents from the Atchafalaya and Mississippi Rivers. For the other months and for the plan channel the bed shear is flood-directed. In June and July the plan condition shears are flood-directed, but much less strongly. So the effect of the drop in Gulf salinity still remains, but the larger channel prevents the complete reversal of direction of the bed shears.

The area around the junction of the Bayport Channel and the Houston Ship Channel shows a disrupted shear pattern. The shear is low in the flare for the Bayport Channel but also in the Houston Ship Channel near

that location. This does not appear when the shear is ebb-directed but does whenever the shear is flood-directed. There is a bend in the Houston Ship Channel just south of this junction that may be the cause.

The shear stresses throughout the upper bay are slightly lower in the plan condition. In the channel the plan condition showed a more significant reduction in shear. This reduced velocity and shear will result in a greater deposition potential.

The TABS-MDS sediment model was used as an analysis tool to determine where suspended sediment travels once it enters the channel and how this pattern changed with the enlarged channel. A single grain was modeled and an equal amount of sediment was introduced into both channel configurations over a 3-day time period. This simulation was conducted for April, May, and June flow conditions - each month modeled separately. The sediment parameters were determined from the field data collection.

The simulations show that the increase in sedimentation in the channel for the larger 45- x 530-ft (13.7- x 162-m) channel is in the range of 20-30 percent. In May and June the increase is concentrated in the upland area around Atkinson Island. In April the increase is concentrated farther oceanward in the Red Fish Reef region. This simulation does not include multiple grains or sediment entering the system from the Trinity or San Jacinto rivers.

Conclusion

This investigation considered the effects of vessels on erosion in and around the channel and the change in currents due to the channel enlargement. These processes will change the channel shoaling long-term. Other processes such as leakage from disposal sites, channel side slope relaxation, and material escape during dredging affect the required maintenance dredging over a short time period (a few dredging cycles). Using a sediment tracer and results from field data, this investigation of the long-term processes only revealed a potential increase in dredging on the order of 20 to 30 percent, which is considerably less than the 100 or more percent increase reported. This would imply that the large increase is due to a short-term process and is not likely to be a permanent state. These results rely upon a sediment model that is not validated to match field results. Sediment is introduced in an artificial manner as a tracer and not through loads in the river system. In the following study (Phase 2), the sediment model will be validated and used to refine the predictions.

References

Berger, R. C., R. T. McAdory, W. D. Martin, and J. H. Schmidt. 1995a. *Houston-Galveston Navigation Channels, Texas Project, Report 3, Three-dimensional hydrodynamic model verification.* Technical Report HL-92-7. Vicksburg, MS: U. S. Army Engineer Waterways Experiment Station.

Berger, R. C, R. T. McAdory, J. H. Schmidt, W. D. Martin, and L. H. Hauck. 1995b. *Houston-Galveston Navigation Channels, Texas Project, Report 4, Three-dimensional numerical modeling of hydrodynamics and salinity*. Technical Report HL-92-7. Vicksburg, MS: U. S. Army Engineer Waterways Experiment Station.

Bobb, W. H., R. A. Boland, and A. J. Banchetti. 1973. *Houston Ship Channel, Galveston Bay, Texas; Report 1: Hydraulic and salinity verification.* Technical Report H-73-12. Vicksburg, MS: U. S. Army Engineer Waterways Experiment Station.

Carrillo, A. R., M. S. Sarruff, and R. C. Berger. 2002. *Effects of adding barge lanes along Houston Ship Channel Through Galveston Bay, Texas.* ERDC/CHL TR-02-23. Vicksburg, MS: U. S. Army Engineer Research and Development Center.

Department of the Army Corps of Engineers. 2006. *Waterborne Commerce of the United States Calendar Year – 2004: Part 2, Waterways and Harbors, Gulf Coast, Mississippi River System and Antilles.* IWR-WCUS-04-2. New Orleans, LA: U.S. Army Corps of Engineer Waterborne Commerce Statistics Center.

Hart, E. D. (Mar) 1969. *Radioactive sediment tracer tests Houston Ship Channel, Houston, Texas.* Vicksburg, MS: U. S. Army Engineer Waterways Experiment Station.

Jansen, P. Ph., and J. B. Schijf. 1953. *18th International Navigation Congress, Rome, Permanent International Association of Navigation Congresses, Section 1, Communication 1*. 175-197.

Krone, R. B. (1962). *Flume studies of the transport of sediment in estuarial shoaling processes.* Final Report, Hydraulic Engrg. Laboratory and Sanitary Engrg. Res. Laboratory, University of California, Berkeley.

Maynord, S. T. (Oct. 12) 2000. *Letter Report on vessel forces at Goat Islands Restoration, Houston Ship Channel.* Prepared for the U.S Army Engineer District, Galveston. Vicksburg, MS: U. S. Army Engineer Research and Development Center, Coastal and Hydraulics Laboratory.

Maynord, S. T. 2005a. Personal communication with R. C. Berger, U. S. Army Engineer Research and Development Center, Vicksburg, MS.

Maynord, S. T. 2005b. *Evaluation of bank recession in existing and proposed channels of the Sabine Neches Waterway*. Memorandum of Record, prepared for the U. S. Army Engineer District, Galveston. Vicksburg, MS: U. S. Army Engineer Research and Development Center, Coastal and Hydraulics Laboratory.

Partheniades, E. 1962. *A study of erosion and deposition of cohesive soils in salt water*. Ph.D. diss., University of California, Berkeley.

Solis, R. S., W. L. Longley, and G. Malstaff. 1994. Influence of inflow on sediment deposition in delta and bay systems. In *Freshwater inflows to Texas bays and estuaries*, W. L. Longley, ed., 56-70. Austin, TX: Texas Water Development Board.

Teeter, A. M., D. Brister, J. W. Parman, and C. J. Coleman. 1999. Ashtabula River, Ohio, sedimentation study, Report 3: Erosion experiments on bed sediments. Technical Report CHL-99-9, Vicksburg, MS: U.S. Army Engineer Waterways Experiment Station.

Teeter, A. 2005. Computational Hydraulics and Transport, LLC. Personal communication with R. C. Berger, U.S. Army Engineer Research and Development Center, Vicksburg, MS.

Ward, G. H., Jr. 1980. Hydrography and circulation processes of Gulf estuaries. In *Estuaries and wetland processes with emphasis on modeling*, P. Hamilton and K. B. Macdonald, ed., 183-215. New York: Plenum Press.

Ward, G. H. and N. E. Armstrong. 1993. *Water and sediment quality of Galveston Bay*. Galveston Bay. National Estuary Program Conference 1993.

White, W. A., R. A. Morton, and C. W. Holmes. 2002. A comparison of factors controlling sedimentation rates and wetland loss in fluvial-deltaic systems, Texas Gulf coast. *Geomorphology* 44, 47-66.

Appendix A: Field Data Analyses

Tables A1-A3 give the date, time, point name, and State Plane coordinates for all of the data points taken by the field team during the data collection on 20-22 August 2004. Following these tables are figures showing reference locations for all of the data points (Figures A1-A4). Table A4 gives the suspended concentration and salinity for many of the field data points.

Sediment bulk density was determined using a pycnometer, following standard procedures. The results of this analysis are given in Table A5.

Table A6 along with Figures A5 and A6 show results of the Vertical Loop Sediment-Water Tunnel (VOST) analysis and Total Suspended Mass analysis. A detailed explanation of the VOST can be found in Teeter et al. (1999). The VOST tests allow for the determination of erosion rate for the sediment being analyzed.

Tables A7 through A18 as well as Figures A7 through A16 present results of sediment settling rates. These tests were performed in the standard method of determining the weight of sediment on the bed over time in order to deduce the remaining concentration in the water column.

Standard sieve analyses were performed on push core #1 and push core #3. These results are presented in Tables A19 and A20.

Figures A17 through A25 show the results of the COULTER® LS Particle Size Analyzer for several field data points. The generated plot gives a visual image of the grain size distribution at the given location.

The sand-silt/clay separation analysis is shown in Table A21 and Figure A26. The percentage of each material type is given for various data points around the channel and into the western shallows.

Table A1. Field data point information for 20 August 2004.

State Plane Coordinates			
NAD-83 Texas South Central (4204), US survey feet			
Date	Point Name	X coordinate	Y coordinate
8/20/2004	8:12:59	3330723.27	13847884.8
8/20/2004	9:00:09	3242272.51	13820918.2
8/20/2004	9:30:17	3242050.23	13820940.4
8/20/2004	9:30:18	3242047.47	13820943.1
8/20/2004	9:38:38	3241411.21	13820748.1
8/20/2004	9:43:19	3241327.98	13820640.6
8/20/2004	9:49:46	3241329.88	13820594.9
8/20/2004	9:51:32	3241285.22	13820565
8/20/2004	9:54:36	3241389.03	13820400.6
8/20/2004	10:03:41	3242393.04	13818555.1
8/20/2004	10:10:43	3242913.22	13819137.1
8/20/2004	10:13:45	3242716.2	13819388.8
8/20/2004	10:22:22	3244030.36	13818857.3
8/20/2004	10:29:55	3245281.24	13819169.3
8/20/2004	10:58:53	3244320.15	13815818.1
8/20/2004	11:03:27	3244583.78	13815865.2
8/20/2004	11:08:20	3245043.95	13816109.6
8/20/2004	11:10:42	3245369.17	13816356.4
8/20/2004	11:24:45	3247491.07	13811357.8
8/20/2004	11:36:23	3247077.98	13810943.9
8/20/2004	11:42:05	3246419.76	13810953.3
8/20/2004	11:45:54	3245862.1	13810894.6
8/20/2004	11:58:19	3248906.4	13807185.7
8/20/2004	12:04:47	3248288.74	13807290.6
8/20/2004	12:11:02	3247773.12	13807193.6
8/20/2004	12:14:18	3247449.68	13807060.3
8/20/2004	12:30:28	3248867.81	13802934.7
8/20/2004	12:34:17	3249297.42	13803056.7
8/20/2004	12:39:24	3250113.36	13803316.9
8/20/2004	12:43:01	3249763.18	13803177.4
8/20/2004	12:58:28	3252139.99	13798414.9
8/20/2004	13:01:34	3251577.37	13798328.3
8/20/2004	13:07:19	3250963.1	13798304.4
8/20/2004	13:07:21	3250960.18	13798304.3
8/20/2004	13:14:42	3250862.83	13797831.2
8/20/2004	13:38:06	3255695.51	13791238.4

8/20/2004	13:43:04	3254581.73	13790652
8/20/2004	13:52:57	3254134.45	13790181.1
8/20/2004	13:58:30	3253879.99	13790108.6
8/20/2004	14:14:10	3246023.46	13804228.7
8/20/2004	14:36:42	3248073.99	13820713.5
8/20/2004	14:43:35	3248213.44	13820088.1
8/20/2004	14:47:59	3248031.28	13819930.9

Table A2. Field data point information for 21 August 2004.

State Plane Coordinates			
NAD-83 Texas South Central (4204), US survey feet			
Date	Point Name	X coordinate	Y coordinate
8/21/2004	10:50:11	3242287.26	13820978.4
8/21/2004	11:00:31	3241888.14	13820729.6
8/21/2004	11:13:54	3242422.8	13818552.9
8/21/2004	11:21:19	3243508.28	13818894.4
8/21/2004	11:26:07	3244183.52	13819120.3
8/21/2004	11:39:40	3243414.15	13819062.8
8/21/2004	11:48:04	3244269.27	13815853.6
8/21/2004	11:55:11	3244588.61	13816215.8
8/21/2004	12:00:34	3245254.54	13816409.4
8/21/2004	12:12:36	3245418.22	13813909.2
8/21/2004	12:19:47	3246711.79	13810646.7
8/21/2004	12:25:40	3247103.04	13810975.8
8/21/2004	12:40:33	3247898.31	13812336.6
8/21/2004	13:12:39	3246677.68	13810631
8/21/2004	13:18:05	3246635.92	13810796.4
8/21/2004	13:20:49	3246122.84	13810465.5
8/21/2004	13:27:01	3246685.03	13810614.6
8/21/2004	13:38:52	3247735.36	13810301.7
8/21/2004	13:46:00	3248966.53	13807163.4
8/21/2004	13:49:16	3248284.92	13807205.9
8/21/2004	13:52:20	3247728.64	13807185.8
8/21/2004	13:55:06	3247426.76	13807076.5
8/21/2004	14:00:16	3248894.96	13802916.9
8/21/2004	14:03:36	3249289.17	13803046.7
8/21/2004	14:08:07	3248392.07	13803763.6
8/21/2004	14:14:38	3249808.53	13803141.8
8/21/2004	14:19:10	3250136.08	13803368.5

8/21/2004	14:31:56	3252139.47	13798449.7
8/21/2004	14:37:46	3251514.64	13798234
8/21/2004	14:45:15	3251141.47	13798334.5
8/21/2004	14:48:24	3250837.6	13798132.6
8/21/2004	15:06:52	3251557.92	13793036.5
8/21/2004	15:22:07	3251551.74	13793069.6
8/21/2004	15:33:38	3254405.26	13790458.9
8/21/2004	15:33:38	3254405.26	13790458.9
8/21/2004	15:44:34	3259121.34	13786438.8
8/21/2004	15:44:34	3259121.34	13786438.8
8/21/2004	16:09:26	3262670.04	13783473.6
8/21/2004	16:25:08	3262696.94	13780637.9
8/21/2004	16:30:07	3262266.83	13780324.8
8/21/2004	16:40:15	3261840.1	13780145.9

Table A3. Field data point information for 22 August 2004.

State Plane Coordinates			
NAD-83 Texas South Central (4204), US survey feet			
Date	Point Name	X coordinate	Y coordinate
8/22/2004	7:41:51	3241917.58	13802086
8/22/2004	8:06:00	3243896.29	13803519.9
8/22/2004	8:21:24	3246521.38	13805371.8
8/22/2004	8:48:36	3257080.3	13804196.1
8/22/2004	9:06:02	3253510.73	13807014.2
8/22/2004	9:26:35	3255865.85	13813601.1
8/22/2004	9:40:26	3253121.33	13818971.5
8/22/2004	10:02:35	3248054.73	13821831.8
8/22/2004	10:20:17	3244940.34	13819569.8
8/22/2004	11:02:25	3238355.16	13822505.4
8/22/2004	12:54:21	3245970.58	13815210.6
8/22/2004	13:08:07	3248407.1	13811501.9
8/22/2004	13:12:52	3248986.2	13807289.3
8/22/2004	13:18:46	3250363.32	13803790.6
8/22/2004	13:24:35	3248624.06	13802756.2
8/22/2004	13:29:21	3247186.98	13806829.2
8/22/2004	13:40:56	3245774.1	13810650.8
8/22/2004	13:52:43	3244610.73	13814099.2

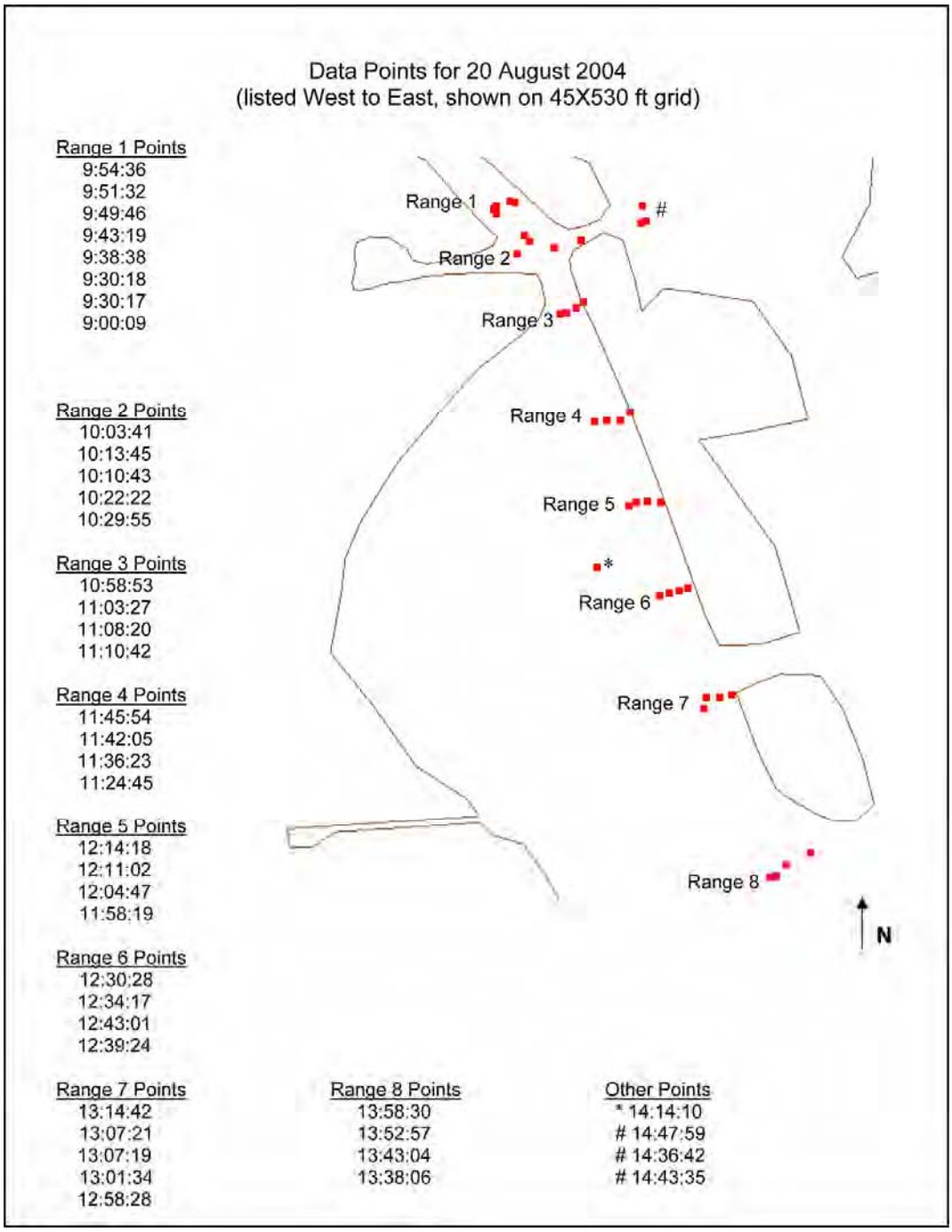

Figure A1. Reference map for 20 August 2004 data collection.

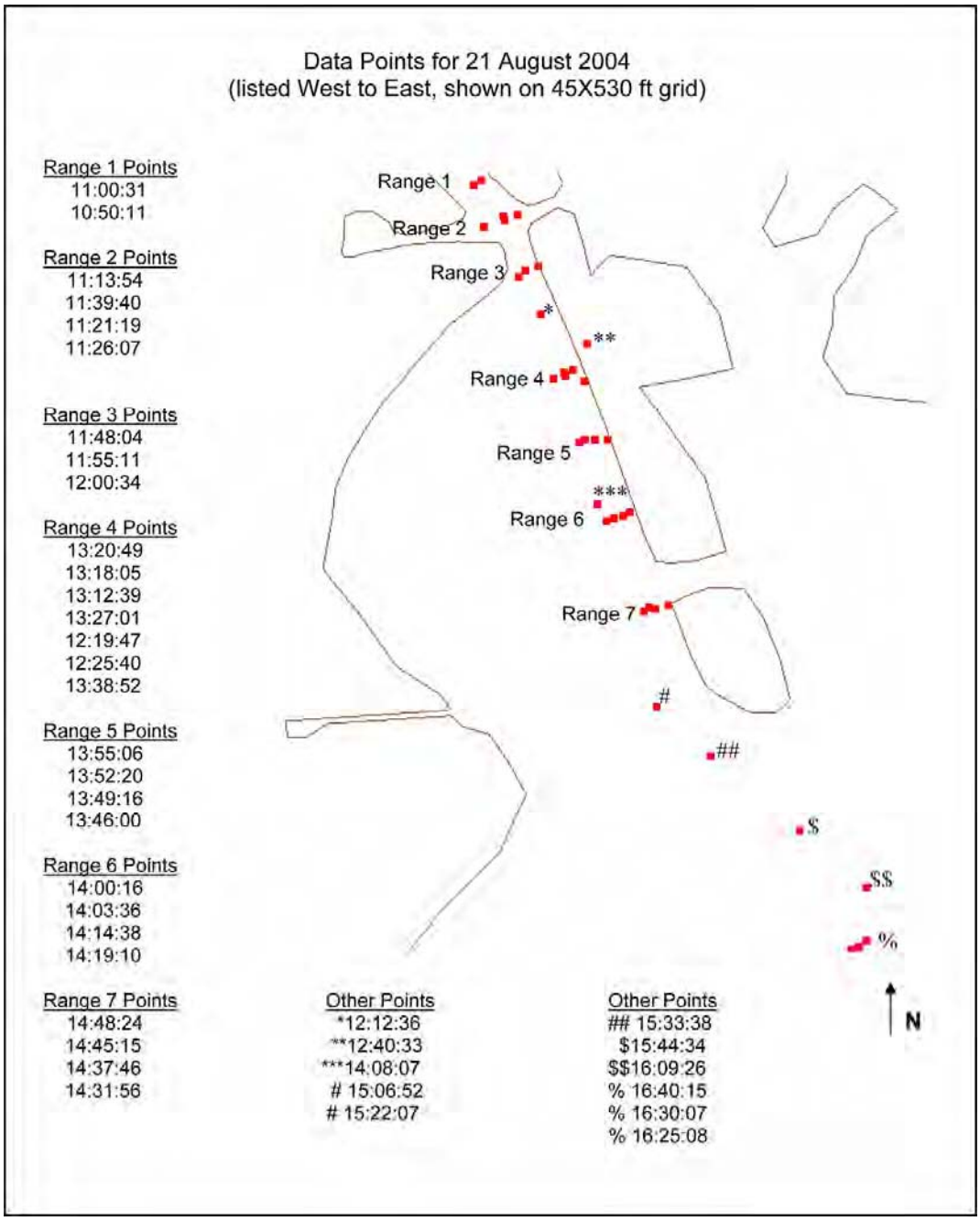

Figure A2. Reference map for 21 August 2004 data collection.

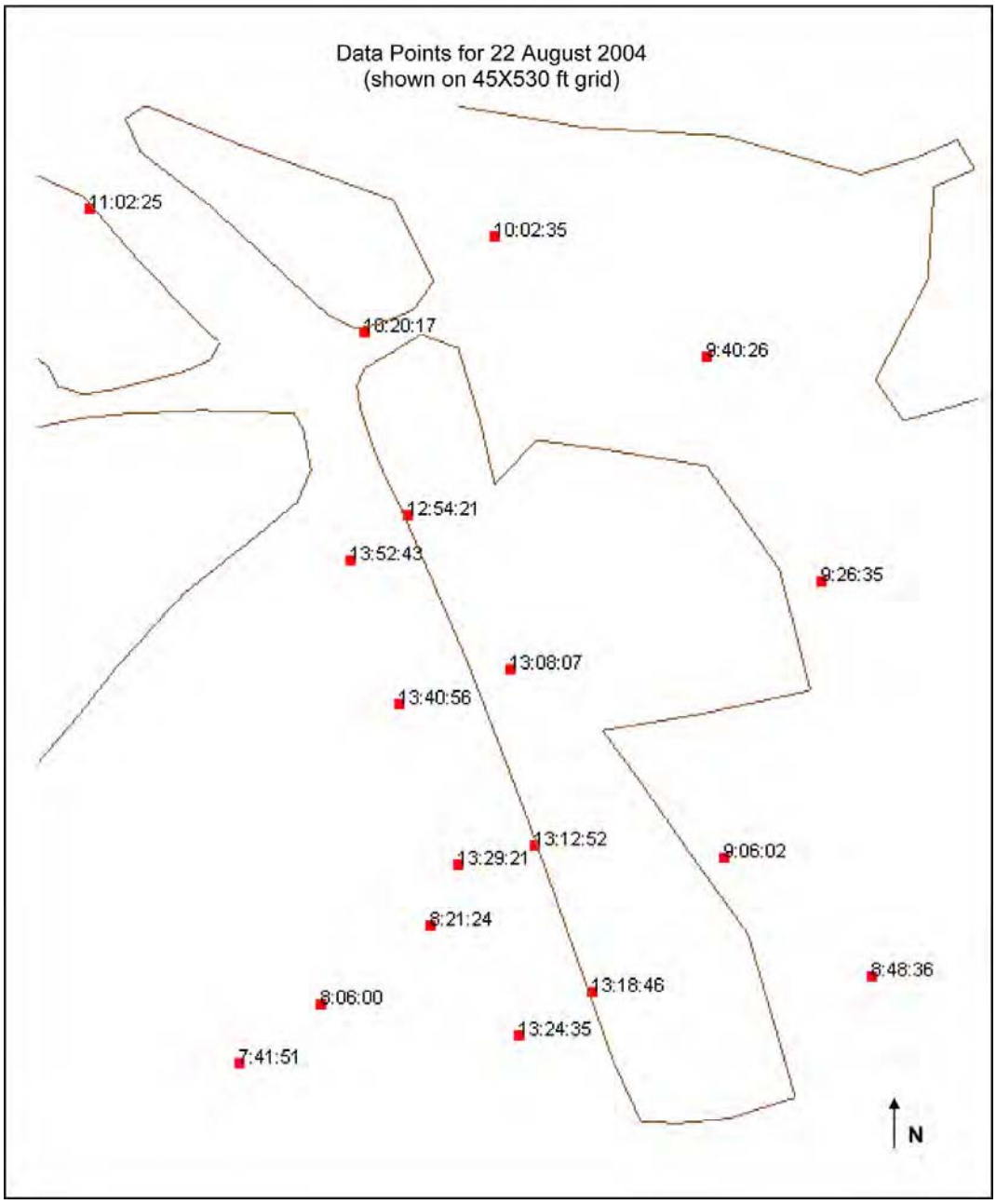

Figure A3. Reference map for 22 August 2004 data collection.

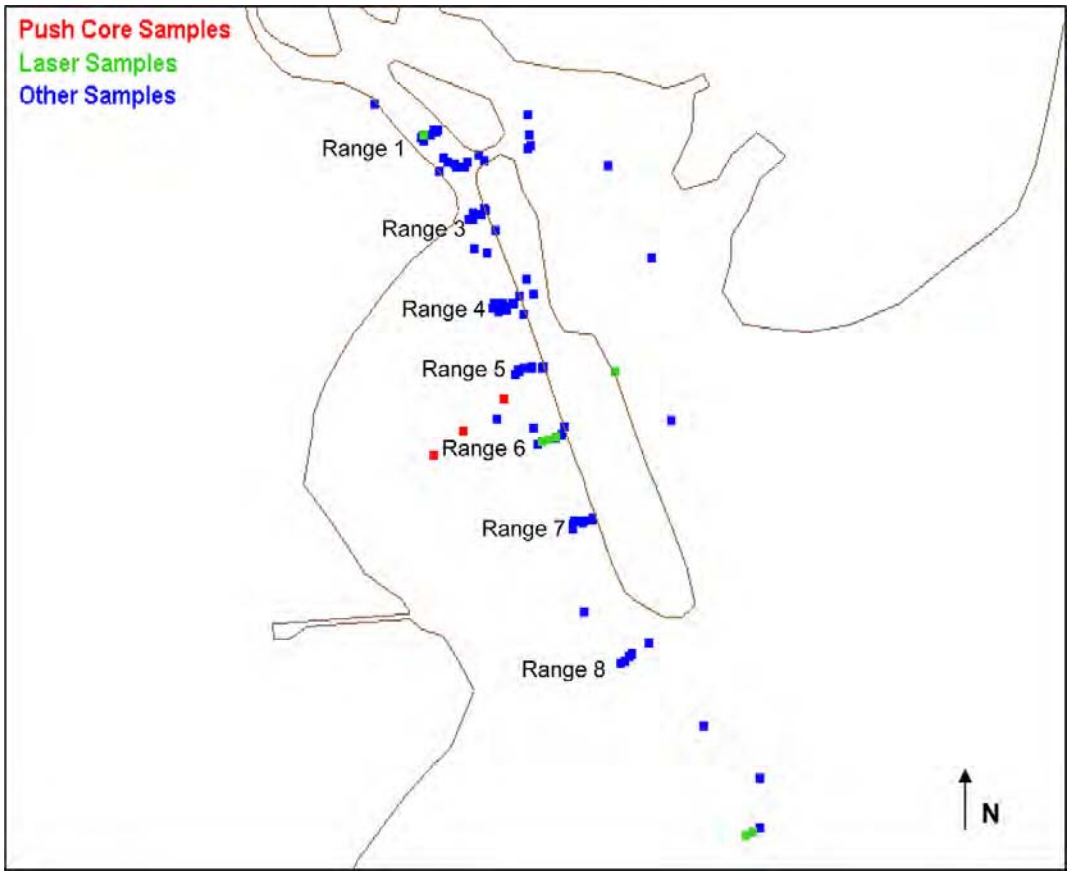

Figure A4. Field data sample types shown on the 40X400 ft grid.

Table A4. Suspended sediment sample analysis results.

SUSPENDED SEDIMENT SAMPLE ANALYSIS					
PROJECT: Houston Ship Channel					
P.I.: C. Berger					
Sampling		Range	Depth	Conc.	Salinity
Date	Time	Sta. #	ft.	mg/l	ppt
8/21/04	105011	1A	6 O.B.	19	14.96
8/21/04	105011	1A	3 O.B.	22	15.03
8/21/04	110031	1CL	3 O.B.	45	15.43
8/21/04	110031	1CL	25 B.S.	28	15.15
8/21/04	110364	2D	3 B.S.	18	14.99
8/21/04	110364	2D	3 O.B.	28	14.99
8/21/04	112119	2CL	3 O.B.	32	15.57
8/21/04	112607	2A	3 O.B.	24	15.08
8/21/04	113940	2CL	3 O.B.	49	15.56
8/21/04	114804	3D	3 O.B.	32	15.18
8/21/04	115511	3CL	3 O.B.	181	15.56
8/21/04	120834	3A	3 B.S.	53	15.20

8/21/04	121236	3CL	3 O.B.	469	15.90
8/21/04	121947	4CL	3 O.B.	290	16.42
8/21/04	121947	4CL	25 B.S.	41	15.87
8/21/04	122540		3 O.B.	25	15.30
8/21/04	124033		3 O.B.	22	15.22
8/21/04	131239		3 O.B.	107	15.82
8/21/04	131805		3 B.S.	46	15.67
8/21/04	132049		3 O.B.	35	15.54
8/21/04	132704		3 B.S.	58	15.65
8/21/04	132704		3 O.B.	2473	16.17
8/21/04	132704	Plume	3 B.S.	128	15.67
8/21/04	133852		3 O.B.	32	15.29
8/21/04	134600		3 O.B.	47	15.44
8/21/04	134916		3 O.B.	145	16.33
8/21/04	135220		3 O.B.	165	16.23
8/21/04	135506		3 O.B.	44	15.72
8/21/04	140006		3 O.B.	51	15.89
8/21/04	140336		3 O.B.	93	16.15
8/21/04	141438		3 O.B.	84	16.19
8/21/04	141910		3 O.B.	46	16.01
8/21/04	143156		3 O.B.	58	15.96
8/21/04	143746		3 O.B.	97	16.33
8/21/04	144515		3 O.B.	131	16.34
8/21/04	144824		3 O.B.	45	16.14
8/21/04	152207		4 O.B.	53	17.84
8/21/04	153338		3 O.B.	138	17.56
8/21/04	154434		3 O.B.	23	13.61
8/21/04	160926		4 B.S.	67	15.61
8/21/04	160926		3 O.B.	55	14.99
8/21/04	162508		3 B.S.	46	15.91
8/21/04	163007		3 O.B.	56	16.25
8/21/04	164015		3 O.B.	202	17.06
8/22/04	080600	Tube #2	3 O.B.	27	15.64
8/22/04	080600	Tube #3	3 O.B.	73	15.62
8/22/04	084836		3 B.S.	22	11.52
8/22/04	092635		3 O.B.	29	12.95
8/22/04	094026		3 B.S.	34	14.72
8/22/04	100235		2.5 B.S.	32	15.38
8/22/04	102017		2.5 B.S.	21	15.31
8/22/04	110225		3 B.S.	33	14.94

Table A5. Bulk density analysis results for several field data points.

BULK DENSITY USING PYCNO BOTTLES									
PROJECT NAME: Houston Ship Channel						P.I. : C. Berger			
Date of Project: Aug. 04						ANALYST: D.B.			
						Analysis date:		9/15/04	
Pycno. bottle #	Sample Date	Sample ID	Temp. C	Tare wt. g	Bottle wt. + sed. g	Bottle wt. + sed. + water g	Density of water	Volume Pycno. bottle	Sediment Density g/cm3
202	8/20/04	090009 10'	22.5	29.6822	53.4343	65.1580	0.998	24.9579	1.798
204	8/20/04	093838 48'	22.5	27.3518	44.8146	55.7142	0.998	25.6506	1.186
205	8/20/04	112445 6'	22.5	28.3951	50.5627	64.0250	0.998	24.9066	1.942
208	8/20/04	114554 11'	22.5	27.3689	49.8874	61.9600	0.998	24.9452	1.753
209	8/20/04	121418 13'	22.5	27.9256	50.4893	63.2080	0.998	25.3391	1.791
202	8/20/04	123028 11'	22.5	29.6817	50.1194	63.0370	0.998	24.9579	1.701
204	8/20/04	123417 39'	22.5	27.3517	49.2058	58.5816	0.998	25.6506	1.344
205	8/20/04	123924 9'	22.5	28.3950	49.6617	63.4850	0.998	24.9066	1.924
208	8/20/04	124301 39'	22.5	27.3688	50.8687	59.4858	0.998	24.9452	1.441
209	8/21/04	163007 13'	22.5	27.9258	44.1559	57.1981	0.998	25.3391	1.323
202	8/21/04	164015 51'	22.5	29.6820	46.0553	57.1184	0.998	24.9579	1.180
204	8/22/04	090602 4'	22.5	27.3518	46.5548	59.2823	0.998	25.6506	1.489
205	8/22/04	080600 9.5' (core tube #2)	22.5	28.3948	46.0233	59.5205	0.998	24.9066	1.549
10/26/04									
202	8/22/04	074151 10.5' (core tube #1)	23.0	29.6821	45.7397	59.1796	0.998	24.9579	1.397
11/3/04									
202	8/22/04	082124 9' (core tube #3)	22.2	29.6820	50.8004	63.0060	0.998	24.9579	1.659

Table A6. Push core sample analysis results.

Project Name: Houston Ship Channel				P.I.: C. Berger				
Date of Project: Aug. 20-22-04				Date of Analysis:		Vloop ran 10/19/04		
Sample I.D.: push core sample #1 surface slice						TSM ran 10/25/04		
	8/22/04 074151 10.5 ft.			Salinity	~15 ppt			
						Gross wt.		
		Shear	Time	Sample	Tare wt.	(g)	Net wt.	Conc.
Bottle #	Voltage	Stress	(min.)	Volume	(g)	filter + sed	(g)	(g/l)
1	3	0.35	10	99	0.0149	0.0150	0.0001	0.0010
2	4	0.50	10	100	0.0152	0.0153	0.0001	0.0010
3	5	0.67	10	99	0.0151	0.0152	0.0001	0.0010
4	6	0.83	10	99	0.0151	0.0153	0.0002	0.0020
5	7	0.98	10	98	0.0147	0.0149	0.0002	0.0020
6	8	1.14	10	100	0.0151	0.0153	0.0002	0.0020
7	8	1.14	15	100	0.0151	0.0157	0.0006	0.0060
8	8	1.14	20	100	0.0148	0.0157	0.0009	0.0090
9	8	1.14	25	98	0.0148	0.0157	0.0009	0.0092
10	8	1.14	30	99	0.0149	0.0158	0.0009	0.0091
11	8	1.14	35	100	0.0152	0.0160	0.0008	0.0080
12	8	1.14	40	100	0.0149	0.0159	0.0010	0.0100
13	8	1.14	45	99	0.0152	0.0161	0.0009	0.0091
14	8	1.14	50	99	0.0150	0.0159	0.0009	0.0091
15	9	1.29	5	100	0.0150	0.0159	0.0009	0.0090
16	9	1.29	10	100	0.0150	0.0161	0.0011	0.0110
17	9	1.29	15	99	0.0149	0.0162	0.0013	0.0131
Project Name: Houston Ship Channel				P.I.: C. Berger				
Date of Project: Aug. 20-22-04				Date of Analysis:		Vloop ran 10/28/04		
Sample I.D.: push core sample #3 surface slice						TSM ran 11/1/04		
	8/22/04 082124 9.0 ft.			Salinity	~15 ppt			
						Gross wt.		
		Shear	Time	Sample	Tare wt.	(g)	Net wt.	Conc.
Bottle #	Voltage	Stress	(min.)	Volume	(g)	filter + sed	(g)	(g/l)
1	3	0.35	10	97	0.0148	0.0149	0.0001	0.0010
2	4	0.50	10	99	0.0145	0.0146	0.0001	0.0010
3	5	0.67	10	97	0.0146	0.0147	0.0001	0.0010
4	6	0.83	10	96	0.0148	0.0149	0.0001	0.0010
5	7	0.98	10	97	0.0147	0.0148	0.0001	0.0010
6	8	1.14	10	100	0.0147	0.0148	0.0001	0.0010
7	9	1.29	10	100	0.0148	0.0149	0.0001	0.0010
8	10	1.45	10	97	0.0148	0.0149	0.0001	0.0010

9	11	1.62	10	98	0.0148	0.0151	0.0003	0.0031
10	12	1.79	10	98	0.0156	0.0159	0.0003	0.0031
11	12	1.79	15	100	0.0156	0.0158	0.0002	0.0020
12	13	1.98	5	99	0.0156	0.0160	0.0004	0.0040
13	13	1.98	10	98	0.0155	0.0161	0.0006	0.0061
14	13	1.98	15	100	0.0157	0.0166	0.0009	0.0090
15	14	2.15	5	100	0.0154	0.0172	0.0018	0.0180
16	14	2.15	10	100	0.0155	0.0181	0.0026	0.0260
17	14	2.15	15	98	0.0156	0.0197	0.0041	0.0418
18	14	2.15	20	98	0.0156	0.0197	0.0041	0.0418

Push Core #1

Volume of Water (L) = 6
Surface Area of Sample (cm^2)= 20.2683

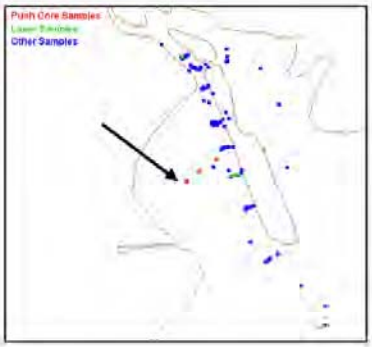

Conc. (g/l)	Conc. (mg/l)	Time (min.)	Total Time (min.)	Shear Stress
0.0010	1.01	10	10	0.35
0.0010	1.00	10	20	0.50
0.0010	1.01	10	30	0.67
0.0020	2.02	10	40	0.83
0.0020	2.04	10	50	0.98
0.0020	2.00	10	60	1.14
0.0060	6.00	15	75	1.14
0.0090	9.00	20	95	1.14
0.0092	9.18	25	120	1.14
0.0091	9.09	30	150	1.14
0.0080	8.00	35	185	1.14
0.0100	10.00	40	225	1.14
0.0091	9.09	45	270	1.14
0.0091	9.09	50	320	1.14
0.0090	9.00	5	325	1.29
0.0110	11.00	10	335	1.29
0.0131	13.13	15	350	1.29

Shear Stress (Pa)	Change in Conc. (mg/L)	Change in Mass (mg)	Erosion Time (min)	Erosion Rate (mg/cm^2*min)
0.6700	0.0100	0.06	30	9.87E-05
0.9800	0.0900	0.54	30	0.000888
1.1400	7.0500	42.3	260	0.008027
1.2900	4.1300	24.78	25	0.048904

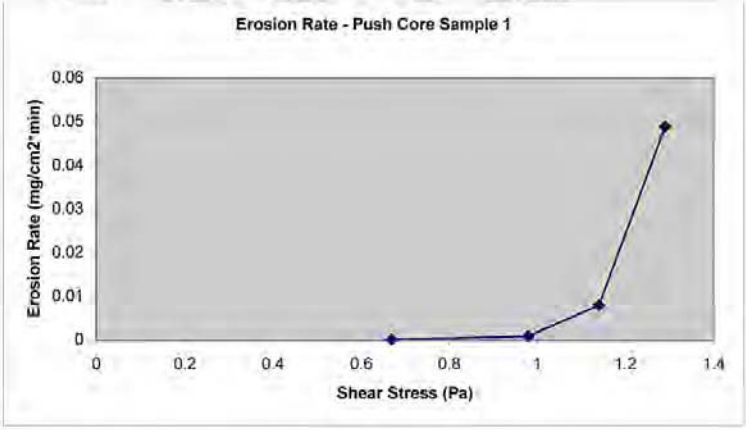

Figure A5. Erosion rate analysis for push core #1.

Push Core #3

Volume of Water (L) = 6
Surface Area of Sample (cm^2)= 20.2683

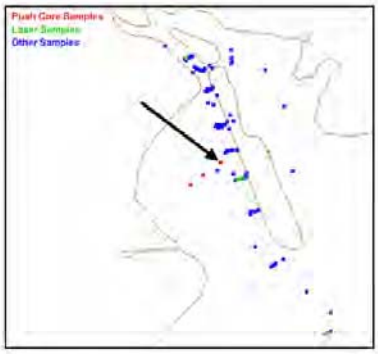

Conc. (g/l)	Conc. (mg/l)	Time (min.)	Total Time (min.)	Shear Stress
0.0010	1.03	10	10	0.35
0.0010	1.01	10	20	0.50
0.0010	1.03	10	30	0.67
0.0010	1.04	10	40	0.83
0.0010	1.03	10	50	0.98
0.0010	1.00	10	60	1.14
0.0010	1.00	10	70	1.29
0.0010	1.03	10	80	1.45
0.0031	3.06	10	90	1.62
0.0031	3.06	10	100	1.79
0.0020	2.00	15	115	1.79
0.0040	4.04	5	120	1.98
0.0061	6.12	10	130	1.98
0.0090	9.00	15	145	1.98
0.0180	18.00	5	150	2.15
0.0260	26.00	10	160	2.15
0.0418	41.84	15	175	2.15
0.0418	41.84	20	195	2.15

Shear Stress (Pa)	Change in Conc. (mg/L)	Change in Mass (mg)	Erosion Time (min)	Erosion Rate (mg/cm^2*min)
1.7900	2.0300	12.18	35	0.01717
1.9800	5.9400	35.64	30	0.058614
2.1500	32.8400	197.04	50	0.194432

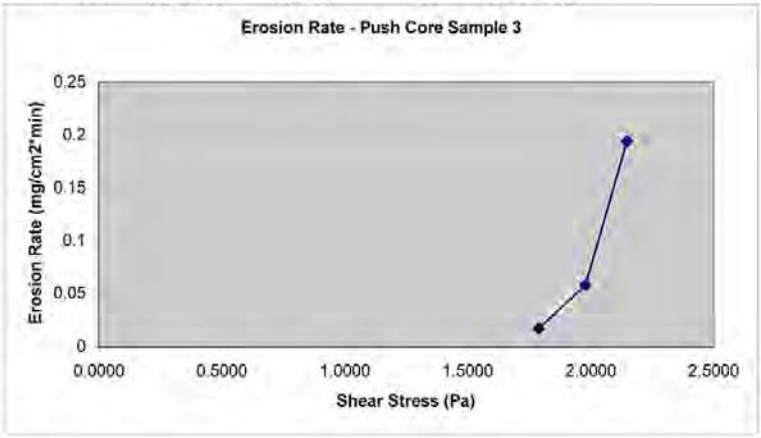

Figure A6. Erosion rate analysis for push core #3.

Table A7. Settling test results for field data point 114554, run 1.

SETTLING TESTS-SUSPENDED SEDIMENT ANALYSIS						1
PROJECT: Houston Ship Channel					Instant Ocean water ~15ppt	
Sample I.D.: 114554 11 ft.						12/8/04
Conc.:		3.4 ml/5 gal. Conc. target:50 mg/l			Analyst:DB	D.B
Height of water in column=186.0 cm				BWD=1.753		
		Vol	Weight, grams			Conc
Time	Notes	ml	Tare	Gross	Net	mg/l
0 min	jerrican	50	0.0156	0.0180	0.0024	48
0 min	column	45	0.0154	0.0186	0.0032	71
20		51	0.0156	0.0190	0.0034	67
40		52	0.0156	0.0183	0.0027	52
60		51	0.0157	0.0180	0.0023	45
90		50	0.0158	0.0179	0.0021	42
120		51	0.0156	0.0175	0.0019	37
150		47	0.0157	0.0173	0.0016	34
200		52	0.0156	0.0173	0.0017	33
250		50	0.0159	0.0175	0.0016	32
300		46	0.0159	0.0173	0.0014	30
350		50	0.0156	0.0171	0.0015	30

Table A8. Settling test results for field data point 114554, run 2.

SETTLING TESTS-SUSPENDED SEDIMENT ANALYSIS						2
PROJECT: Houston Ship Channel					Instant Ocean water ~15ppt	
Sample I.D.: 114554 11 ft.						12/9/04
Conc.:	13.6 ml/5 gal. Conc. target:200 mg/l				Analyst:	D.B.
Height of water in column=186.0 cm				BWD=1.753		
		Vol	Weight, grams			Conc
Time	Notes	ml	Tare	Gross	Net	mg/l
0 min	jerrican	50	0.0155	0.0248	0.0093	186
0 min	column	47	0.0155	0.0247	0.0092	196
20		50	0.0158	0.0229	0.0071	142
40		50	0.0157	0.0217	0.0060	120
60		53	0.0157	0.0214	0.0057	108
90		46	0.0155	0.0201	0.0046	100
120		45	0.0156	0.0200	0.0044	98
150		50	0.0155	0.0203	0.0048	96
200		50	0.0157	0.0200	0.0043	86
250		50	0.0158	0.0196	0.0038	76
300		50	0.0156	0.0186	0.0030	60
350		47	0.0158	0.0181	0.0023	49

Table A9. Settling test results for field data point 114554, run 3.

SETTLING TESTS-SUSPENDED SEDIMENT ANALYSIS						3
PROJECT: Houston Ship Channel					Instant Ocean water ~15ppt	
Sample I.D.: 114554 11 ft.						12/13/04
Conc.:	13.6 + 20.6= 34.2 ml/5 gal. Conc. target: 500 mg/l Analyst: D.B.					
Height of water in column=186.0 cm				BWD=1.753		
		Vol	Weight, grams			Conc
Time	Notes	ml	Tare	Gross	Net	mg/l
0 min	jerrican	50	0.0156	0.0603	0.0447	894
0 min	column	51	0.0158	0.0503	0.0345	676
20		51	0.0157	0.0339	0.0182	357
40		53	0.0156	0.0309	0.0153	289
60		50	0.0156	0.0291	0.0135	270
90		48	0.0158	0.0282	0.0124	258
120		47	0.0156	0.0264	0.0108	230
150		50	0.0155	0.0233	0.0078	156
200		50	0.0157	0.0208	0.0051	102
250		46	0.0157	0.0193	0.0036	78
300		50	0.0159	0.0189	0.0030	60
350		54	0.0158	0.0183	0.0025	46

Table A10. Settling test results for field data point 163007, run 1.

SETTLING TESTS-SUSPENDED SEDIMENT ANALYSIS					1	
PROJECT: Houston Ship Channel					Instant Ocean water ~15ppt	
Sample I.D.: 163007 13 ft.						12/8/04
Conc.:		3.4 ml/5 gal. Conc. target:50 mg/l			Analyst:	D.B.
Height of water in column=186.0 cm				BWD=1.323		
Time	Notes	Vol ml	Weight, grams Tare	Gross	Net	Conc mg/l
0 min	jerrican	50	0.0156	0.0200	0.0044	88
0 min	column	56	0.0156	0.0213	0.0057	102
20		53	0.0155	0.0217	0.0062	117
40		51	0.0154	0.0201	0.0047	92
60		54	0.0155	0.0200	0.0045	83
90		51	0.0155	0.0197	0.0042	82
120		56	0.0156	0.0199	0.0043	77
150		54	0.0156	0.0196	0.0040	74
200		56	0.0155	0.0196	0.0041	73
250		56	0.0156	0.0194	0.0038	68
300		52	0.0156	0.0188	0.0032	62
350		51	0.0156	0.0185	0.0029	57

Table A11. Settling test results for field data point 163007, run 2.

SETTLING TESTS-SUSPENDED SEDIMENT ANALYSIS						2
PROJECT: Houston Ship Channel					Instant Ocean water ~15ppt	
Sample I.D.: 163007 13 ft.						12/9/04
Conc.:		13.6 ml/5 gal. Conc. target:200 mg/l			Analyst:	D.B.
Height of water in column=186.0 cm				BWD=1.323		
		Vol	Weight, grams			Conc
Time	Notes	ml	Tare	Gross	Net	mg/l
0 min	jerrican	50	0.0155	0.0253	0.0098	196
0 min	column	48	0.0155	0.0280	0.0125	260
20		55	0.0154	0.0281	0.0127	231
40		50	0.0154	0.0263	0.0109	218
60		52	0.0153	0.0263	0.0110	212
90		49	0.0155	0.0258	0.0103	210
120		53	0.0155	0.0264	0.0109	206
150		52	0.0154	0.0245	0.0091	175
200		50	0.0156	0.0223	0.0067	134
250		51	0.0156	0.0202	0.0046	90
300		54	0.0156	0.0191	0.0035	65
350		54	0.0156	0.0185	0.0029	54

Table A12. Settling test results for field data point 163007, run 3.

SETTLING TESTS-SUSPENDED SEDIMENT ANALYSIS						3
PROJECT: Houston Ship Channel					Instant Ocean water 15ppt	
Sample I.D.: 163007 13 ft.						12/13/04
Conc.:	13.6 + 20.6= 34.2 ml/5 gal. Conc. target: 500 mg/l Analyst: D.B.					
Height of water in column=186.0 cm				BWD=1.323		
		Vol	Weight, grams			Conc
Time	Notes	ml	Tare	Gross	Net	mg/l
0 min	jerrican	50	0.0157	0.0489	0.0332	664
0 min	column	48	0.0156	0.0529	0.0373	777
20		50	0.0156	0.0546	0.0390	780
40		56	0.0156	0.0601	0.0445	795
60		53	0.0156	0.0576	0.0420	792
90		53	0.0155	0.0534	0.0379	715
120		55	0.0158	0.0398	0.0240	436
150		56	0.0157	0.0271	0.0114	204
200		54	0.0156	0.0217	0.0061	113
250		53	0.0155	0.0199	0.0044	83
300		55	0.0158	0.0195	0.0037	67
350		54	0.0154	0.0185	0.0031	57

Table A13. Settling test results for field data point 090009, run 1.

SETTLING TESTS-SUSPENDED SEDIMENT ANALYSIS						1
PROJECT: Houston Ship Channel					Instant Ocean water ~15ppt	
Sample I.D.: 090009 10 ft.						12/14/04
Conc.:	3.4 ml/5 gal. Conc. target:50 mg/l				Analyst:	D.B.
Height of water in column=186.0 cm				BWD=1.798		
		Vol	Weight, grams			Conc
Time	Notes	ml	Tare	Gross	Net	mg/l
0 min	jerrican	50	0.0156	0.0180	0.0024	48
0 min	column	48	0.0156	0.0193	0.0037	77
20		50	0.0156	0.0169	0.0013	26
40		53	0.0156	0.0168	0.0012	23
60		48	0.0156	0.0166	0.0010	21
90		48	0.0156	0.0166	0.0010	21
120		47	0.0157	0.0166	0.0009	19
150		48	0.0156	0.0165	0.0009	19
200		47	0.0157	0.0166	0.0009	19
250		46	0.0155	0.0163	0.0008	17
300		51	0.0155	0.0163	0.0008	16
350		50	0.0156	0.0164	0.0008	16

Table A14. Settling test results for field data point 090009, run 2.

SETTLING TESTS-SUSPENDED SEDIMENT ANALYSIS						2
PROJECT: Houston Ship Channel					Instant Ocean water ~15ppt	
Sample I.D.: 090009 10 ft.						12/15/04
Conc.:	13.6 ml/5 gal. Conc. target:200 mg/l				Analyst:	D.B.
Height of water in column=186.0 cm				BWD=1.798		
		Vol	Weight, grams			Conc
Time	Notes	ml	Tare	Gross	Net	mg/l
0 min	jerrican	50	0.0155	0.0217	0.0062	124
0 min	column	47	0.0157	0.0212	0.0055	117
20		50	0.0153	0.0195	0.0042	84
40		52	0.0155	0.0194	0.0039	75
60		48	0.0156	0.0187	0.0031	65
90		47	0.0154	0.0182	0.0028	60
120		46	0.0158	0.0185	0.0027	59
150		48	0.0159	0.0186	0.0027	56
200		49	0.0154	0.0181	0.0027	55
250		49	0.0156	0.0181	0.0025	51
300		46	0.0158	0.0181	0.0023	50
350		51	0.016	0.0184	0.0024	47

Table A15. Settling test results for field data point 090009, run 3.

SETTLING TESTS-SUSPENDED SEDIMENT ANALYSIS						3
PROJECT: Houston Ship Channel					Instant Ocean water ~15ppt	
Sample I.D.: 090009 10 ft.					12/16/04	
Conc.:	13.6 + 20.6= 34.2 ml/5 gal. Conc. target: 500 mg/l Analyst: D.B.					
Height of water in column=186.0 cm				BWD=1.798		
		Vol	Weight, grams			Conc
Time	Notes	ml	Tare	Gross	Net	mg/l
0 min	jerrican	50	0.0154	0.0306	0.0152	304
0 min	column	47	0.0152	0.0261	0.0109	232
20		51	0.0154	0.0247	0.0093	182
40		47	0.0151	0.0225	0.0074	157
60		51	0.0155	0.0228	0.0073	143
90		51	0.0153	0.0223	0.0070	137
120		46	0.0155	0.0216	0.0061	133
150		48	0.0155	0.0216	0.0061	127
200		50	0.0153	0.0208	0.0055	110
250		50	0.0154	0.0194	0.0040	80
300		47	0.0156	0.0185	0.0029	62
350		49	0.0153	0.0180	0.0027	55

Table A16. Settling test results for field data point 090602, run 1.

SETTLING TESTS-SUSPENDED SEDIMENT ANALYSIS						1
PROJECT: Houston Ship Channel				Instant Ocean water ~15ppt		
Sample I.D.: 090602 4.0 ft.					12/14/04	
			3.4 ml/5 gal. Conc. target:50 mg/l			
Conc.:					Analyst:	D.B.
Height of water in column=186.0 cm				BWD=1.489		
		Vol	Weight, grams			Conc
Time	Notes	ml	Tare	Gross	Net	mg/l
0 min	jerrican	50	0.0156	0.0209	0.0053	106
0 min	column	48	0.0157	0.0235	0.0078	163
20		52	0.0156	0.0219	0.0063	121
40		54	0.0156	0.0194	0.0038	70
60		53	0.0155	0.0184	0.0029	55
90		49	0.0157	0.0183	0.0026	53
120		50	0.0157	0.0181	0.0024	48
150		54	0.0158	0.0183	0.0025	46
200		53	0.0154	0.0178	0.0024	45
250		57	0.0155	0.0180	0.0025	44
300		52	0.0153	0.0177	0.0024	46
350		60	0.0154	0.0182	0.0028	47

Table A17. Settling test results for field data point 090602, run 2.

SETTLING TESTS-SUSPENDED SEDIMENT ANALYSIS						2
PROJECT: Houston Ship Channel					Instant Ocean water ~15ppt	
Sample I.D.: 090602 4.0 ft.						12/15/04
Conc.:	13.6 ml/5 gal. Conc. target:200 mg/l Analyst: D.B.					
Height of water in column=185.0 cm					BWD=1.489	
		Vol	Weight, grams			Conc
Time	Notes	ml	Tare	Gross	Net	mg/l
0 min	jerrican	50	0.0154	0.0334	0.0180	360
0 min	column	52	0.0157	0.0389	0.0232	446
20		50	0.0155	0.0363	0.0208	416
40		59	0.0159	0.0324	0.0165	280
60		57	0.0152	0.0284	0.0132	232
90		51	0.0154	0.0267	0.0113	222
120		53	0.0155	0.0266	0.0111	209
150		53	0.0159	0.0257	0.0098	185
200		50	0.0158	0.0232	0.0074	148
250		52	0.0152	0.0205	0.0053	102
300		51	0.0155	0.0193	0.0038	75
350		59	0.0155	0.0191	0.0036	61

Table A18. Settling test results for field data point 090602, run 3.

SETTLING TESTS-SUSPENDED SEDIMENT ANALYSIS						3
PROJECT: Houston Ship Channel					Instant Ocean water ~15ppt	
Sample I.D.: 090602 4.0 ft.					12/16/04	
Conc.:	13.6 + 20.6= 34.2 ml/5 gal. Conc. target: 500 mg/l Analyst: D.B.					
Height of water in column=186.0 cm				BWD=1.489		
		Vol	Weight, grams			Conc
Time	Notes	ml	Tare	Gross	Net	mg/l
0 min	jerrican	51	0.0154	0.0737	0.0583	1143
0 min	column	48	0.0153	0.0649	0.0496	1033
20		53	0.0154	0.0597	0.0443	836
40		55	0.0155	0.0521	0.0366	665
60		52	0.0154	0.0449	0.0295	567
90		51	0.0153	0.0386	0.0233	457
120		53	0.0153	0.0304	0.0151	285
150		52	0.0156	0.0242	0.0086	165
200		56	0.0153	0.0218	0.0065	116
250		52	0.0155	0.0199	0.0044	85
300		55	0.0157	0.0192	0.0035	64
350		54	0.0152	0.0180	0.0028	52

Table 18. Settling test results for field data point 090602, run 3.

090009_1

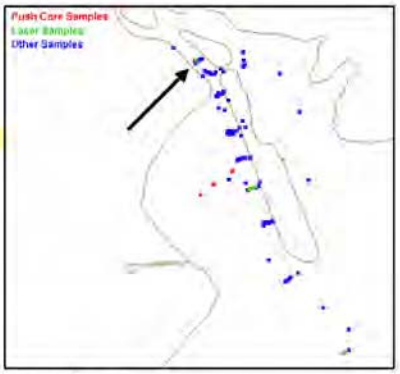

Settling Chamber Experiment Results and Settling Velocity Determination
20-Jun-05
Jennifer N. Tate

INPUT:

	Time (min)	Concentration (g/l)
1	#	0.048
2	#	0.077083333
3	20	0.026
4	40	0.022641509
5	60	0.020833333
6	90	0.020833333
7	120	0.019148936
8	150	0.01875
9	200	0.019148936
10	250	0.017391304
11	300	0.015686275
12	350	0.016
13	#	#
14	#	#
15	#	#
16	#	#
17	#	#
18	#	#
19	#	#
20	#	#
21	#	#
22	#	#
23	#	#
24	#	#
25	#	#
26	#	#
27	#	#
28	#	#
29	#	#
30	#	#

CALCULATE:

Fraction of Concentration Removed	Ln (Time)
#	#
#	#
0.458333333	2.9957323
0.528301887	3.6888795
0.565972222	4.0943446
0.565972222	4.4998097
0.60106383	4.7874917
0.609375	5.0106353
0.60106383	5.2983174
0.637681159	5.5214609
0.673202614	5.7037825
0.666666667	5.8579332
#	#
#	#
#	#
#	#
#	#
#	#
#	#
#	#
#	#
#	#
#	#
#	#
#	#
#	#
#	#
#	#
#	#
#	#

Slope	Y-intercept	Roots
0.0680755	0.26768812	-3.5102

Chart 1

A	B	C
-0.03	0.3417	-0.3871

z-values	b =	decile check
0.1	0.05830689	OK
0.2	0.04630689	OK
0.3	0.03430689	OK
0.4	0.02230689	OK
0.5	0.01030689	OK
0.6	-0.0016931	Imaginary
0.7	-0.0136931	Imaginary
0.8	-0.0256931	Imaginary
0.9	-0.0376931	Imaginary

mm/sec

Ws Deciles
5.833
3.764
2.284
1.256
0.566
#NUM!
#NUM!
#NUM!
#NUM!

Chart 2

A	B	C
-0.0453	0.4138	-0.3757

z-values	b =	decile check
0.1	0.0850336	OK
0.2	0.0669136	OK
0.3	0.0487936	OK
0.4	0.0306736	OK
0.5	0.0125536	OK
0.6	-0.0055664	Imaginary
0.7	-0.0236864	Imaginary
0.8	-0.0418064	Imaginary
0.9	-0.0599264	Imaginary

Ws Deciles
8.047
5.595
3.687
2.225
1.109
#NUM!
#NUM!
#NUM!
#NUM!

Figure A7. Settling chamber analysis for determination of settling velocity for Point 090009, run 1.

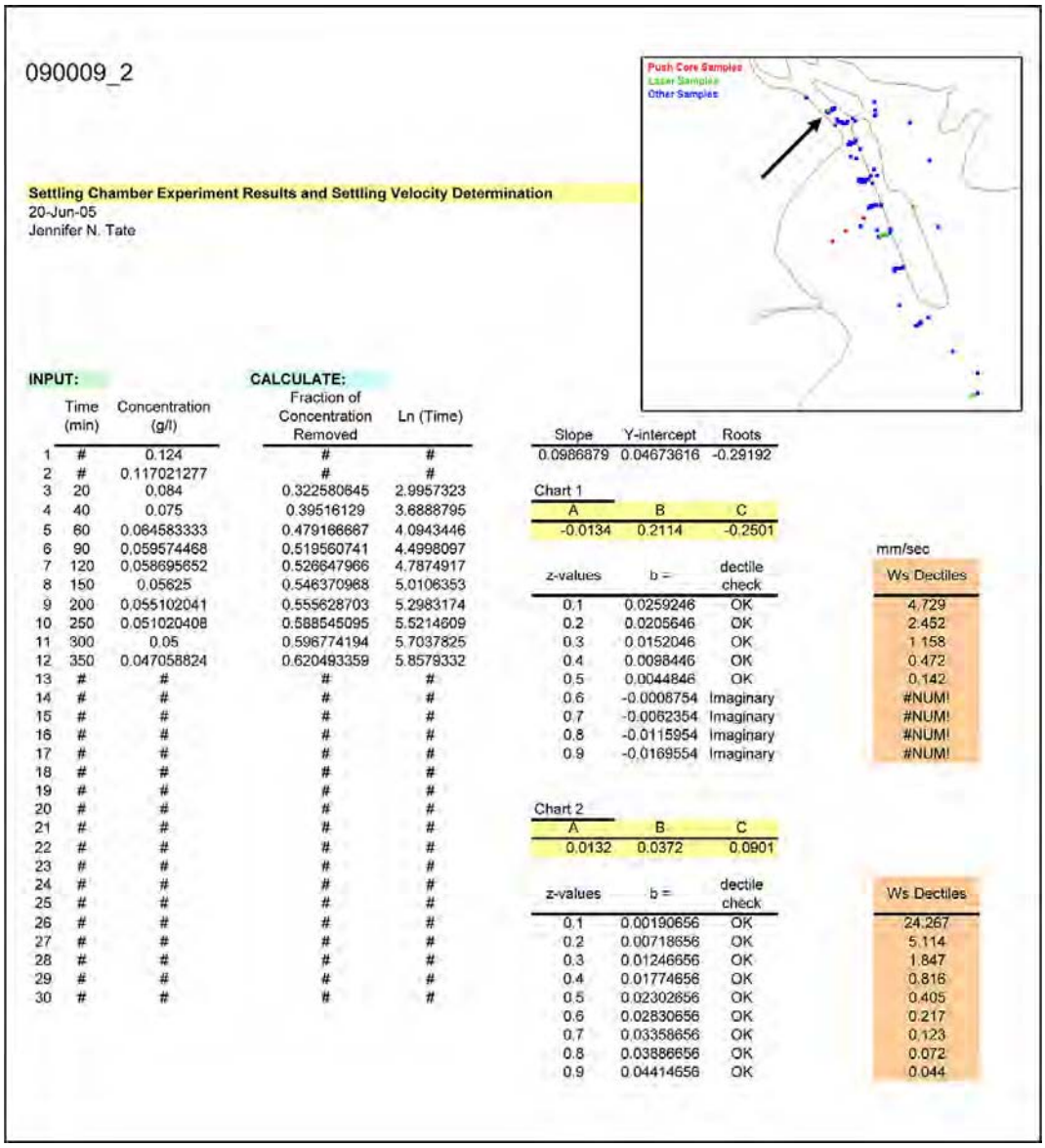

090009_2

Push Core Samples
Laser Samples
Other Samples

Settling Chamber Experiment Results and Settling Velocity Determination
20-Jun-05
Jennifer N. Tate

INPUT: **CALCULATE:**

	Time (min)	Concentration (g/l)	Fraction of Concentration Removed	Ln (Time)
1	#	0.124	#	#
2	#	0.117021277	#	#
3	20	0.084	0.322580645	2.9957323
4	40	0.075	0.39516129	3.6888795
5	60	0.064583333	0.479166667	4.0943446
6	90	0.059574468	0.519560741	4.4998097
7	120	0.058695652	0.526647966	4.7874917
8	150	0.05625	0.546370968	5.0106353
9	200	0.055102041	0.555628703	5.2983174
10	250	0.051020408	0.588545095	5.5214609
11	300	0.05	0.596774194	5.7037825
12	350	0.047058824	0.620493359	5.8579332
13	#	#	#	#
14	#	#	#	#
15	#	#	#	#
16	#	#	#	#
17	#	#	#	#
18	#	#	#	#
19	#	#	#	#
20	#	#	#	#
21	#	#	#	#
22	#	#	#	#
23	#	#	#	#
24	#	#	#	#
25	#	#	#	#
26	#	#	#	#
27	#	#	#	#
28	#	#	#	#
29	#	#	#	#
30	#	#	#	#

Slope	Y-intercept	Roots
0.0986879	0.04673616	-0.29192

Chart 1

A	B	C
-0.0134	0.2114	-0.2501

z-values	b =	decile check
0.1	0.0259246	OK
0.2	0.0205646	OK
0.3	0.0152046	OK
0.4	0.0098446	OK
0.5	0.0044846	OK
0.6	-0.0008754	Imaginary
0.7	-0.0062354	Imaginary
0.8	-0.0115954	Imaginary
0.9	-0.0169554	Imaginary

mm/sec

Ws Deciles
4.729
2.452
1.158
0.472
0.142
#NUM!
#NUM!
#NUM!
#NUM!

Chart 2

A	B	C
0.0132	0.0372	0.0901

z-values	b =	decile check
0.1	0.00190656	OK
0.2	0.00718656	OK
0.3	0.01246656	OK
0.4	0.01774656	OK
0.5	0.02302656	OK
0.6	0.02830656	OK
0.7	0.03358656	OK
0.8	0.03886656	OK
0.9	0.04414656	OK

Ws Deciles
24.267
5.114
1.847
0.816
0.405
0.217
0.123
0.072
0.044

Figure A8. Settling chamber analysis for determination of settling velocity for Point 090009, run 2.

090009_3

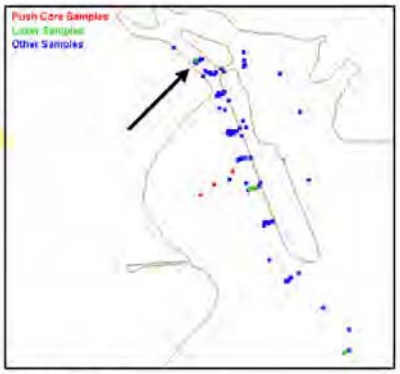

Settling Chamber Experiment Results and Settling Velocity Determination
20-Jun-05
Jennifer N. Tate

INPUT: **CALCULATE:**

	Time (min)	Concentration (g/l)	Fraction of Concentration Removed	Ln (Time)
1	#	0.304	#	#
2	#	0.231914894	#	#
3	20	0.182352941	0.400154799	2.9957323
4	40	0.157446809	0.482082867	3.6888795
5	60	0.143137255	0.529153767	4.0943446
6	90	0.137254902	0.548503612	4.4998097
7	120	0.132608696	0.563787185	4.7874917
8	150	0.127083333	0.581962719	5.0106353
9	200	0.11	0.638157895	5.2983174
10	250	0.08	0.736842105	5.5214609
11	300	0.061702128	0.797032475	5.7037825
12	350	0.055102041	0.818743287	5.8579332
13	#	#	#	#
14	#	#	#	#
15	#	#	#	#
16	#	#	#	#
17	#	#	#	#
18	#	#	#	#
19	#	#	#	#
20	#	#	#	#
21	#	#	#	#
22	#	#	#	#
23	#	#	#	#
24	#	#	#	#
25	#	#	#	#
26	#	#	#	#
27	#	#	#	#
28	#	#	#	#
29	#	#	#	#
30	#	#	#	#

Slope	Y-intercept	Roots
0.1392844	-0.0513794	0.829392

Chart 1

A	B	C
-0.0235	0.2905	-0.3338

z-values	b =	decile check
0.1	0.04361305	OK
0.2	0.03421305	OK
0.3	0.02481305	OK
0.4	0.01541305	OK
0.5	0.00601305	OK
0.6	-0.003387	Imaginary
0.7	-0.012787	Imaginary
0.8	-0.022187	Imaginary
0.9	-0.031587	Imaginary

mm/sec

Ws Deciles
5.455
3.283
1.831
0.900
0.334
#NUM!
#NUM!
#NUM!
#NUM!

Chart 2

A	B	C
-0.0311	0.3338	-0.3214

z-values	b =	decile check
0.1	0.05900028	OK
0.2	0.04656028	OK
0.3	0.03412028	OK
0.4	0.02168028	OK
0.5	0.00924028	OK
0.6	-0.0031997	Imaginary
0.7	-0.0156397	Imaginary
0.8	-0.0280797	Imaginary
0.9	-0.0405197	Imaginary

Ws Deciles
7.189
4.648
2.821
1.544
0.679
#NUM!
#NUM!
#NUM!
#NUM!

Figure A9. Settling chamber analysis for determination of settling velocity for Point 090009, run 3.

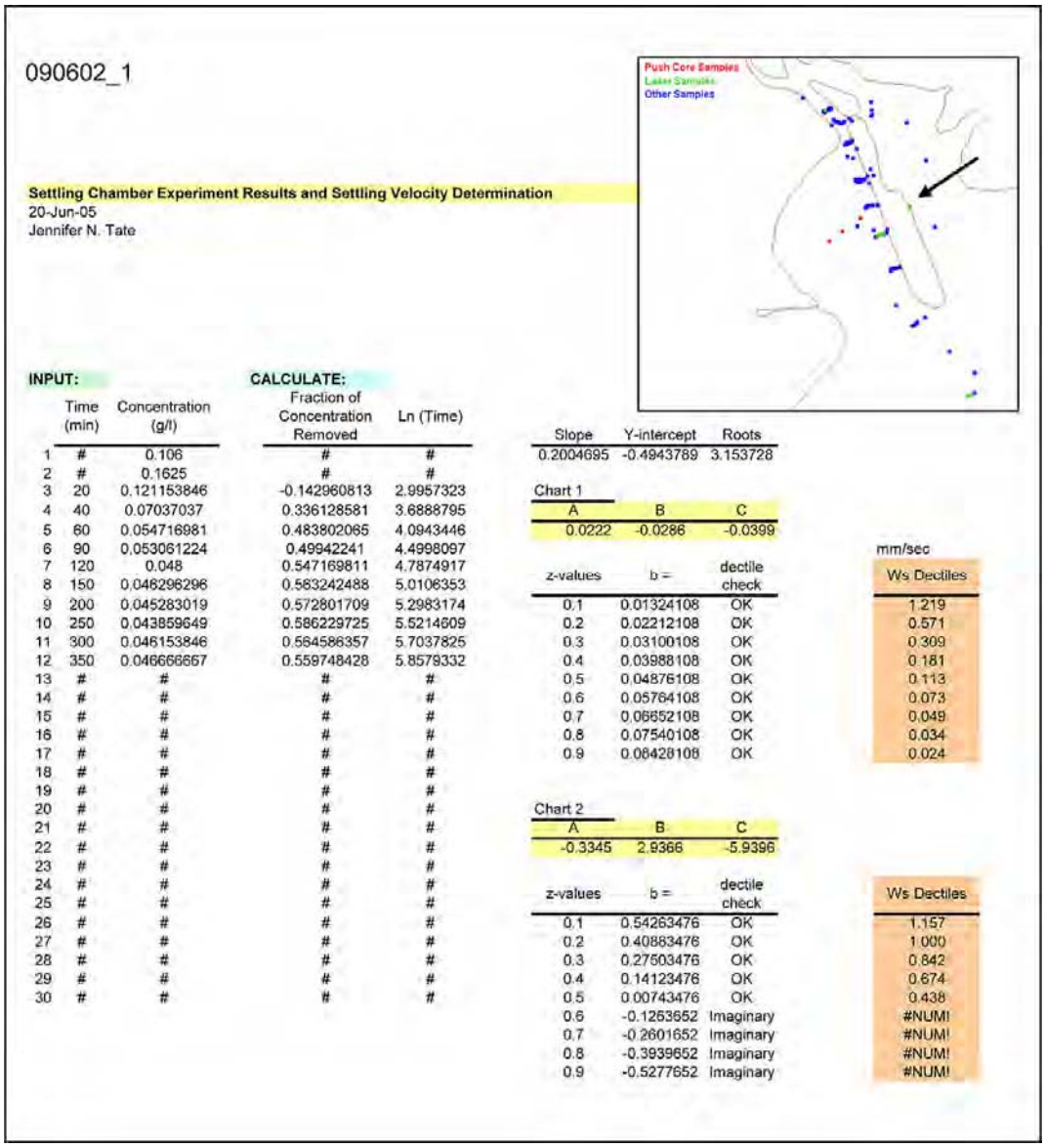

090602_1

Push Core Samples
Laser Samples
Other Samples

Settling Chamber Experiment Results and Settling Velocity Determination
20-Jun-05
Jennifer N. Tate

INPUT: **CALCULATE:**

	Time (min)	Concentration (g/l)	Fraction of Concentration Removed	Ln (Time)
1	#	0.106	#	#
2	#	0.1625	#	#
3	20	0.121153846	-0.142960813	2.9957323
4	40	0.07037037	0.336128581	3.6888795
5	60	0.054716981	0.483802065	4.0943446
6	90	0.053061224	0.49942241	4.4998097
7	120	0.048	0.547169811	4.7874917
8	150	0.046296296	0.563242488	5.0106353
9	200	0.045283019	0.572801709	5.2983174
10	250	0.043859649	0.586229725	5.5214609
11	300	0.046153846	0.564586357	5.7037825
12	350	0.046666667	0.559748428	5.8579332
13	#	#	#	#
14	#	#	#	#
15	#	#	#	#
16	#	#	#	#
17	#	#	#	#
18	#	#	#	#
19	#	#	#	#
20	#	#	#	#
21	#	#	#	#
22	#	#	#	#
23	#	#	#	#
24	#	#	#	#
25	#	#	#	#
26	#	#	#	#
27	#	#	#	#
28	#	#	#	#
29	#	#	#	#
30	#	#	#	#

Slope	Y-intercept	Roots
0.2004695	-0.4943789	3.153728

Chart 1

A	B	C
0.0222	-0.0286	-0.0399

z-values	b =	decile check
0.1	0.01324108	OK
0.2	0.02212108	OK
0.3	0.03100108	OK
0.4	0.03988108	OK
0.5	0.04876108	OK
0.6	0.05764108	OK
0.7	0.06652108	OK
0.8	0.07540108	OK
0.9	0.08428108	OK

mm/sec

Ws Deciles
1.219
0.571
0.309
0.181
0.113
0.073
0.049
0.034
0.024

Chart 2

A	B	C
-0.3345	2.9366	-5.9396

z-values	b =	decile check
0.1	0.54263476	OK
0.2	0.40883476	OK
0.3	0.27503476	OK
0.4	0.14123476	OK
0.5	0.00743476	OK
0.6	-0.1263652	Imaginary
0.7	-0.2601652	Imaginary
0.8	-0.3939652	Imaginary
0.9	-0.5277652	Imaginary

Ws Deciles
1.157
1.000
0.842
0.674
0.438
#NUM!
#NUM!
#NUM!
#NUM!

Figure A10. Settling chamber analysis for determination of settling velocity for Point 090602, run 1.

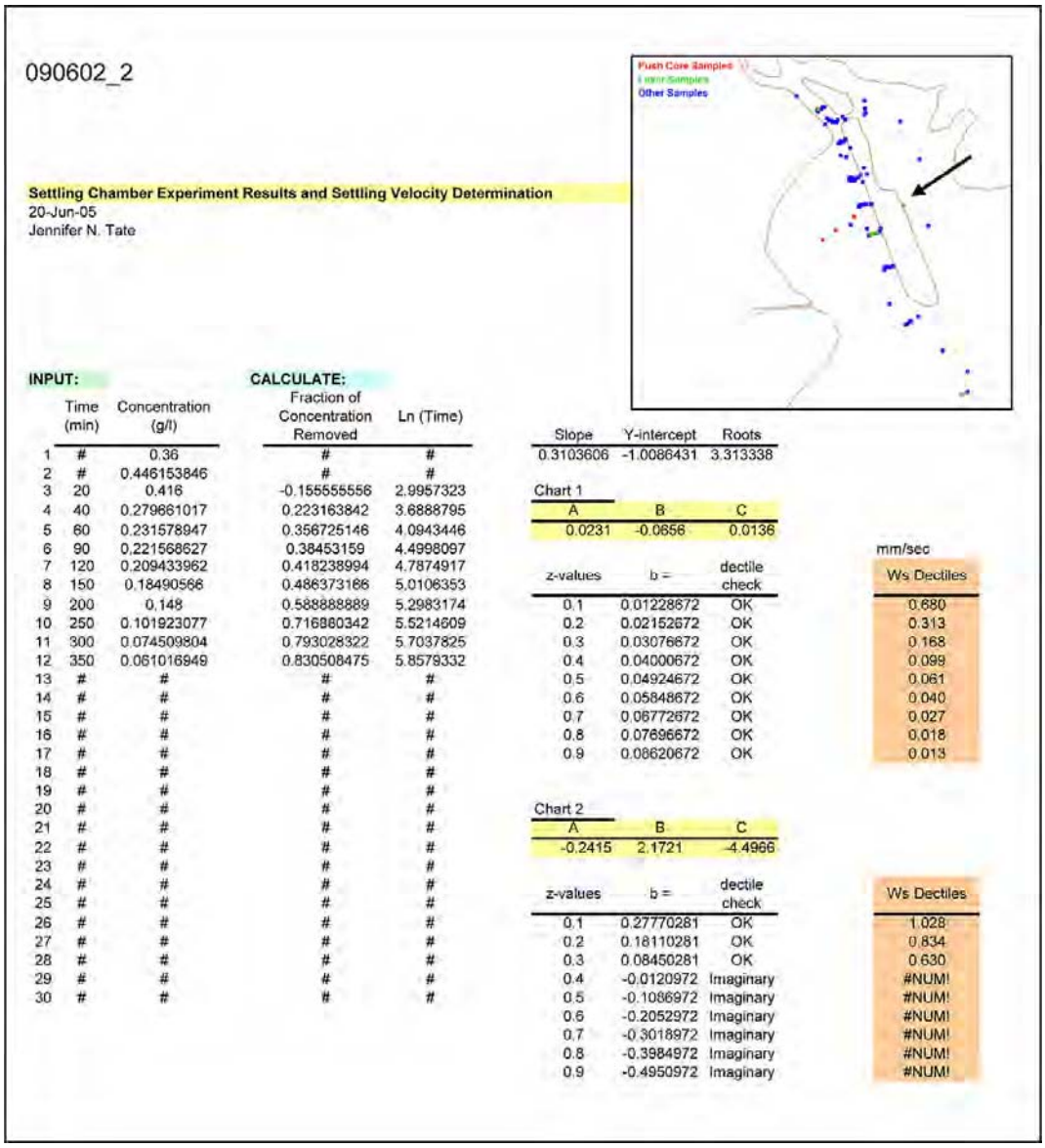

090602_2

Push Core Samples
Other Samples

Settling Chamber Experiment Results and Settling Velocity Determination
20-Jun-05
Jennifer N. Tate

INPUT:

	Time (min)	Concentration (g/l)
1	#	0.36
2	#	0.446153846
3	20	0.416
4	40	0.279661017
5	60	0.231578947
6	90	0.221568627
7	120	0.209433962
8	150	0.18490566
9	200	0.148
10	250	0.101923077
11	300	0.074509804
12	350	0.061016949
13	#	#
14	#	#
15	#	#
16	#	#
17	#	#
18	#	#
19	#	#
20	#	#
21	#	#
22	#	#
23	#	#
24	#	#
25	#	#
26	#	#
27	#	#
28	#	#
29	#	#
30	#	#

CALCULATE:

Fraction of Concentration Removed	Ln (Time)
#	#
#	#
-0.155555556	2.9957323
0.223163842	3.6888795
0.356725146	4.0943446
0.38453159	4.4998097
0.418238994	4.7874917
0.486373166	5.0106353
0.588888889	5.2983174
0.716880342	5.5214609
0.793028322	5.7037825
0.830508475	5.8579332
#	#
#	#
#	#
#	#
#	#
#	#
#	#
#	#
#	#
#	#
#	#
#	#
#	#
#	#
#	#
#	#
#	#
#	#

Slope	Y-intercept	Roots
0.3103606	-1.0086431	3.313338

Chart 1

A	B	C
0.0231	-0.0656	0.0136

z-values	b =	decile check
0.1	0.01228672	OK
0.2	0.02152672	OK
0.3	0.03076672	OK
0.4	0.04000672	OK
0.5	0.04924672	OK
0.6	0.05848672	OK
0.7	0.06772672	OK
0.8	0.07696672	OK
0.9	0.08620672	OK

mm/sec

Ws Deciles
0.680
0.313
0.168
0.099
0.061
0.040
0.027
0.018
0.013

Chart 2

A	B	C
-0.2415	2.1721	-4.4966

z-values	b =	decile check
0.1	0.27770281	OK
0.2	0.18110281	OK
0.3	0.08450281	OK
0.4	-0.0120972	Imaginary
0.5	-0.1086972	Imaginary
0.6	-0.2052972	Imaginary
0.7	-0.3018972	Imaginary
0.8	-0.3984972	Imaginary
0.9	-0.4950972	Imaginary

Ws Deciles
1.028
0.834
0.630
#NUM!
#NUM!
#NUM!
#NUM!
#NUM!
#NUM!

Figure A11. Settling chamber analysis for determination of settling velocity for Point 090602, run 2.

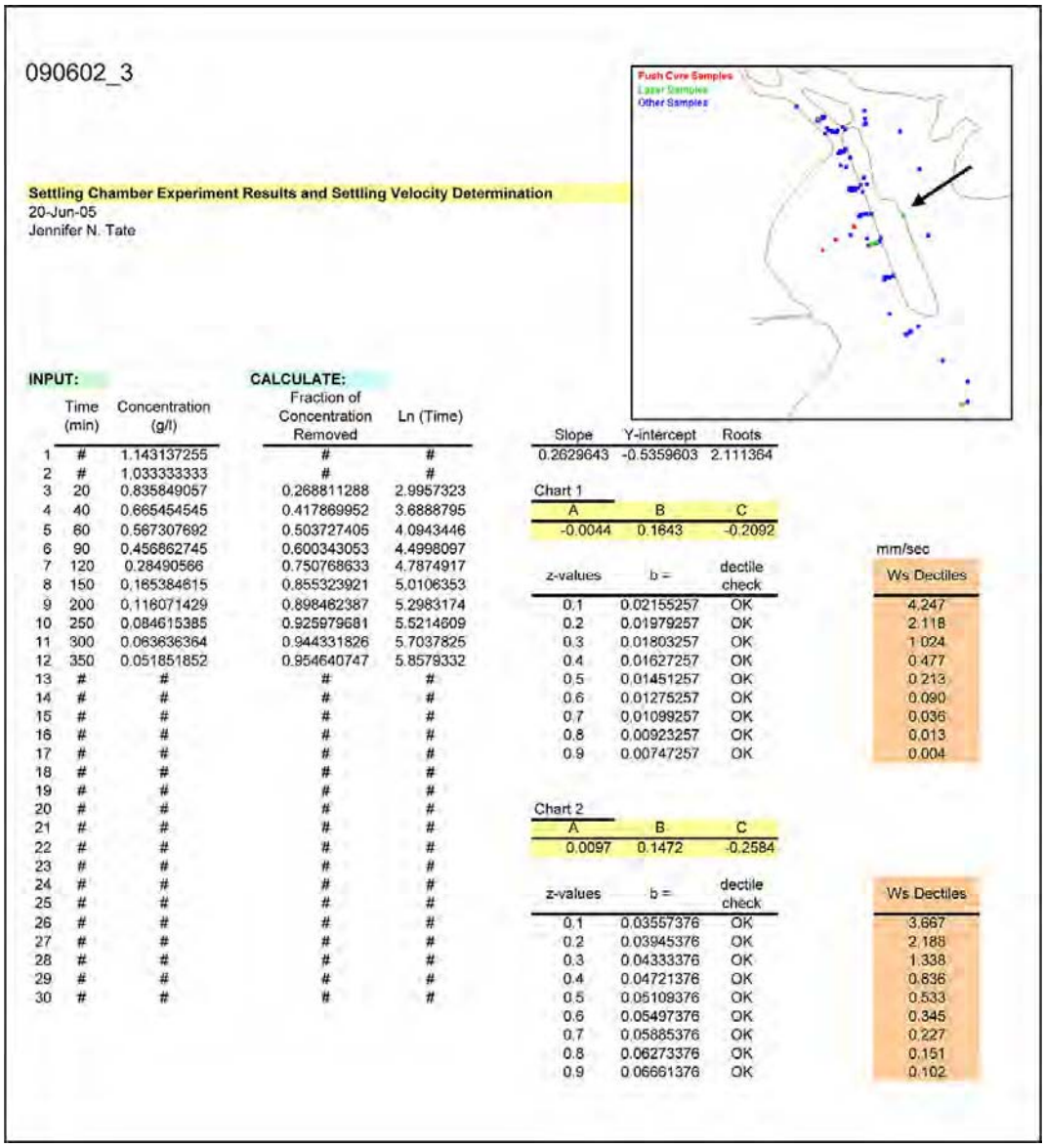

090602_3

Push Core Samples
Laser Samples
Other Samples

Settling Chamber Experiment Results and Settling Velocity Determination
20-Jun-05
Jennifer N. Tate

INPUT:

	Time (min)	Concentration (g/l)
1	#	1.143137255
2	#	1.033333333
3	20	0.835849057
4	40	0.665454545
5	60	0.567307692
6	90	0.456862745
7	120	0.28490566
8	150	0.185384615
9	200	0.116071429
10	250	0.084615385
11	300	0.063636364
12	350	0.051851852
13	#	#
14	#	#
15	#	#
16	#	#
17	#	#
18	#	#
19	#	#
20	#	#
21	#	#
22	#	#
23	#	#
24	#	#
25	#	#
26	#	#
27	#	#
28	#	#
29	#	#
30	#	#

CALCULATE:

Fraction of Concentration Removed	Ln (Time)
#	#
#	#
0.268811288	2.9957323
0.417869952	3.6888795
0.503727405	4.0943446
0.600343053	4.4998097
0.750768633	4.7874917
0.855323921	5.0106353
0.898462387	5.2983174
0.925979681	5.5214609
0.944331826	5.7037825
0.954640747	5.8579332
#	#
#	#
#	#
#	#
#	#
#	#
#	#
#	#
#	#
#	#
#	#
#	#
#	#
#	#
#	#
#	#
#	#
#	#

Slope	Y-intercept	Roots
0.2629643	-0.5359603	2.111364

Chart 1

A	B	C
-0.0044	0.1643	-0.2092

z-values	b =	decile check
0.1	0.02155257	OK
0.2	0.01979257	OK
0.3	0.01803257	OK
0.4	0.01627257	OK
0.5	0.01451257	OK
0.6	0.01275257	OK
0.7	0.01099257	OK
0.8	0.00923257	OK
0.9	0.00747257	OK

mm/sec

Ws Deciles
4.247
2.118
1.024
0.477
0.213
0.090
0.036
0.013
0.004

Chart 2

A	B	C
0.0097	0.1472	-0.2584

z-values	b =	decile check
0.1	0.03557376	OK
0.2	0.03945376	OK
0.3	0.04333376	OK
0.4	0.04721376	OK
0.5	0.05109376	OK
0.6	0.05497376	OK
0.7	0.05885376	OK
0.8	0.06273376	OK
0.9	0.06661376	OK

Ws Deciles
3.667
2.188
1.338
0.836
0.533
0.345
0.227
0.151
0.102

Figure A12. Settling chamber analysis for determination of settling velocity for Point 090602, run 3.

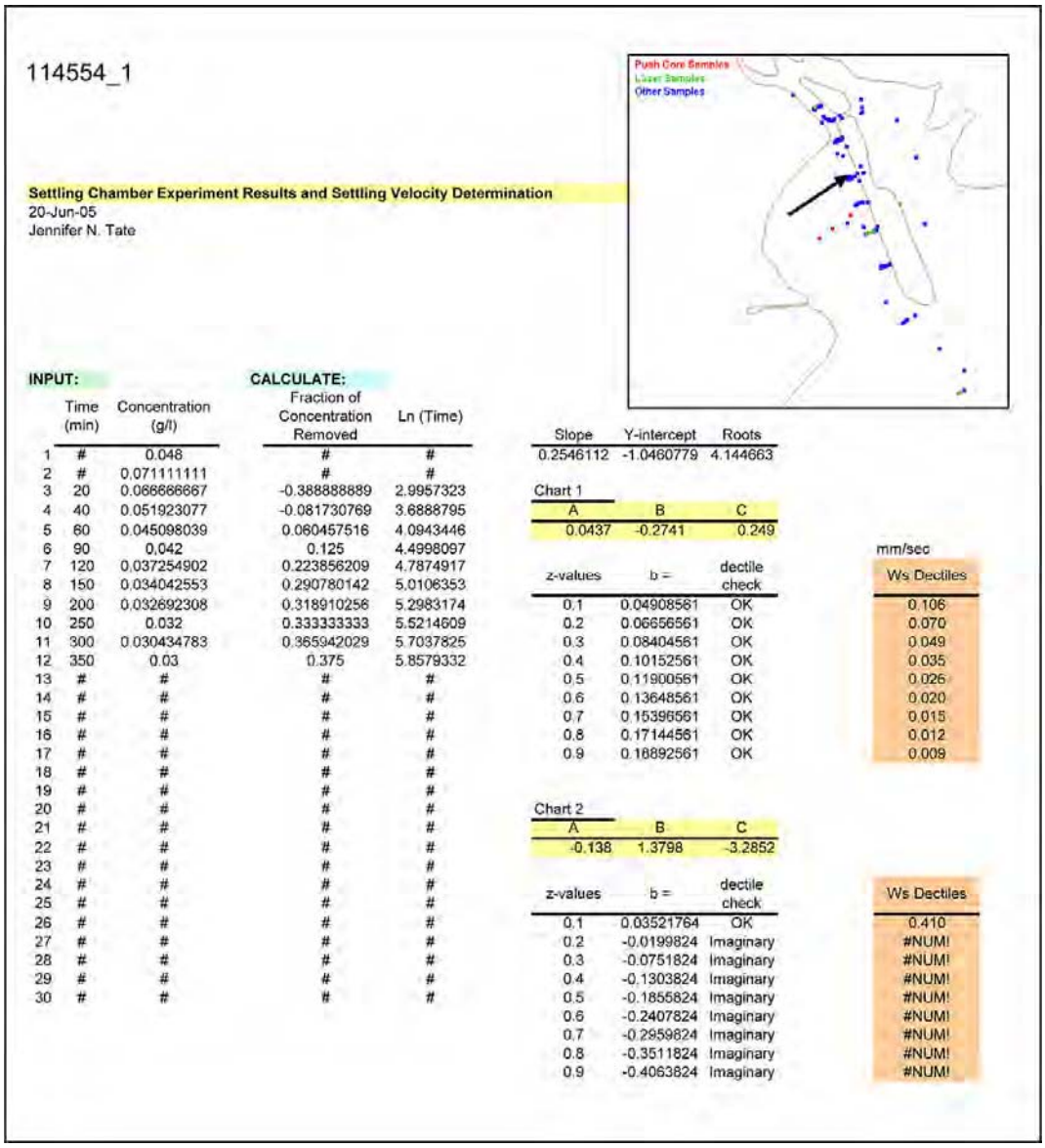

114554_1

Push Core Samples
Laser Samples
Other Samples

Settling Chamber Experiment Results and Settling Velocity Determination
20-Jun-05
Jennifer N. Tate

INPUT: **CALCULATE:**

	Time (min)	Concentration (g/l)	Fraction of Concentration Removed	Ln (Time)
1	#	0.048	#	#
2	#	0.071111111	#	#
3	20	0.066666667	-0.388888889	2.9957323
4	40	0.051923077	-0.081730769	3.6888795
5	60	0.045098039	0.060457516	4.0943446
6	90	0.042	0.125	4.4998097
7	120	0.037254902	0.223856209	4.7874917
8	150	0.034042553	0.290780142	5.0106353
9	200	0.032692308	0.318910256	5.2983174
10	250	0.032	0.333333333	5.5214609
11	300	0.030434783	0.365942029	5.7037825
12	350	0.03	0.375	5.8579332
13	#	#	#	#
14	#	#	#	#
15	#	#	#	#
16	#	#	#	#
17	#	#	#	#
18	#	#	#	#
19	#	#	#	#
20	#	#	#	#
21	#	#	#	#
22	#	#	#	#
23	#	#	#	#
24	#	#	#	#
25	#	#	#	#
26	#	#	#	#
27	#	#	#	#
28	#	#	#	#
29	#	#	#	#
30	#	#	#	#

Slope	Y-intercept	Roots
0.2546112	-1.0460779	4.144663

Chart 1

A	B	C
0.0437	-0.2741	0.249

z-values	b =	decile check
0.1	0.04908561	OK
0.2	0.06656561	OK
0.3	0.08404561	OK
0.4	0.10152561	OK
0.5	0.11900561	OK
0.6	0.13648561	OK
0.7	0.15396561	OK
0.8	0.17144561	OK
0.9	0.18892561	OK

mm/sec

Ws Deciles
0.106
0.070
0.049
0.035
0.026
0.020
0.015
0.012
0.009

Chart 2

A	B	C
-0.138	1.3798	-3.2852

z-values	b =	decile check
0.1	0.03521764	OK
0.2	-0.0199824	Imaginary
0.3	-0.0751824	Imaginary
0.4	-0.1303824	Imaginary
0.5	-0.1855824	Imaginary
0.6	-0.2407824	Imaginary
0.7	-0.2959824	Imaginary
0.8	-0.3511824	Imaginary
0.9	-0.4063824	Imaginary

Ws Deciles
0.410
#NUM!
#NUM!
#NUM!
#NUM!
#NUM!
#NUM!
#NUM!
#NUM!

Figure A13. Settling chamber analysis for determination of settling velocity for Point 114554, run 1.

114554_2

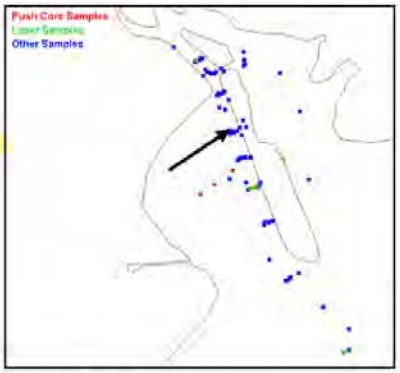

Settling Chamber Experiment Results and Settling Velocity Determination
20-Jun-05
Jennifer N. Tate

INPUT: **CALCULATE:**

	Time (min)	Concentration (g/l)	Fraction of Concentration Removed	Ln (Time)
1	#	0.186	#	#
2	#	0.195744681	#	#
3	20	0.142	0.23655914	2.9957323
4	40	0.12	0.35483871	3.6888795
5	60	0.10754717	0.42178941	4.0943446
6	90	0.1	0.462365591	4.4998097
7	120	0.097777778	0.474313023	4.7874917
8	150	0.096	0.483870968	5.0106353
9	200	0.086	0.537634409	5.2983174
10	250	0.076	0.591397849	5.5214609
11	300	0.06	0.677419355	5.7037825
12	350	0.04893617	0.736902311	5.8579332
13	#	#	#	#
14	#	#	#	#
15	#	#	#	#
16	#	#	#	#
17	#	#	#	#
18	#	#	#	#
19	#	#	#	#
20	#	#	#	#
21	#	#	#	#
22	#	#	#	#
23	#	#	#	#
24	#	#	#	#
25	#	#	#	#
26	#	#	#	#
27	#	#	#	#
28	#	#	#	#
29	#	#	#	#
30	#	#	#	#

Slope	Y-intercept	Roots
0.1531719	-0.2292201	1.716505

Chart 1

A	B	C
-0.0085	0.165	-0.2029

z-values	b =	decile check
0.1	0.0169264	OK
0.2	0.0135264	OK
0.3	0.0101264	OK
0.4	0.0067264	OK
0.5	0.0033264	OK
0.6	-7.36E-05	Imaginary
0.7	-0.0034736	Imaginary
0.8	-0.0068736	Imaginary
0.9	-0.0102736	Imaginary

mm/sec

Ws Deciles
3.958
1.758
0.699
0.234
0.056
#NUM!
#NUM!
#NUM!
#NUM!

Chart 2

A	B	C
-0.0317	0.3893	-0.6462

z-values	b =	decile check
0.1	0.05693633	OK
0.2	0.04425633	OK
0.3	0.03157633	OK
0.4	0.01889633	OK
0.5	0.00621633	OK
0.6	-0.0064637	Imaginary
0.7	-0.0191437	Imaginary
0.8	-0.0318237	Imaginary
0.9	-0.0445037	Imaginary

Ws Deciles
2.863
1.834
1.095
0.581
0.230
#NUM!
#NUM!
#NUM!
#NUM!

Figure A14. Settling chamber analysis for determination of settling velocity for Point 114554, run 2.

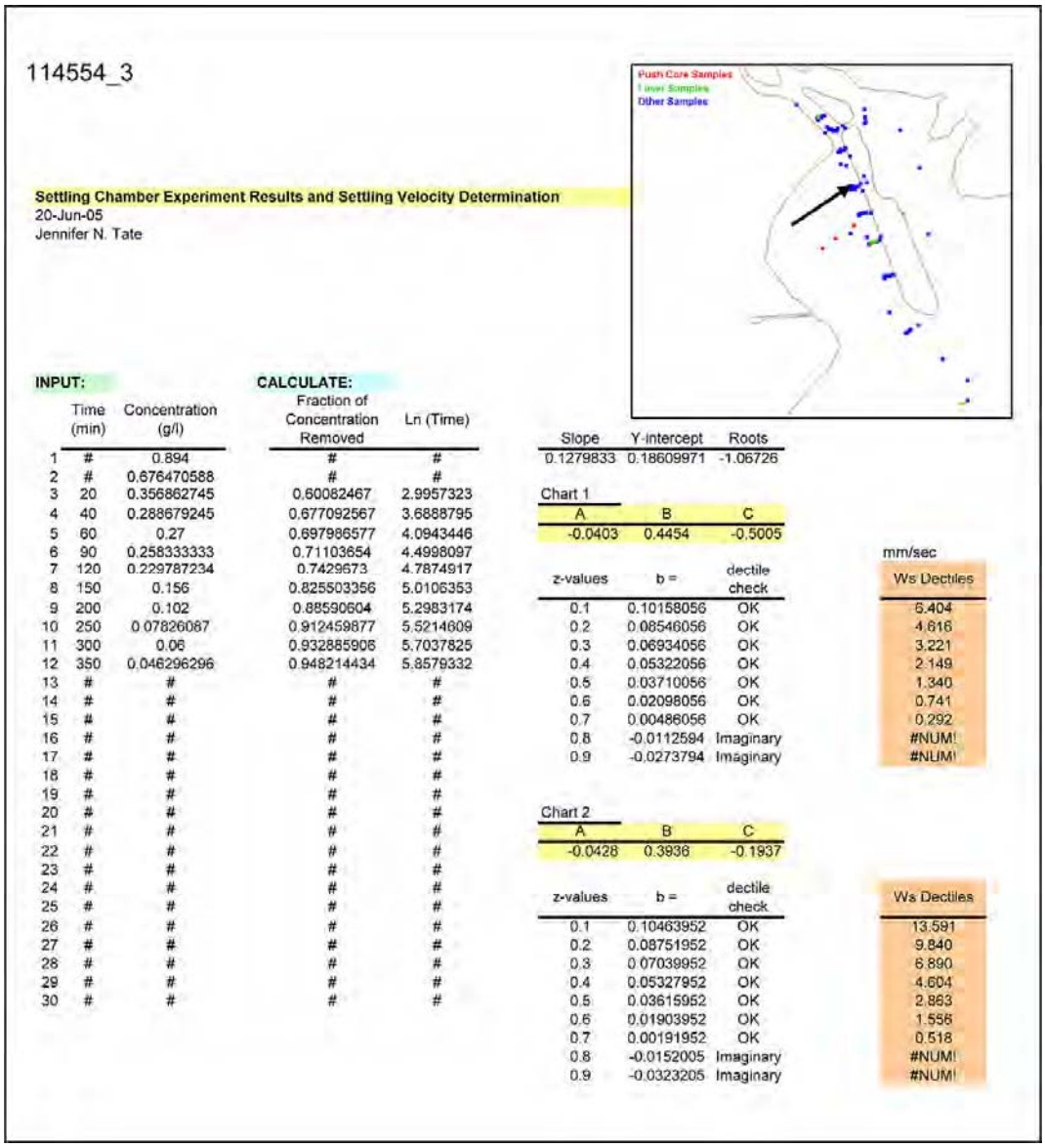

114554_3

Push Core Samples
Liner Samples
Other Samples

Settling Chamber Experiment Results and Settling Velocity Determination
20-Jun-05
Jennifer N. Tate

INPUT: **CALCULATE:**

	Time (min)	Concentration (g/l)	Fraction of Concentration Removed	Ln (Time)
1	#	0.894	#	#
2	#	0.676470588	#	#
3	20	0.356862745	0.60082467	2.9957323
4	40	0.288679245	0.677092567	3.6888795
5	60	0.27	0.697986577	4.0943446
6	90	0.258333333	0.71103654	4.4998097
7	120	0.229787234	0.7429673	4.7874917
8	150	0.156	0.825503356	5.0106353
9	200	0.102	0.88590604	5.2983174
10	250	0.07826087	0.912459877	5.5214609
11	300	0.06	0.932885906	5.7037825
12	350	0.046296296	0.948214434	5.8579332
13	#	#	#	#
14	#	#	#	#
15	#	#	#	#
16	#	#	#	#
17	#	#	#	#
18	#	#	#	#
19	#	#	#	#
20	#	#	#	#
21	#	#	#	#
22	#	#	#	#
23	#	#	#	#
24	#	#	#	#
25	#	#	#	#
26	#	#	#	#
27	#	#	#	#
28	#	#	#	#
29	#	#	#	#
30	#	#	#	#

Slope	Y-intercept	Roots
0.1279833	0.18609971	-1.06726

Chart 1

A	B	C
-0.0403	0.4454	-0.5005

z-values	b =	decile check
0.1	0.10158056	OK
0.2	0.08546056	OK
0.3	0.06934056	OK
0.4	0.05322056	OK
0.5	0.03710056	OK
0.6	0.02098056	OK
0.7	0.00486056	OK
0.8	-0.0112584	Imaginary
0.9	-0.0273794	Imaginary

mm/sec

Ws Deciles
6.404
4.616
3.221
2.149
1.340
0.741
0.292
#NUM!
#NUM!

Chart 2

A	B	C
-0.0428	0.3936	-0.1937

z-values	b =	decile check
0.1	0.10463952	OK
0.2	0.08751952	OK
0.3	0.07039952	OK
0.4	0.05327952	OK
0.5	0.03615952	OK
0.6	0.01903952	OK
0.7	0.00191952	OK
0.8	-0.0152005	Imaginary
0.9	-0.0323205	Imaginary

Ws Deciles
13.591
9.840
6.890
4.604
2.863
1.556
0.518
#NUM!
#NUM!

Figure A15. Settling chamber analysis for determination of settling velocity for Point 114554, run 3.

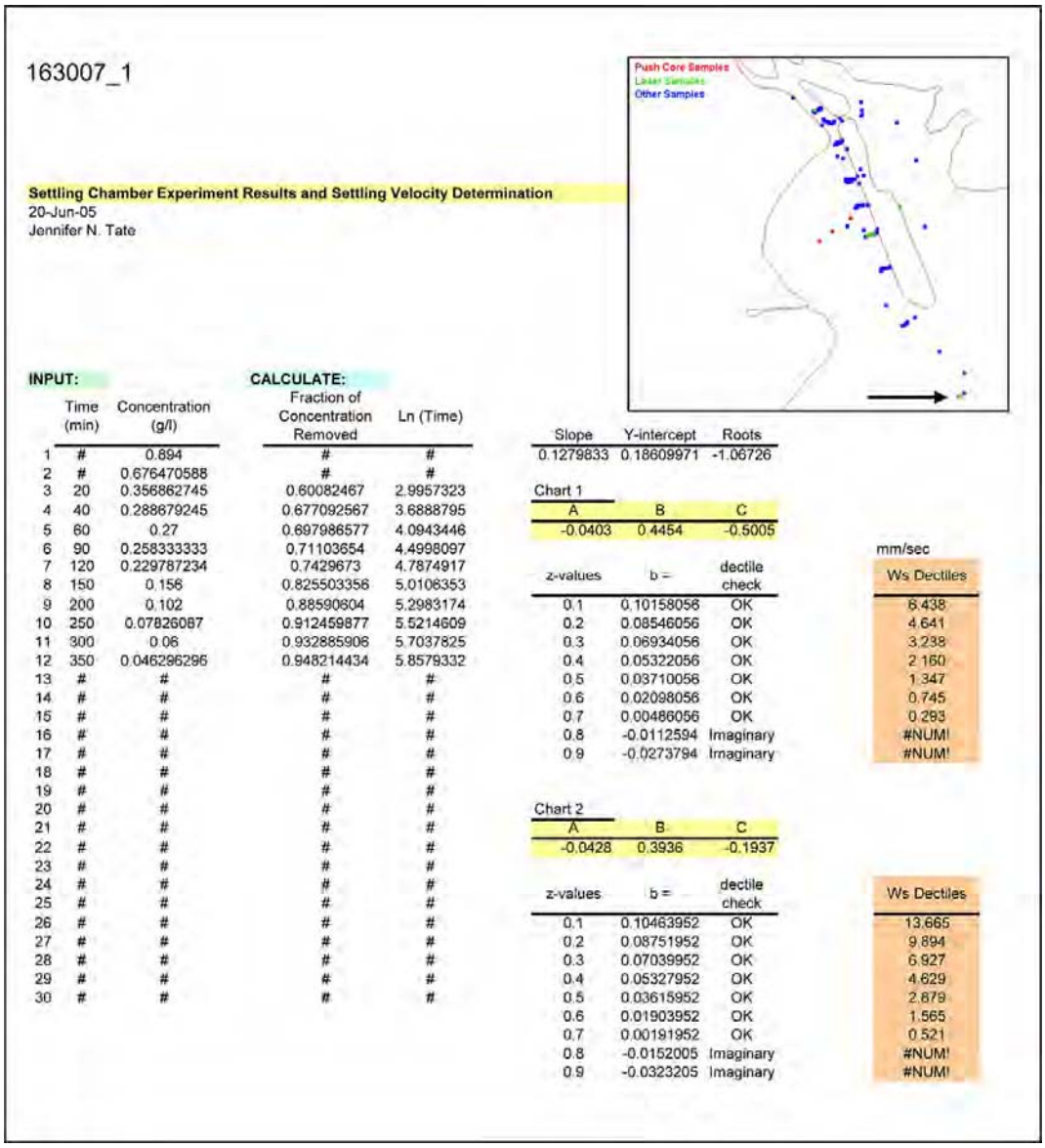

163007_1

Push Core Samples
Laser Samples
Other Samples

Settling Chamber Experiment Results and Settling Velocity Determination
20-Jun-05
Jennifer N. Tate

INPUT:

	Time (min)	Concentration (g/l)
1	#	0.894
2	#	0.676470588
3	20	0.356862745
4	40	0.288679245
5	60	0.27
6	90	0.258333333
7	120	0.229787234
8	150	0.156
9	200	0.102
10	250	0.07826087
11	300	0.06
12	350	0.046296296
13	#	#
14	#	#
15	#	#
16	#	#
17	#	#
18	#	#
19	#	#
20	#	#
21	#	#
22	#	#
23	#	#
24	#	#
25	#	#
26	#	#
27	#	#
28	#	#
29	#	#
30	#	#

CALCULATE:

Fraction of Concentration Removed	Ln (Time)
#	#
#	#
0.60082467	2.9957323
0.677092567	3.6888795
0.697986577	4.0943446
0.71103654	4.4998097
0.7429673	4.7874917
0.825503356	5.0106353
0.88590604	5.2983174
0.912459877	5.5214609
0.932885906	5.7037825
0.948214434	5.8579332
#	#
#	#
#	#
#	#
#	#
#	#
#	#
#	#
#	#
#	#
#	#
#	#
#	#
#	#
#	#
#	#
#	#
#	#

Slope	Y-intercept	Roots
0.1279833	0.18609971	-1.06726

Chart 1

A	B	C
-0.0403	0.4454	-0.5005

z-values	b =	decile check
0.1	0.10158056	OK
0.2	0.08546056	OK
0.3	0.06934056	OK
0.4	0.05322056	OK
0.5	0.03710056	OK
0.6	0.02098056	OK
0.7	0.00486056	OK
0.8	-0.0112594	Imaginary
0.9	-0.0273794	Imaginary

mm/sec

Ws Deciles
6.438
4.641
3.238
2.160
1.347
0.745
0.293
#NUM!
#NUM!

Chart 2

A	B	C
-0.0428	0.3936	-0.1937

z-values	b =	decile check
0.1	0.10463952	OK
0.2	0.08751952	OK
0.3	0.07039952	OK
0.4	0.05327952	OK
0.5	0.03615952	OK
0.6	0.01903952	OK
0.7	0.00191952	OK
0.8	-0.0152005	Imaginary
0.9	-0.0323205	Imaginary

Ws Deciles
13.665
9.894
6.927
4.629
2.879
1.565
0.521
#NUM!
#NUM!

Figure A16. Settling chamber analysis for determination of settling velocity for Point 163007, run 1.

Table A19. Sieve analysis results for push code #1.

SIEVE ANALYSIS

PROJECT: Houston Ship Channel
SAMPLE ID: Core Tube #1 1-1/4 to 2 in. below sample surface
FILE IS: Core 1

SIEVE SIZE MILLIMETERS	OR NUMBER	WEIGHT RETAINED IN GRAMS	PERCENT RETAINED PARTIAL	PERCENT RETAINED TOTAL	FINER BY WEIGHT
76.200	3 in				
50.800	2 in				
38.100	1-1/2 in				
25.400	1 in				
19.050	3/4 in				
12.700	1/2 in				
9.525	3/8 in				
6.727	No.3				
4.760	No.4				
4.000	No.5				
3.360	No.6				
2.380	No.8				
2.000	No.10				
1.414	No.14				
1.190	No.16				
1.000	No.18				
.840	No.20				
.590	No.30				
.500	No.35	.0000	.000	.000	100.000
.420	No.40	.0015	.208	.208	99.792
.297	No.50				
.250	No.60				
.210	No.70	.0117	1.621	1.829	98.171
.149	No.100	.0153	2.120	3.950	96.050
.125	No.120				
.105	No.140				
.074	No.200	.3409	47.242	51.192	48.808
.063	No.230	.2064	28.603	79.795	20.205
	PAN	.1458	20.205	100.000	.000
TOTAL WEIGHT IN GRAMS		.7216			

D95 =	.1467 mm	D90 =	.1362 mm	D85 =	.1265 mm
D80 =	.1175 mm	D75 =	.1091 mm	D70 =	.1013 mm
D65 =	.0941 mm	D60 =	.0873 mm	D55 =	.0811 mm
D50 =	.0753 mm	D45 =	.0724 mm	D40 =	.0704 mm
D35 =	.0685 mm	D30 =	.0666 mm	D25 =	.0647 mm

Table A20. Sieve analysis results for push core #3.

SIEVE ANALYSIS

PROJECT: Houston Ship Channel
SAMPLE ID: Core Tube #3 1-1/4 to 2 in. below sample surface
FILE IS: Core 3

SIEVE SIZE MILLIMETERS	SIEVE SIZE NUMBER	WEIGHT RETAINED IN GRAMS	PERCENT RETAINED PARTIAL	PERCENT RETAINED TOTAL	FINER BY WEIGHT
76.200	3 in				
50.800	2 in				
38.100	1-1/2 in				
25.400	1 in				
19.050	3/4 in				
12.700	1/2 in				
9.525	3/8 in				
6.727	No.3				
4.760	No.4				
4.000	No.5				
3.360	No.6				
2.380	No.8				
2.000	No.10				
1.414	No.14				
1.190	No.16				
1.000	No.18				
.840	No.20				
.590	No.30				
.500	No.35	.0000	.000	.000	100.000
.420	No.40	.0077	.132	.132	99.868
.297	No.50				
.250	No.60				
.210	No.70	.0684	1.170	1.302	98.698
.149	No.100	.1041	1.781	3.084	96.916
.125	No.120				
.105	No.140				
.074	No.200	3.3412	57.175	60.259	39.741
.063	No.230	1.2523	21.430	81.688	18.312
	PAN	1.0701	18.312	100.000	.000
TOTAL WEIGHT IN GRAMS		5.8438			

D95 = .1455 mm	D90 = .1369 mm	D85 = .1288 mm
D80 = .1211 mm	D75 = .1139 mm	D70 = .1072 mm
D65 = .1008 mm	D60 = .0948 mm	D55 = .0892 mm
D50 = .0839 mm	D45 = .0789 mm	D40 = .0742 mm
D35 = .0714 mm	D30 = .0688 mm	D25 = .0662 mm
D20 = .0638 mm		

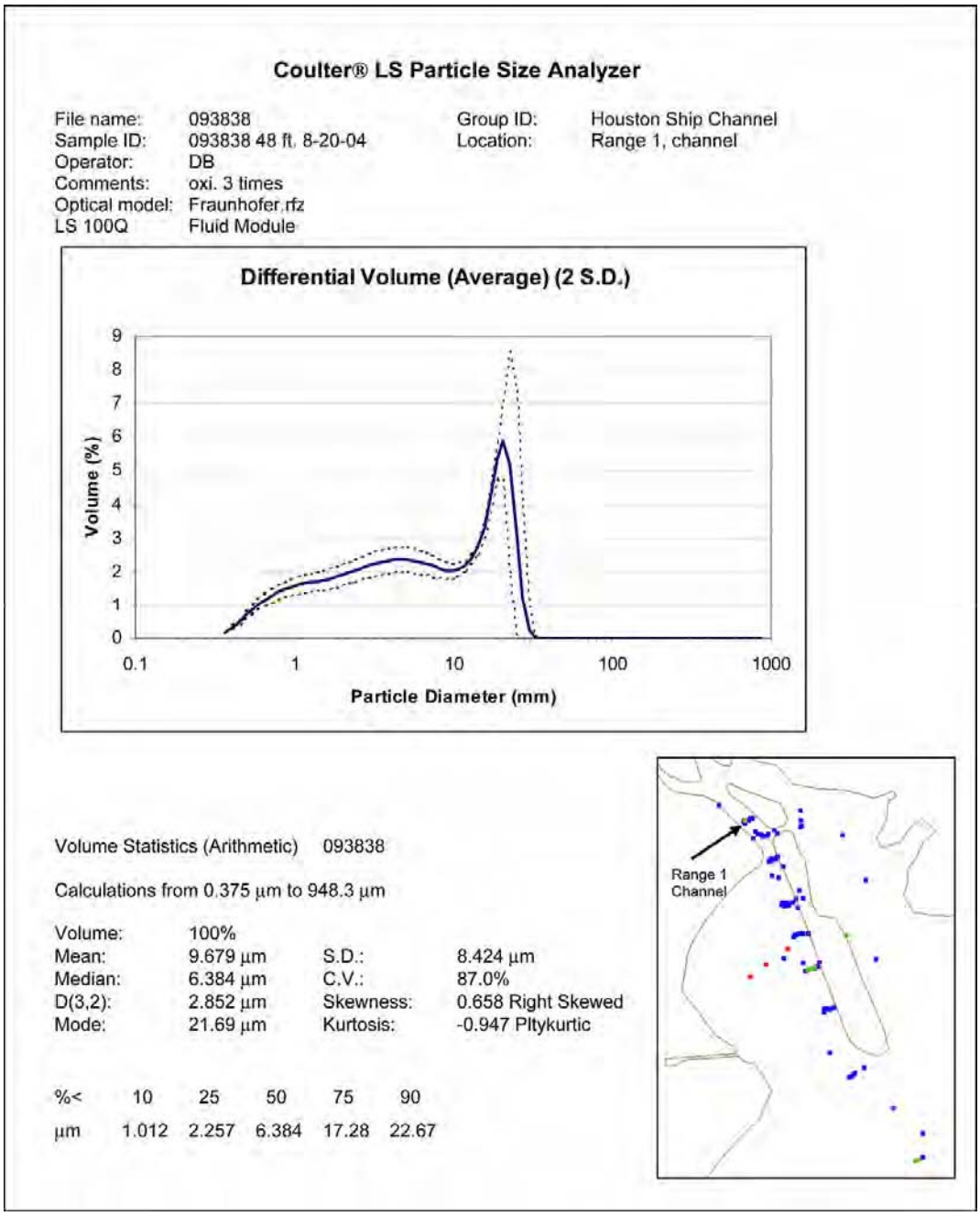

Figure A17. Coulter counter analysis for Point 093838.

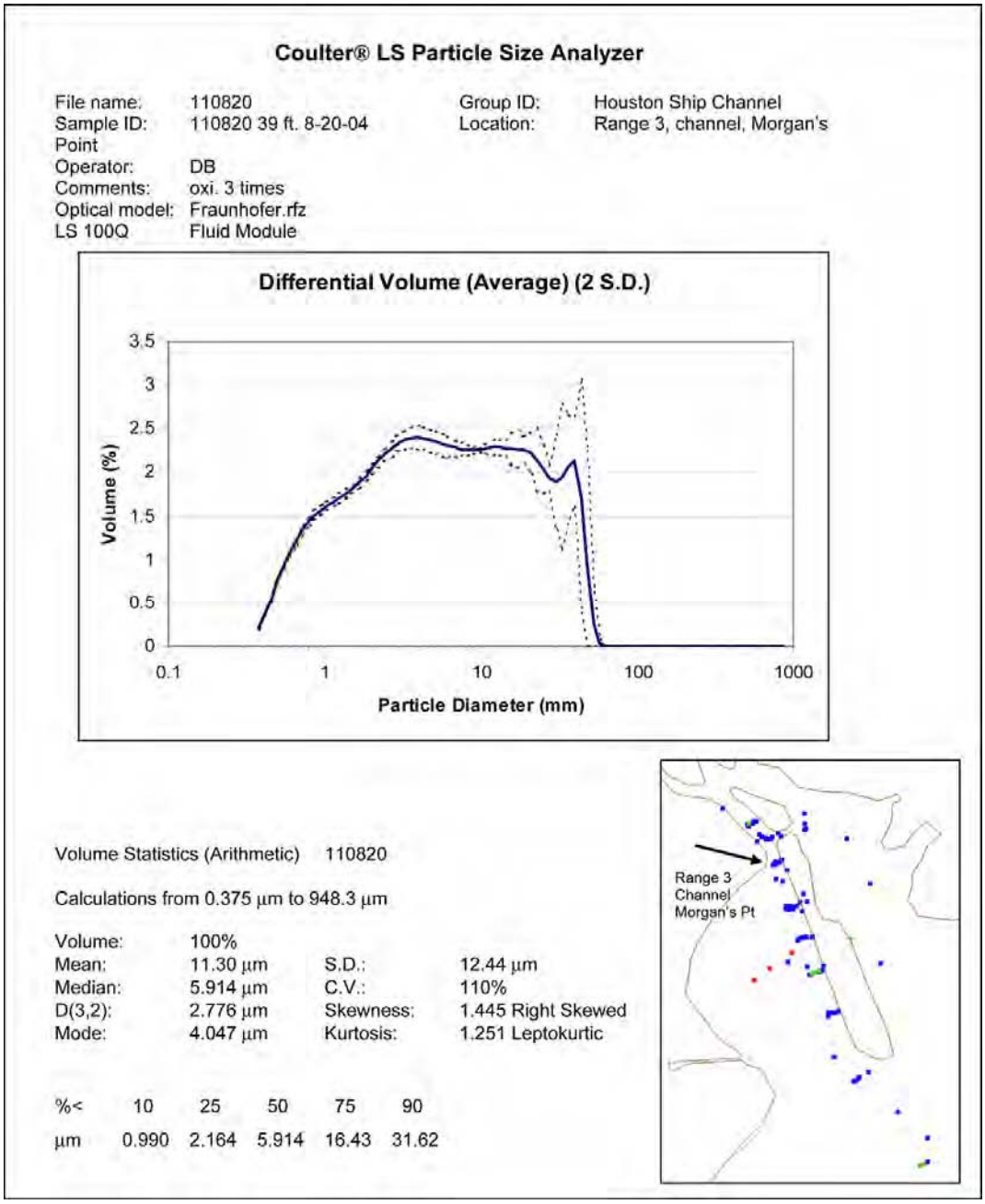

Figure A18. Coulter counter analysis for Point 110820.

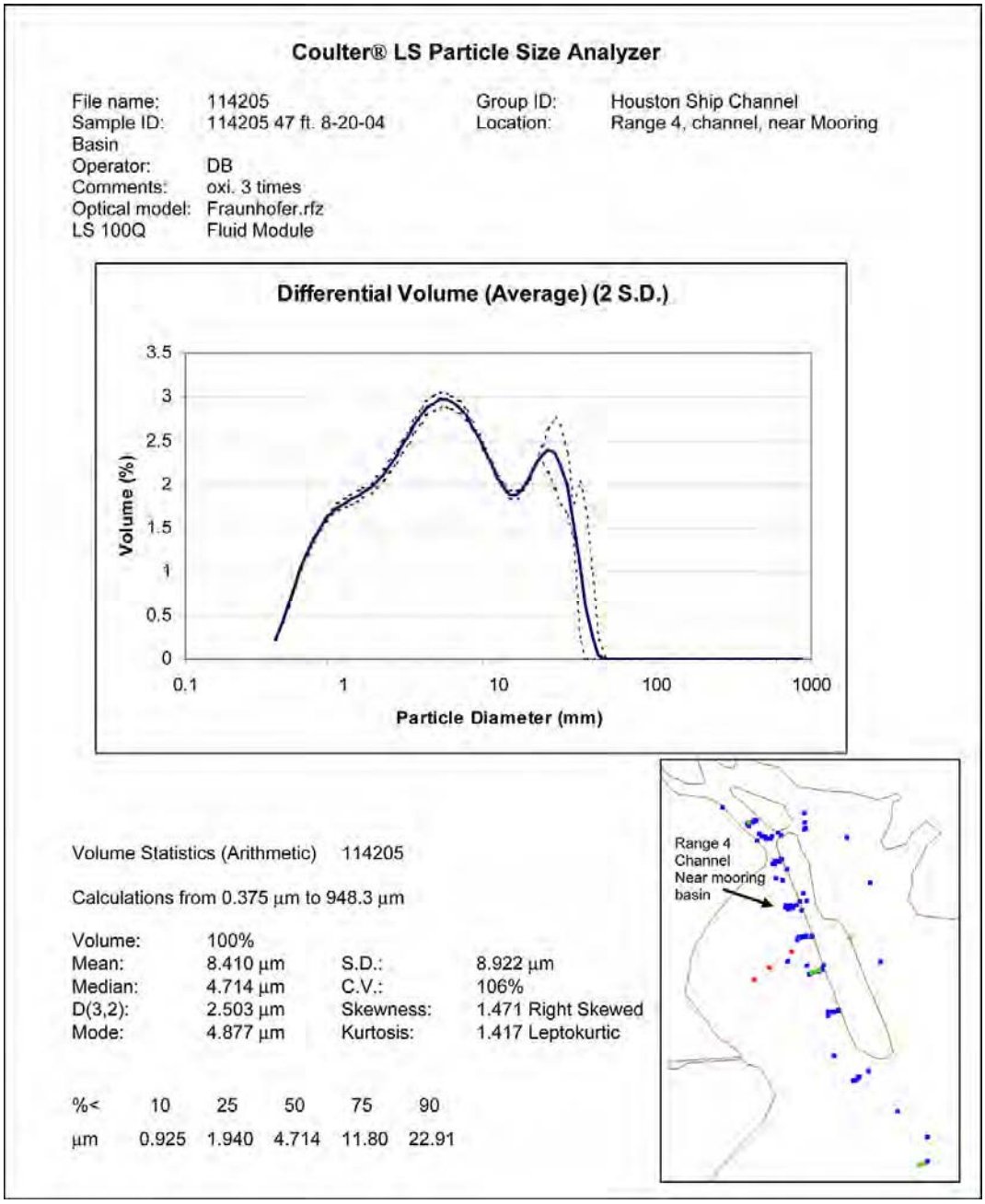

Figure A19. Coulter counter analysis for Point 114205.

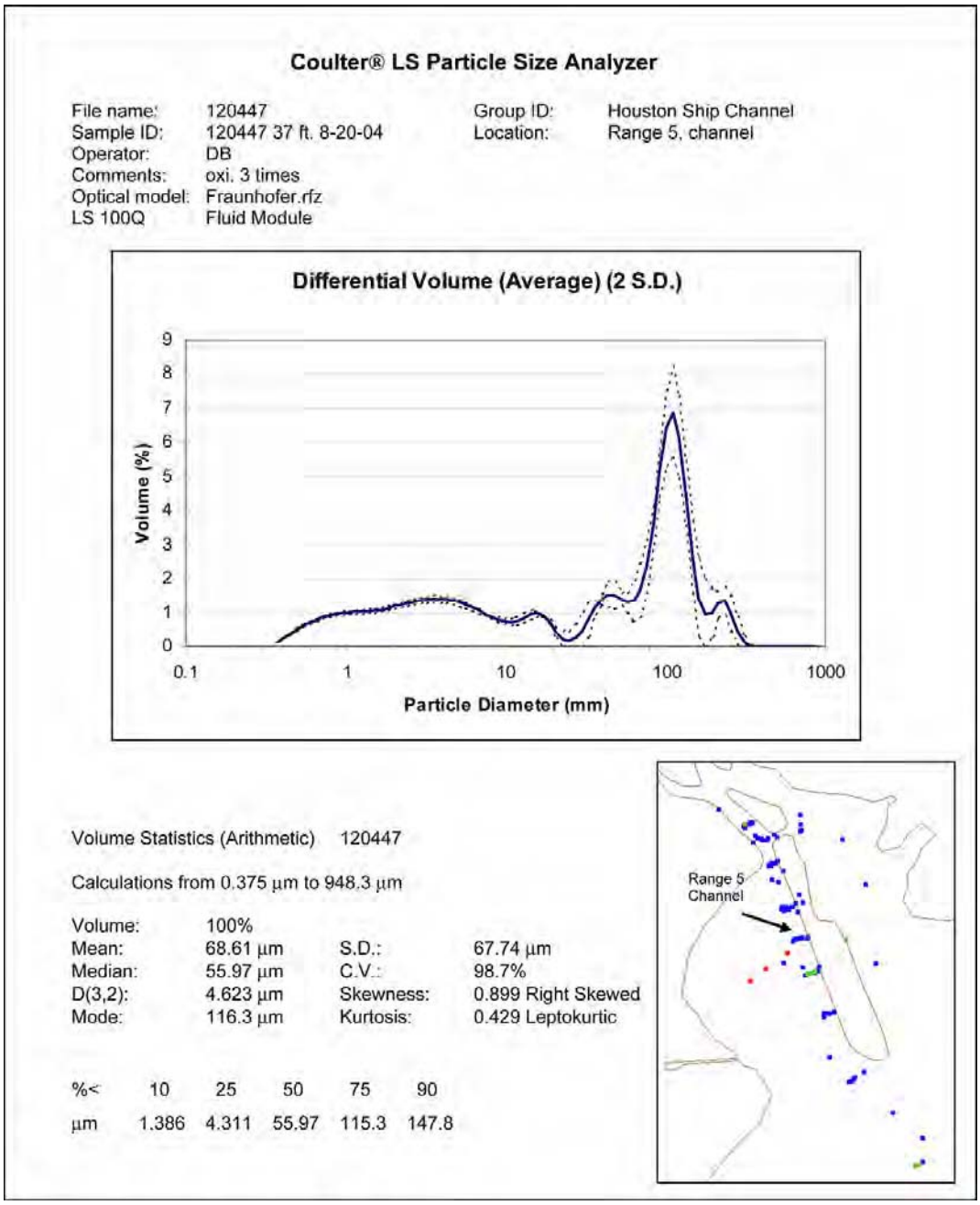

Figure A20. Coulter counter analysis for Point 120447.

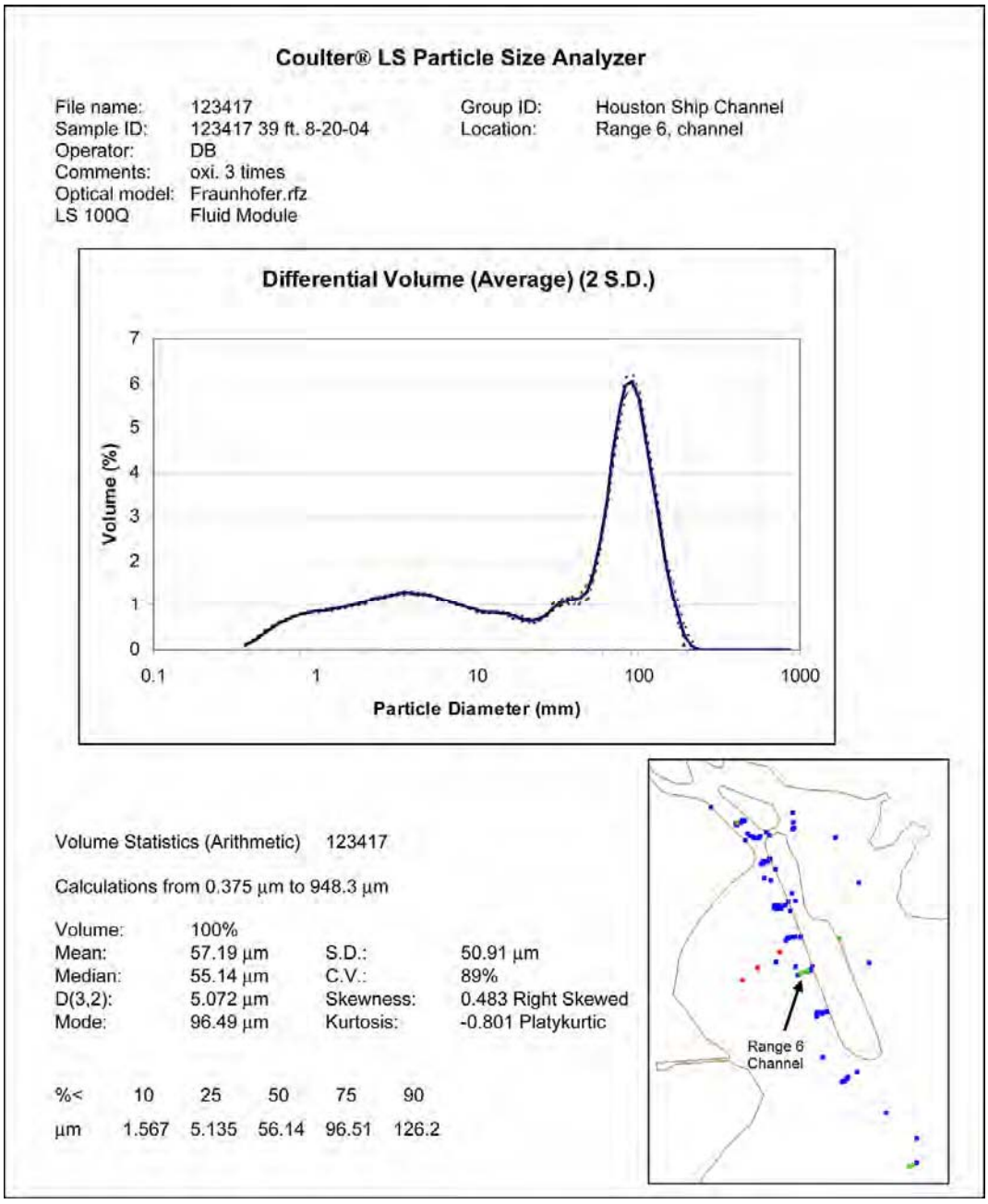

Figure A21. Coulter counter analysis for Point 123417.

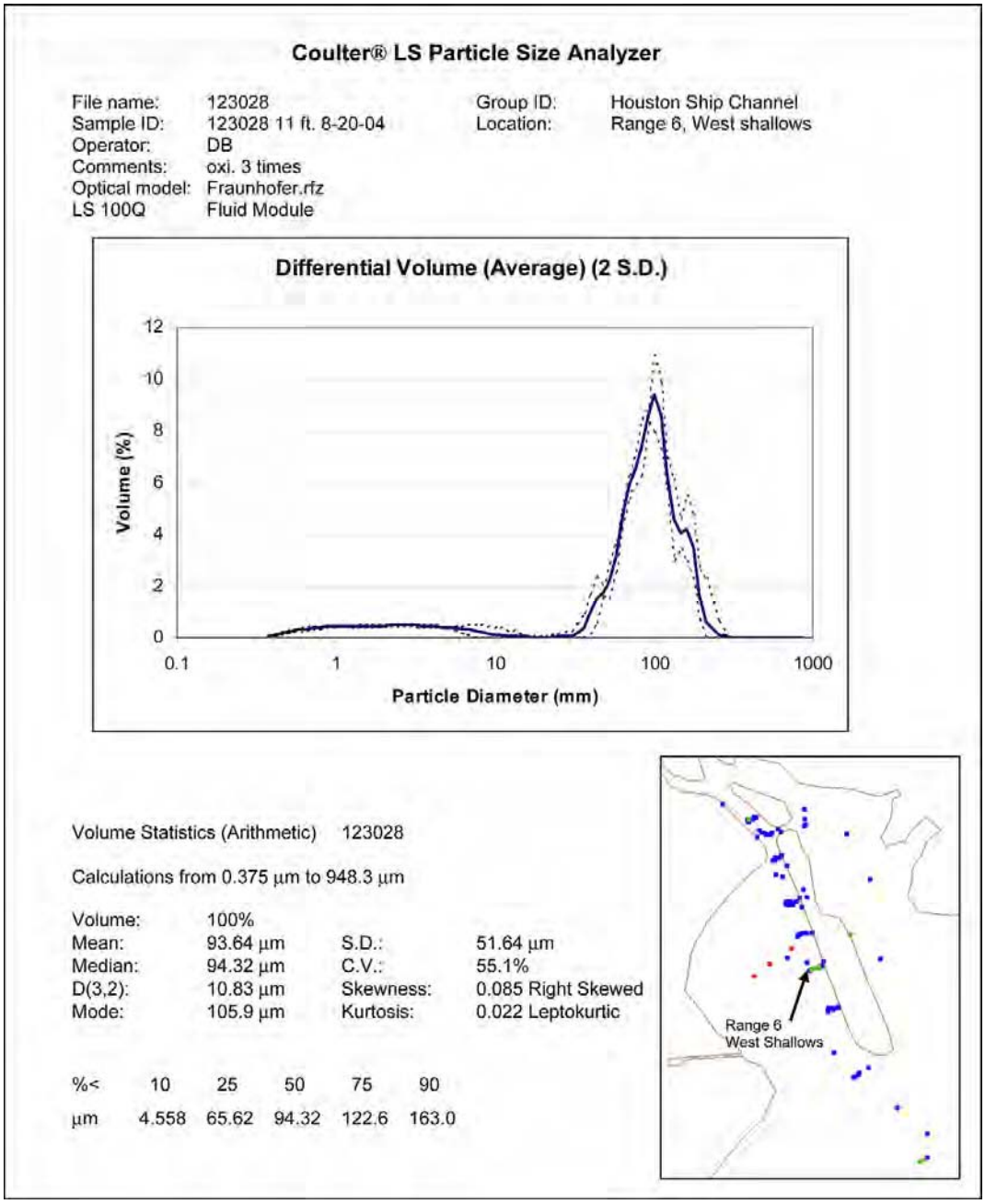

Figure A22. Coulter counter analysis for Point 123028.

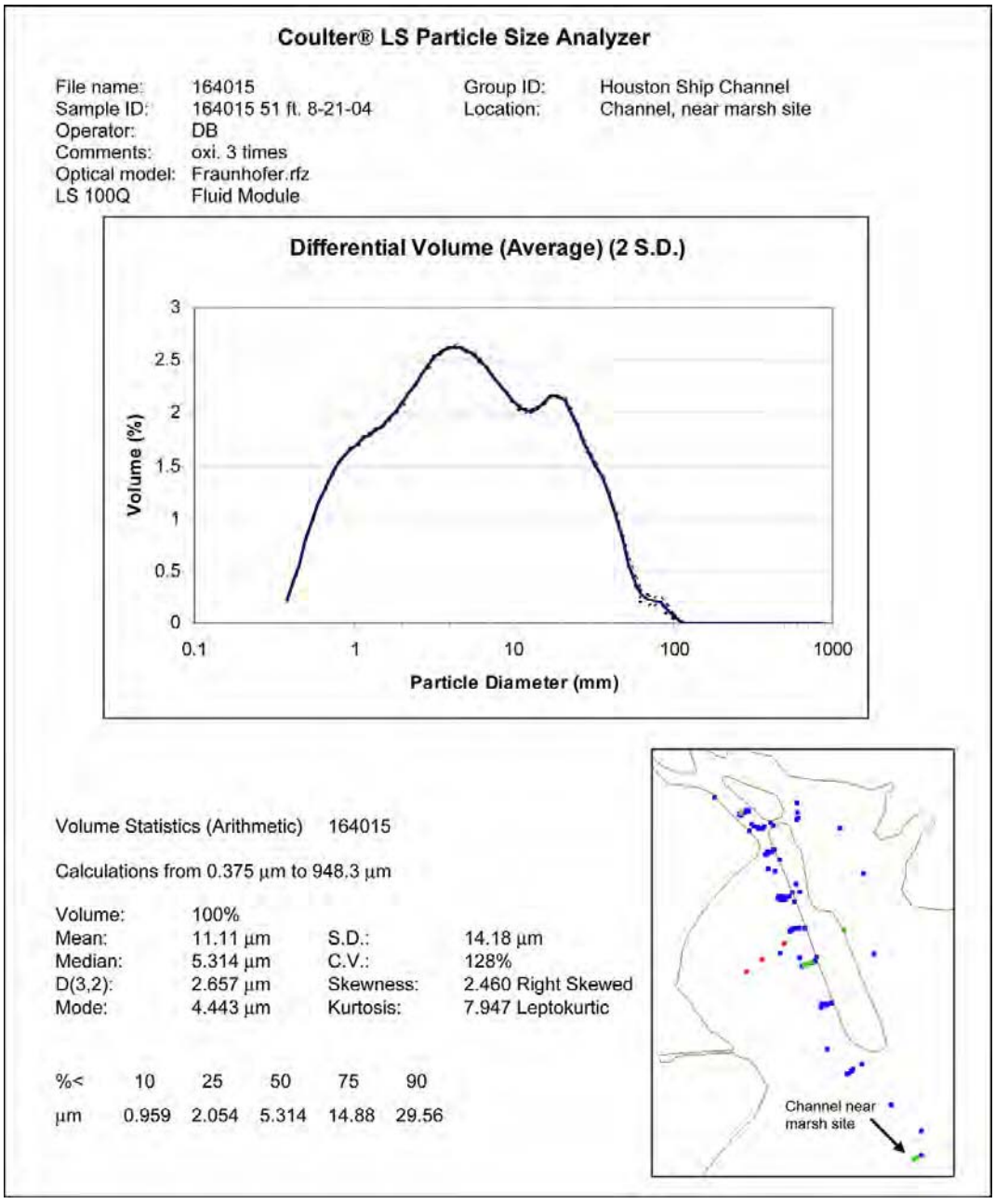

Figure A23. Coulter counter analysis for Point 164015.

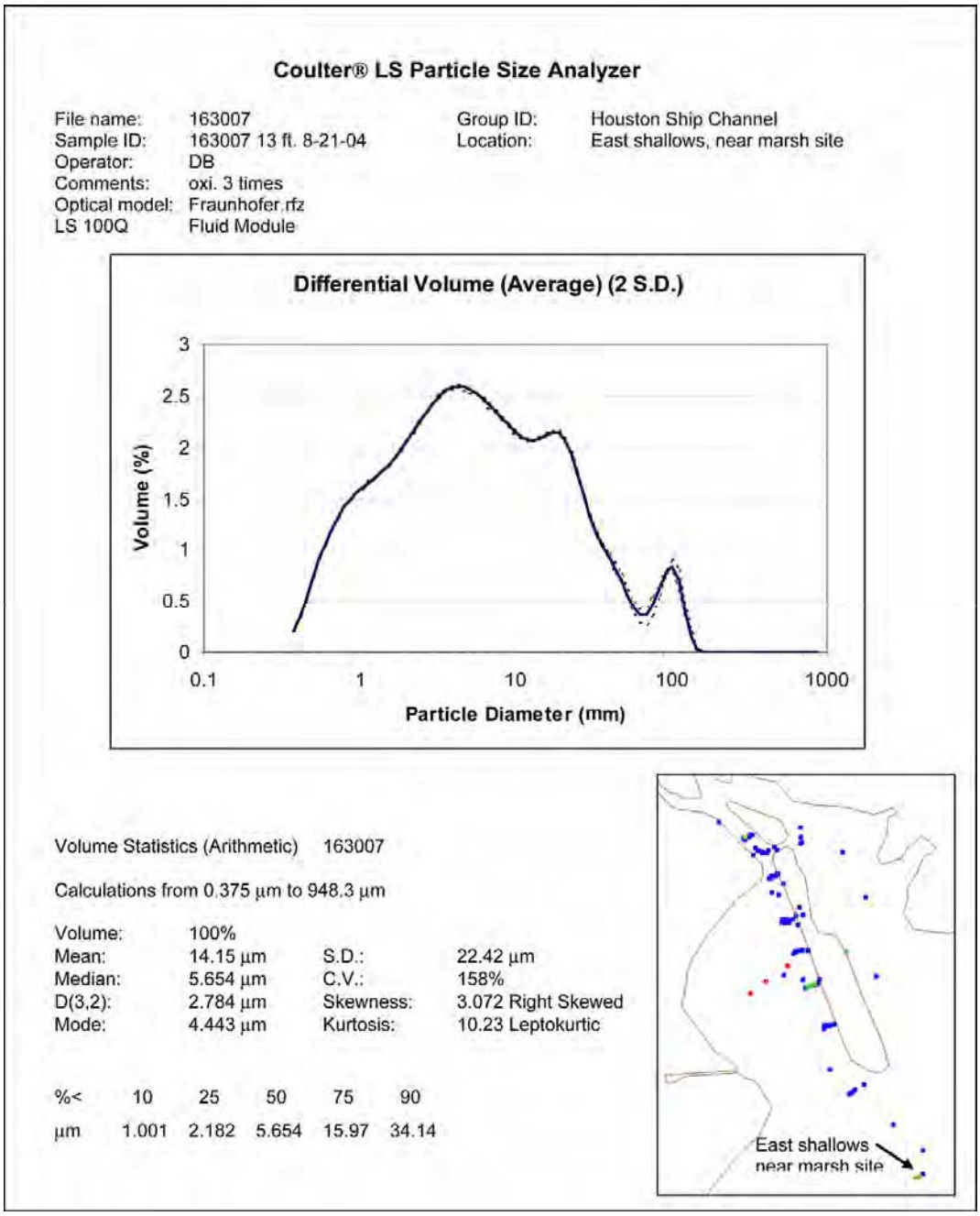

Figure A24. Coulter counter analysis for Point 163007.

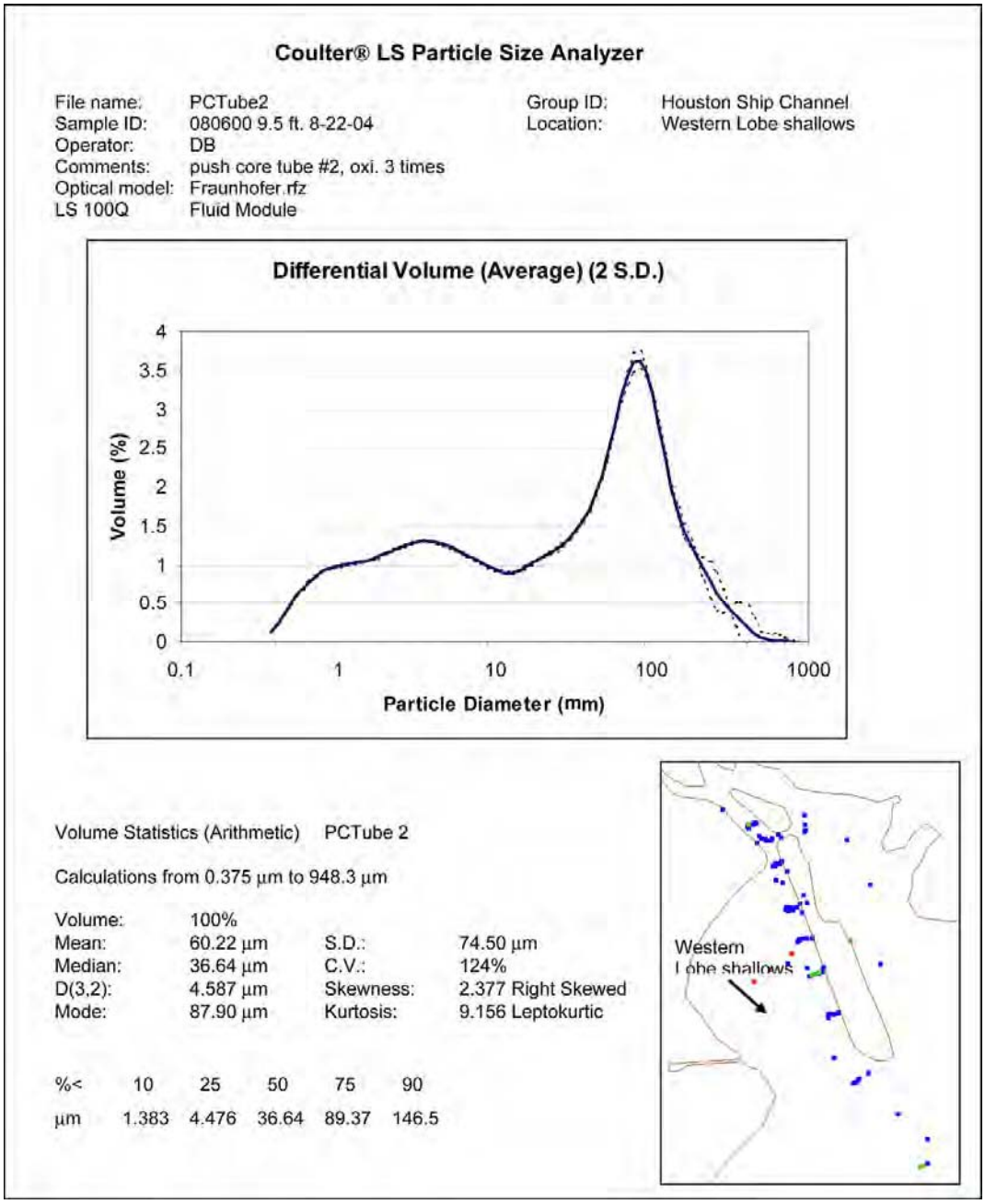

Figure A25. Coulter counter analysis for Point 0806009.

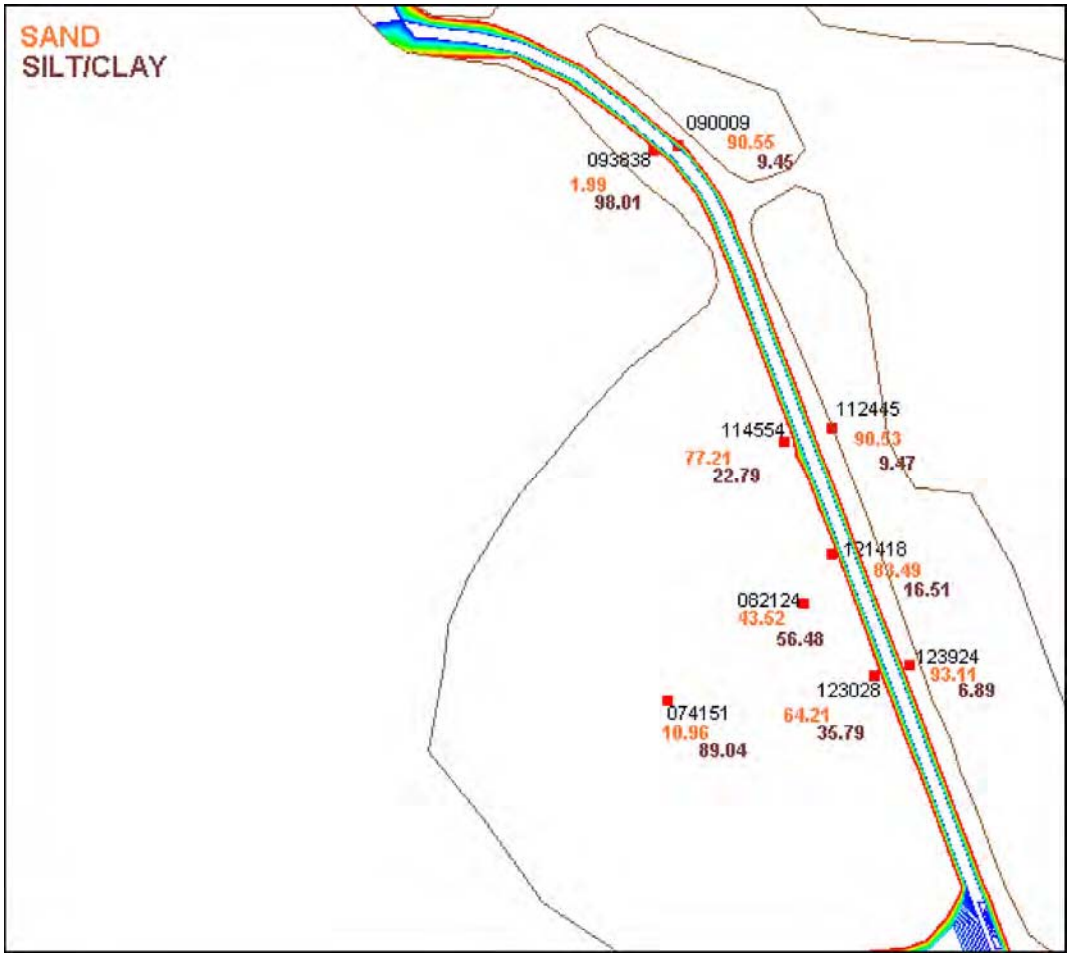

Figure A26. Grain class separation percentages for several field data points.

REPORT DOCUMENTATION PAGE

Form Approved
OMB No. 0704-0188

1. REPORT DATE *(DD-MM-YYYY)*	2. REPORT TYPE	3. DATES COVERED *(From - To)*
August 2006	Final Report	

4. TITLE AND SUBTITLE

Houston-Galveston Navigation Channels, Texas Project Navigation Channel Sediment Study

5a. CONTRACT NUMBER

5b. GRANT NUMBER

5c. PROGRAM ELEMENT NUMBER

6. AUTHOR(S)
J. N. Tate and R. C. Berger

5d. PROJECT NUMBER

5e. TASK NUMBER

5f. WORK UNIT NUMBER

7. PERFORMING ORGANIZATION NAME(S) AND ADDRESS(ES)

U. S. Army Engineer Research and Development Center
Coastal and Hydraulics Laboratory
3909 Halls Ferry Road
Vicksburg, MS 39180-6199

8. PERFORMING ORGANIZATION REPORT NUMBER

ERDC/CHL TR-06-8

9. SPONSORING / MONITORING AGENCY NAME(S) AND ADDRESS(ES)

U.S. Army Engineer District, Galveston
P.O. Box 1229
Galveston, TX 77553-1229

10. SPONSOR/MONITOR'S ACRONYM(S)

11. SPONSOR/MONITOR'S REPORT NUMBER(S)

12. DISTRIBUTION / AVAILABILITY STATEMENT
Approved for public release; distribution is unlimited

13. SUPPLEMENTARY NOTES

14. ABSTRACT

The U.S. Army Engineer District, Galveston, has recently enlarged the Houston Ship Channel from a 40-ft (12.2-m) depth by 400-ft (122-m) width to a 45-ft (13.7-m) depth by 530-ft (162-m) width. Previously, a three-dimensional (3-D) numerical model study was implemented at the U.S. Army Engineer Research and Development Center's Coastal and Hydraulics Laboratory to evaluate the salinity and circulation impact of this enlargement. The enlarged channel is nearly complete. Preliminary evaluations indicate a higher than anticipated rate of deposition in the channel reach near Atkinson Island. The purpose of this investigation was to determine if this new shoaling rate was a permanent feature of this new channel or a single anomalous event. If this considerably larger deposition is a permanent condition then the planned disposal locations must be expanded. The project will determine the possible effects on sedimentation in the channel based on dredging records, field data, vessel effects, and hydrodynamic changes due to the channel's enlargement.

15. SUBJECT TERMS

Channel deepening	Houston-Galveston Ship Channel	Shoaling
Dredging records	Hydrodynamics model	Vessel effects

16. SECURITY CLASSIFICATION OF:			17. LIMITATION OF ABSTRACT	18. NUMBER OF PAGES	19a. NAME OF RESPONSIBLE PERSON
a. REPORT	b. ABSTRACT	c. THIS PAGE			19b. TELEPHONE NUMBER *(include area code)*
Unclassified	Unclassified	Unclassified		131	